VALIDATION OF DISCHARGE PREDICTION APPROACHES IN A STRAIGHT COMPOUND CHANNEL

A Thesis Submitted in Partial Fulfillment of the Requirements for the Degree of

Master of Technology
In
Civil Engineering

ELLORA PADHI

DEPARTMENT OF CIVIL ENGINEERING
NATIONAL INSTITUTE OF TECHNOLOGY, ROURKELA
2014

VALIDATION OF DISCHARGE PREDICTION APPROACHES IN A STRAIGHT COMPOUND CHANNEL

A thesis
Submitted by

Ellora Padhi

(212CE4491)

In partial fulfillment of the requirements
for the award of the degree of

Master of Technology

In

Civil Engineering

(Water Resources Engineering)

Under The Guidance of
Dr. K.C. Patra

Department of Civil Engineering
National Institute of Technology Rourkela
Orissa -769008, India
May 2014

NATIONAL INSTITUTE OF TECHNOLOGY ROURKELA, ORISSA -769008, INDIA

CERTIFICATE

*This is to certify that the thesis entitled, "**Validation of discharge prediction approaches in a straight compound channel**" submitted by **Ellora Padhi** in partial fulfillment of the requirement for the award of **Master of Technology** degree in **Civil Engineering** with specialization in **Water Resources Engineering** at the National Institute of Technology Rourkela is an authentic work carried out by her under our supervision and guidance. To the best of our knowledge, the matter embodied in the thesis has not been submitted to any other University/Institute for the award of any degree or diploma.*

Research Guide

Dr. K. C. Patra
Professor
National Institute Of Technology

Place: Rourkela
Date:

ACKNOWLEDGEMENT

First and foremost, I am glad and thankful to God for the blessing that has given upon me in all my endeavors.

I am deeply indebted to **Dr. K.C. Patra Professor** of Water Resources Engineering specialization, my supervisor, for the motivation, guidance and patience throughout the research work. Along with that I really glad to **Dr. K. K. Khatua** Associate Professor of Water Resources Engineering specialization, for helping me in my research work during my project. I appreciate their broad range of expertise and attention to detail, as well as the constant encouragement they have given me over the years.

I am grateful to **Prof. N Roy**, Head of the Department of Civil Engineering for his valuable suggestions during the synopsis meeting and necessary facilities for the research work, and also I am sincerely thankful to **Prof. Ramakar Jha, and Prof. A. Kumar** for their kind cooperation and necessary advice.

I extend my sincere thanks to **Mrs Bandita Naik** the senior research scholar of Water Resources Engineering Specialization for giving a chance to work with her at the time of experiment. I am really thankful to her for constantly encouraging me for this work. I am grateful for friendly atmosphere of the Water Resources Engineering specialization and all kind and helpful professors that I have met during my course.

I would like thank my parents, and family members. Without their love, patience and support, I could not have completed this work. Finally, I wish to thank many friends especially, **Aparupa, Mona, Abinash, Santosh** for the giving me support and encouragement during these difficult years,

Ellora Padhi

Table of Contents

List of Figure

Title **Page No**

List of Tables

Title **Page No**

List of Symbols

A	Area of the compound channel
a	Rating curve constant
$A_{full\ bank}$	Area of the main channel at full bank depth
A_{fp}	Area of the flood plain
A_{mc}	Area of the main channel
A_r	Area ratio
A_{total}	Total area of the compound channel
B	Top width of the compound channel
b	Bottom width of the main channel
b_1	Rating curve constant
C	Chezy's constant
C_d	Co-efficient of discharge
D	Hydraulic depth
d	The diameter of the pitot tube
f	Darcy- weisbach co-efficient of friction
f_{mc}	Co efficient of friction in the main channel
f_{fp}	Co efficient of friction in the flood plain
F_r	Froude's number
g	Acceleration due to gravity
H	Depth of flow
h	Full bank depth
Hn	The height of water flowing above the notch
h_{int}	Interface depth
L	The length of the notch,
n	manning's roughness coefficient
N_{fp}	No of flood plain
n_{fp}	Manning's roughness for flood plain
n_{mc}	Manning's roughness for main channel
$P_{full\ bank}$	Perimeter of the main channel at full bank depth

P_{fp}	perimeter of the flood plain
P_{mc}	Perimeter of the main channel
P_r	Perimeter ratio
P_{total}	Total perimeter of the compound channel
Q	Discharge of the channel
Q_{actual}	*Actual discharge of the channel*
$Q_{full\ bank}$	Discharge of the main channel at full bank depth
Q_r	Discharge ratio
Q_{total}	Total discharge of the channel for a given flow
R	Hydraulic radius of the channel
R_e	Reynolds number of the flowing fluid
R_{fp}	Hydraulic radius of the flood plain
R_{mc}	Hydraulic radius of the main channel
S_0	Bed slope of the channel
s	lateral slope of the channel
U_d	Depth averaged velocity
U_{fp}	Velocity of the flood plain
$U_{fp,0}$	Velocities of flood plain when co-efficient of interface is zero
U_{mc}	Velocity of the main channel
$U_{mc,0}$	Velocities of the main channel when co-efficient of interface is zero
V	Mean velocity of the channel
V_d	Lateral depth averaged velocity
$W_{full\ bank}$	Width of the main channel at full bank depth
W_{fp}	Width of the flood plain
W_{mc}	Width of the main channel
W_r	Width ratio
W_{total}	Total width of the compound channel
X_{fp}	Interface length for flood plain
X_{mc}	Interface length for the main channel
τ_b	Bed shear stress
γ	Co-efficient of interface

ρ	Density of water
λ	Eddy viscosity
τ_{int}	Interface shear stress
ν	Kinematic viscosity
$\%S_{fp}$	Percentage of shear force in the flood plain
Δp	Pressure difference between the total pressure and the static pressure at the wall
β	Relative depth
Γ	Secondary current
τ_w	Wall shear stress
α	Width ratio

Abstract

The flow pattern of a compound channel becomes complicated due to the transfer of momentum between the main channel and the adjoining floodplains. Experiments are carried out to compute the velocity as well as boundary shear along the wetted perimeter of a straight compound channel to quantify the momentum transfer along the expected interfaces originating at the junction region between main channel and flood plain. This is helpful to evaluate the stage-discharge relationship for a compound channel accurately. Discharge calculation can be done by using various hydraulic models. But the traditional discharge prediction models such as SCM, DCM fail to give accurate discharge as they don't consider the effect of momentum transfer. Therefore some new models are being developed which makes discharge prediction more accurate than the traditional method by considering the effect of momentum transfer. In this study the experimental data reported by other investigators as well as data from the present series of experiments are used through the hydraulic models such as DCM, IDCM, MDCM,CES to evaluate the discharge estimation and the results are compared with the experimental observations by keeping Manning's n value constant with respect to the surface roughness. But apart from surface roughness Manning's n is dependent upon many other factors such as depth of flow, shape of the channel, alignment of the channel etc.. So by varying the value of manning's n with respect to depth of flow the discharge is being computed through MDCM and the percentage of error is found out. Modification to MDCM is applied for the variation of n values.

INTRODUCTION

1.1 Introduction

There is a very close relationship exists between civilization and the rivers from the last decades, as they provide many contribution to the human society like water for house hold work, irrigation, navigation, hydro electricity generation, water supply for consumption and industrial applications and disposal of waste. Therefore it is seen that the surroundings of the river have been popular settling areas of the human civilization. Due to consequently increased use of rivers large amount of settlements have been developed on the river flood plains and its nearby areas. As a result the river may be a threat to the activities that has been taking places in its vicinity, at extreme discharge condition flood may occur that may cause loss of life and damage to the infrastructure of the surrounding area.

River engineers are therefore more and more solicited to mitigate the flood impacts. Previously flood control work was associated with many alleviation works like improvement on dikes and detention reservoirs. But it was cost effective and the outcome was not so effective as the morphological response of the river is unpredictable. Therefore some sustainable solution are being adopted such as, surrounding of the rivers are allocated with much space or made free by withdrawing dikes and abandoning possible settlements areas or using the surrounding area of the river seasonally (Bhattacharya and Bora 1997). Apart from this to reduce the flood risk, hydro-dynamic models of river flow may also help in achieving better flood protection measures against the upcoming flood. To forecast the flood is required and for that many hydraulic models are being developed by different investigators which are helpful in estimating the discharge for given flow condition of the rivers. There are many hydraulic models have been developed by the researchers which are helpful in discharge prediction of a channel. Initially Single channel method (SCM) and Divided channel method (DCM) are the two most common methods which are used by the river engineers but these methods are that reliable as these methods do not consider the effect of momentum transfer therefore other new discharge prediction methods are being developed. IDCM, MDCM, EDM, SKM, MSKM LDM are the examples of the standard hydraulic models. Apart from discharge prediction these models are helpful in velocity as well as

boundary shear stress measurement. But for this the hydraulic behaviors of the river is required to be investigated. So for this investigation, the types of flow, type of channel, factor affecting the hydraulic behavior of the channel, channel geometry etc. has to be studied.

1.2 Types of Flow

Generally there are two types of flow exist. One is free surface flow and another one is pressure flow. The flow is said to be free surface flow if is subjected to atmospheric pressure and the flow is said to be pressure flow if it is running at full flow condition with in a conduit. But in open channel the flow type is free surface as it is open to atmosphere. But apart from this depending upon the hydraulic characteristics the flow is again categorized such as steady and unsteady flow, uniform and non-uniform flow, laminar and turbulent flow and lastly depending upon the energy level it is subdivided into critical, subcritical and supercritical flow.

1.2.1 Steady and unsteady flow

When the flow velocity at a given point does not change with respect to time then the flow is said to be steady flow. If the velocity at a given point changes with respect to time the flow is said to be unsteady flow. This is based on variation of velocity with respect to time at a particular location. The mean local acceleration is considered to be zero for steady state flow condition i.e. partial derivative of the velocity components with respect to time (t) are zero.

1.2.2 Uniform and non-uniform flow

If the flow velocity at a given time does not change within a given length of the channel, the flow is said to be uniform flow and if the flow velocity at a given time changes with respect to space the flow is called as non-uniform flow. This is based on the variation of flow velocity with respect to space at a particular time. Here the conservative acceleration in uniform flow is zero i.e partial derivative of the velocity components with respect to space (x, y, z) are all zero.

1.2.3. Laminar and turbulent flow

If the flow particle of the water appear to move in a definite path and the flow appears to be in the patterns of layer upon layer, the type of flow is said to be laminar flow. In turbulent flow the particle of water moves in an irregular path which are not constant with respect to time or space. Whether the flow is laminar or turbulent, it depends upon the relative magnitude of the viscous force and the inertia force. The flow should be laminar if the viscous force is

predominant and the flow will be turbulent if the inertia force is predominant. The ratio of viscous force and the inertia force is called as Reynolds number. If the Reynolds number is less than 500, the flow comes under laminar flow category. If the Reynolds number id greater than 2000 the flow type is turbulent and if it lies between 500 and 2000, it comes under transition zone.

1.2.4. Critical, Subcritical, Super critical flow

Depending upon the level of specific energy the flow is again characterized in to three parts, such as critical, subcritical, super critical flow etc.

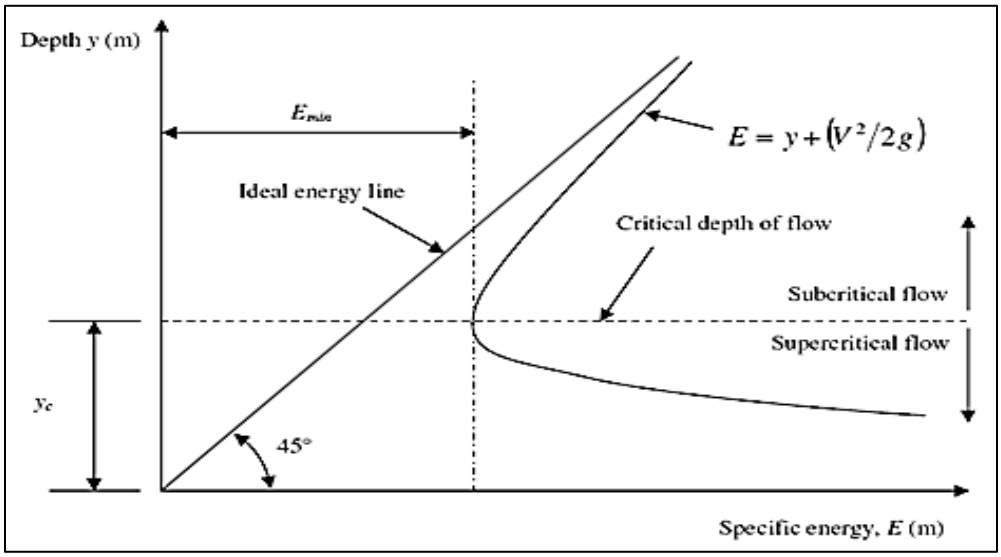

Fig 1.1 The specific energy curve in an open channel

In the fig.1.1 a graph is plotted between the depth and specific energy where y is depth of flow, V is the mean velocity of flow, g is the acceleration due to gravity and y_c denotes the critical depth where the value of specific energy (E) is minimum. A flow is said to be critical if the velocity of flow is equal to velocity of a gravity wave having small amplitude. A gravity wave can be formed by changing the flow depth. The flow is said to be subcritical if the velocity of flow is less than the critical velocity and the flow is said to be supercritical if the flow velocity is greater than the critical velocity. If we consider critical flow in terms of depth then we can say that the if the depth of flow is greater than critical flow depth then the flow is called as subcritical flow and if the depth of flow is less than the critical flow depth then the flow is said to be supercritical flow.

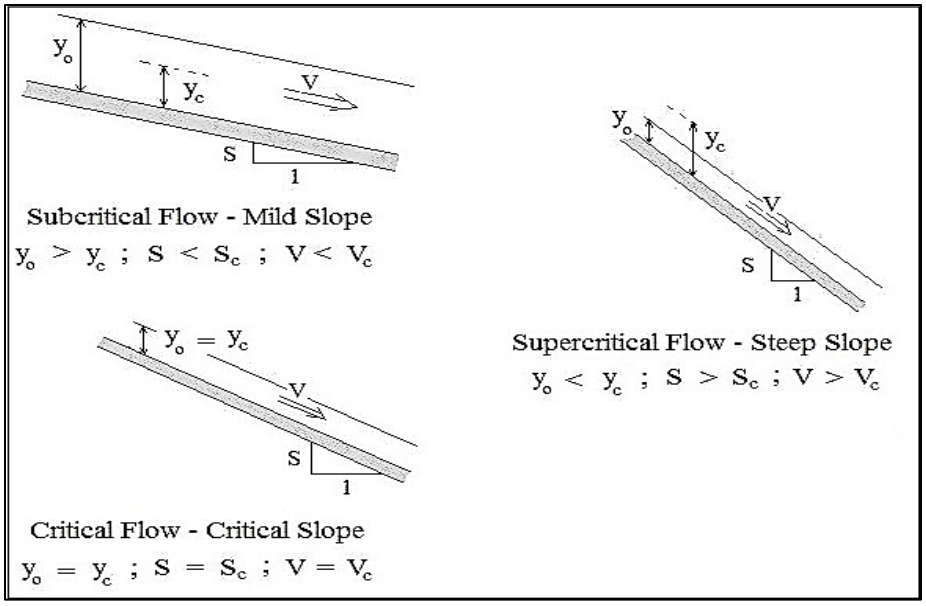

Fig.1.2 The Subcritical, supercritical and critical flow conditions

Apart from these, whether the flow is critical, subcritical or supercritical, it can be known from the value of Froude's number. The ratio of inertia force and gravitational force is called Froude's number. For an open channel,$F_r = \frac{V}{\sqrt{gd}}$, where d is hydraulic depth, V is the flow velocity and g is the gravitational acceleration. But a rectangular channel, d term'd' is replaced by 'y' where y is the depth of flow. As it is mentioned before depending upon the value of Froude's number the flow can be classified, so here the categorization is given i.e. for Froude's number less than one the flow is a subcritical flow, for Froude's number greater than one, the flow is said to be a supercritical flow and for critical flow condition the Froude's number should be equal to one.

1.3 Types of Channel

Streams are responsible for erosion, transportation, and deposition of sediments. Energy of the stream controls these function. the slope of the stream determines the energy of the stream and discharge. The discharge of a stream can be measured by multiplying area of the cross section of the stream with the velocity of the stream. there are some factors which are affecting the discharge such as the shape of the channel, the smoothness of the channel sides and bottom, and obstacles in the stream. Velocity of the stream determines the capability of the stream whether it can carry large size of particle or not and as discharge is the function of velocity it

also determines the total capacity of the channel. Through its complete path, a river may be classified into three different types of streams as it travels through dissimilar sites.

Three major streams are three types

1. Braided Channel
2. Straight Channel
3. Meandering Channel.

1.3.1. Braided channel

Braided streams are having less energy deficient and have a tendency to change the flow path constantly due to deposition of large sediment loads they carry. Braided streams are often originated in outwash plains at the head of glaciers.

1.3.2. Straight Channel

Straight stream channels are rare. The straight channels are the channels which are having sinuosity as one. There is no much variation occurs along its flow path. These are mainly unstable in nature. Along the lines of faults and joints, on steep slopes where the surface gradient are closely followed by hills, the straight are developed. In the experimental laboratory it is seen that the flume of straight channels are having uniform cross section quickly develop pool-and-riffle orders.

Fig.1.3.(i)Three dimensional view of a straight channel.

Fig1.3.(ii) Straight reach of River Great Ouse in United Kingdom

Fig1.3.(iii) Straight reach of River Jhelum in Srinagar

Fig1.3. (i)-(iii) shows straight channels in India as well as in abroad

Straight channels are having excess of energy and mostly have a single channel. Straight streams erode towards the downstream and thus have channels with steep walls and large slope. Even in straight channel segments water flows in a sinuous fashion, with the deepest part of the channel changing from near one bank to near the other. Velocity is highest in the zone overlying the deepest part of the stream. In these areas, sediment is transported readily resulting in pools. Where the velocity of the stream is low, sediment is deposited to form bars. The bank closest to the zone of highest velocity is usually eroded and results in a cut-bank.

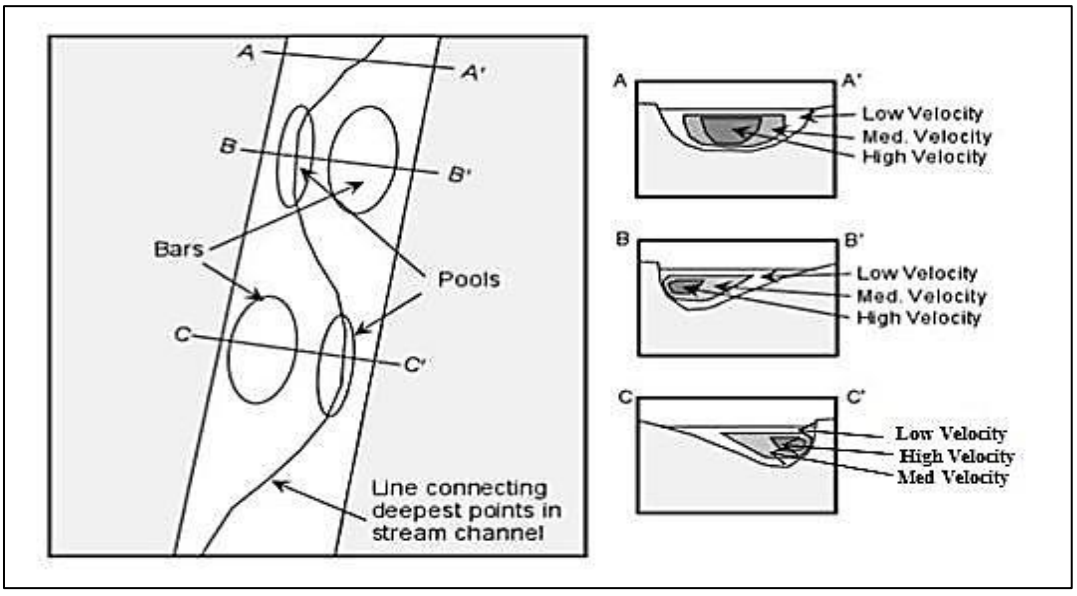

Fig1.4. Deposition of sediments along the path of the straight channel.

1.3.3. Meandering channel

Meandering channel are the channel which are having sinuosity more than one. These are the channels which are having small straight reaches and the variation occurs along the flow path. When there is an obstacle occurs the river deviates from its path and goes towards the low resistance path due to which a meandering channel is developed. these streams have a balance of energy. They are mainly characterized by slow moving water, low slopes, but having high capacity. Meandering streams erode laterally across an active meandering floodplain creating cut-banks on the outside of the bends where the bank of the stream is being eroded away, point bars on the inside of the bends where sediments are accumulating, and oxbows where the bends have been cut off from the main stream Oxbows may or may not have water in them. They are often left only as depressions in the ground that have been overgrown with vegetation.

Fig.1.5: Meandering River Okavango

Depending upon the channel geometry the channels are also classified as rectangular, trapezoidal circular etc. The compound channels are also asymmetric if there is one floodplain along the side of the main channel. The compound channel is said to be symmetric if it has same floodplain along both side of the main channel and it is said to be unsymmetrical if its main channel has two flood plain but they unequal in size.

1.4. Stage Discharge Relationship

Estimation stream discharge is often area of interest of river engineers and watershed managers. Rate of flow of water passing a point on a stream at an unit duration of time is known as discharge; therefore, it is harder to measure the discharge of a river continuously and it is cost effective task in hydrology. To overcome this problem an empirical or theoretical relationship is

being developed by the researchers between the water level and the quantity of water passing through a point at a particular instant of time. This relationship is called as stage discharge relationship or it is called as a rating curve. A **Rating curve** is a graph of discharge versus water level (stage) for a given point on a stream. Frequent measurements of discharge of the stream are taken over a range of stream stages. A rating curve is usually plotted as stage on y-axis versus discharge on x-axis.

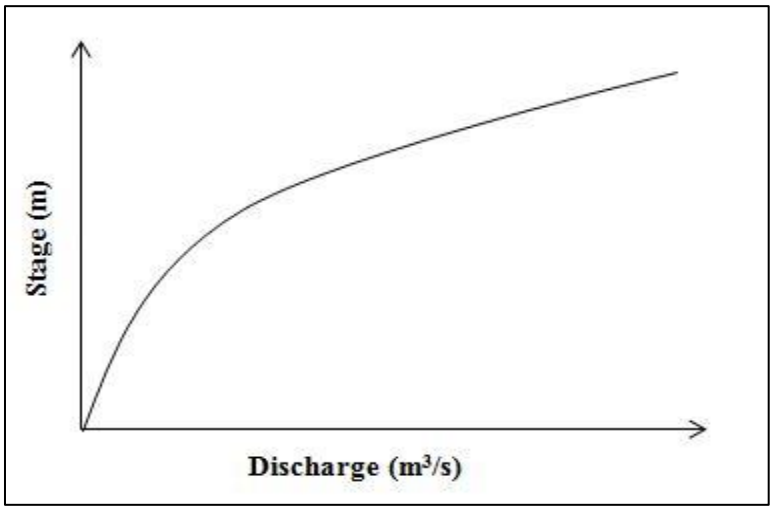

Fig.1.6: Rating curve plotted between Stage and discharge

While a rating curve is generated it includes two steps. In the first step by measuring the stage and corresponding discharge in the river the relationship between stage and discharge is established. In the second step, measurement of stage of river is done by gauge and then discharge is calculated by the help of the relationship established in the first step. When the stage-discharge relationship is constant with respect to time, it is called permanent control and when the relationship does change, it is called shifting control. due to erosion or deposition of sediment at the stage measurement site, situation of shifting control occurs. Situation of permanent controls occur where bed of the river is rock type or the bottom of the river is of concrete, though it is not available always,

The relationship between stage and discharge can be estimated with the equation (1.1).

$$Q = aH^{b_1} \tag{1.1}$$

Where H represents water level (stage) for discharge Q, a and b_1 are rating curve constants.

1.5. Estimation of Stage-Discharge

Generally the stage discharge relationship is required to predict the discharge. Therefore an empirical relationship is established which is used for steady and uniform flow condition so that we can get an ideal rating curve, other than this we can calculate it directly by multiplying area with the average velocity of the river, but for this the mean velocity and the cross sectional area of the stream should be known. Sometimes it is very difficult to go to the site and take the measurement. So we cannot be more dependent on the rating curve formula. But apart from this there are other traditional formulae which are used to estimate the discharge such as Manning's formula, Chezy's formula and Darcy's Weisbach formula etc.

So according to Mannings formula

$$V = \frac{1}{n} R^{\frac{2}{3}} S_o^{1/2} \tag{1.2}$$

According to Chezy's formula

$$V = C\sqrt{RS_o} \tag{1.3}$$

According to Darcy's Weisbach formula

$$V = \sqrt{\frac{8gRS_o}{f}} \tag{1.4}$$

After finding out the velocity discharge can be calculated by multiplying area with it. In the above equations V is the mean velocity, R is the hydraulic radius, S_o is the bed slope, g is acceleration due to gravity, f is the co-efficient of friction and C is the Chezy's Constant.

The problem with three formulae is they are mainly useful to simple channel and they fails to fails to predict the discharge large compound channels due to changes in geometry and variability in hydraulic parameters. Therefore some new models are developed to predict the discharge. Initially single channel method was used but as it gives overestimated discharge so divided channel method was developed but both methods do not consider the effect of momentum transfer.

Momentum transfer occurs at the junction of the main channel and the flood plain, due to difference in local velocities of both main channel and flood plain. Due to this difference formation of vortices occurs at the junction. A shear layer is formed because of these vortices.

Apart from this there is a secondary current develops at the boundary of the channel due to turbulence and also there is a frictional force develops between the water and the boundary of the channel which give resistance to flow. Due to secondary current, viscosity and shear stress the discharge prediction was getting difficult.

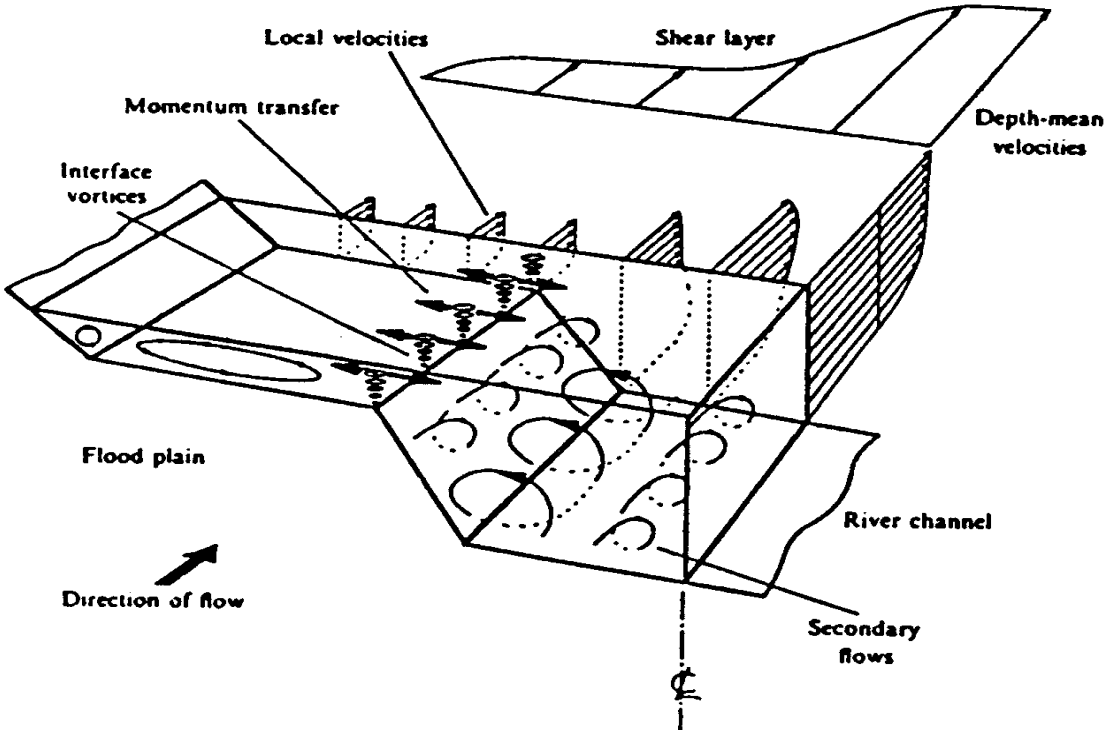

Fig1.7: Flow structure in a compound channel (Shiono and Knight 1991)

So by considering these effects Shiono and Kinight developed a model which gives better discharge prediction than those conventional methods. But later on some researchers found that effect of secondary current is negligible therefore some new methods are being developed without considering that. MDCM is the method which is used to predict the discharge by quantifying the momentum transfer in terms of interface length. Interacting divided channel method is another which is also used to measure the discharge by considering momentum transfer in terms of shear stress.

With these numerical methods some computational are developed which also give good discharge prediction such as HEC-RAS, MIKE11, CES, ANN etc. So here we should go for a comparison study between these numerical and computational method so we can come to a conclusion that which method give better discharge prediction.

LITERETURE REVIEW

2.1. Introduction

Prediction of discharge is one of the important works in river flow analysis. Discharge prediction is required to establish the stage discharge relationship in a channel which will be help full to the River Engineers for flood forecasting, bank protection etc. Discharge calculation is influenced by various hydraulic parameters as well as geometric parameters of the channel. But still discharge prediction in the simple channel is easy and it can be done using manning's equation, chazy's equation or by using darcy-weibach' equation. But when it is required to calculate the discharge in compound channel then these equations do not give adequate answers. So for finding out the reasons of not getting good result, initially some researchers divided the compound channel in to various segments and tried to calculate the discharge for each segment. By integrating the discharge for the segments, the total discharge for the compound channel was found out. But this method also did not work. So after having several investigations by the researchers it was found that the reason behind inaccurate discharge value is due to exchange of momentum. They stated that Momentum transfer occurs at the junction of flood plain and the main channel due to difference in velocities. Generally in bank flow condition water flows in certain velocity with in the main channel but due to flood, it overtops the main channel and flow over the flood plain. As the flow area for flood plain is less than the main channel so initially the effect of shear stress is more. Due to this there is difference in velocity generated which resulting in the formation of vortices at the junction. This difference in velocity leads to create problem in calculation of discharge. So now a days many researchers are trying hard to work on momentum transfer and also to understand how it is affecting the velocity of the compound channel and shear stress at the bed as well as on the wall for an over bank flow condition.

In this chapter the works of various investigators on experimental research and studies on discharge prediction, momentum transfer phenomenon and calculation of boundary shear stress for straight compound channels are presented.

2.2 Literature on Discharge, Momentum Transfer, Boundary Shear Stress

Sellin (1964) made sure the presence of the secondary current after conducting number of laboratory studies and shown the presence of vortices at the junction of main channel and flood plain. Here the channel velocities and discharge was being studied under both in-bank and over bank flow conditions by putting a thin impermeable film at the junction and it was observed that velocity in the main channel was more under in bank flow condition, than the over bank flow condition.

Zheleznyakov (1965) investigated the interaction at the junction of main channel and the adjoining floodplains. He studied the effect of momentum transfer mechanism by conducting experiments in the laboratory conditions. He stated that due to momentum transfer the overall rate of discharge is decreased for the lower floodplain depths and as the floodplain depth goes on increasing the effect of momentum transfer goes on decreasing. Apart from this he conducted field experiments where he had shown the importance of momentum transfer in the calculation of overall discharge. The dragging and accelerating forces acting upon the higher main channel flow velocity and slower flood plain flow velocity respectively are main cause of transfer of momentum at the junction which is called as kinematics effect.

Ghosh and Kar (1975) studied the boundary shear distribution in straight compound channels for both smooth and rough surface. The distribution of drag forces on different parts of the channel sections were being related with the co-efficient of roughness and depth of flow.

Yen and Overton (1973) used isovel plots to get the exact position of zero shear interface plane. By using this method data had been collected and they showed that with increase in depth of flow over the flood plain, the angle of inclination the horizontal of the interface plane also increased.

Myers and Elswy (1975) reported studies on the effect of momentum transfer at the junction of main channel and flood plain and distribution of shear stress at complex sections of a compound channel. Here shear stress were calculated at different section of the compound channel and it is found that with respect to in flow condition there is a decrease of 22 percent in main channel shear stress and increase of 260 percent in flood plain shear stress. The possible area of erosion and scour of channel bed and the flow pattern in a compound section can be known through this.

Rajaratnam and Ahmadi (1979) reported the study on the interaction of flow velocity between main channel and floodplain with smooth boundary surface in a straight channel. The transfer of longitudinal momentum from main channel to flood plain was presented. It is seen that due to flow interaction at the junction of flood plain and main channel, the bed shear in floodplain considerably increased while the main channel shear decreased at the same time. It is observed that the effect of flow interaction was reduced as the flow depth in the floodplain increased.

Wormleaton *et. al.* (1982) carried out a series of laboratory experiments in straight compound channels with symmetrical floodplains and by using "divide channel" method discharge was estimated. By measuring boundary shear stress, apparent shear stress at the horizontal, vertical and diagonal interface planes generated between the main channel-floodplain junction could also be evaluated. For calculating discharge, an apparent shear stress ratio was proposed which was useful in selecting the best method of dividing the channel. It was found that the horizontal and diagonal interface divided channel method gave better discharge results than the vertical interface divided channel method at lower floodplains depth.

Knight and Demetriou (1983) undertook series of experiments in straight symmetrical compound channels to understand the characteristics of discharge, distributions of boundary shear stress and boundary shear force in the given section. Equations for calculating the percentage of shear force carried by floodplain were being proposed. They also presented an equation for the proportions of total flow in various sub-parts of compound section in terms of two dimensionless channel parameters. The apparent shear force was found to be more at lower flow depth and also for high floodplain widths for vertical interface between main channel and floodplain.

Knight and Hamed (1984) further extended the work of Knight and Demetriou (1983) from smooth flood plains to rough floodplains. The floodplains were roughened through six different

materials to study the effect of different roughness between floodplain and main channel on flow interaction process. Using four dimensionless channel parameters, they proposed equations for the percentage shear force carried by floodplains and the apparent shear force in vertical, horizontal, diagonal interface planes. From the results of apparent shear force and discharge data the efficiency of these four commonly adopted design methods for predicting discharge could be known.

Wormleaton and Hadjipanos (1985) reported a study on flow distribution in compound channels and showed that even though a discharge prediction method may be efficient can give good results on overall discharge in a compound channel but the velocity flow distribution between floodplain and main channel may not be good. In general, the floodplain flow is found to be underestimated and the flow distribution in the main channel is overestimated.

Myers (1987) proposed the theoretical considerations of ratios of velocity of main channel and to the velocity of floodplain and discharge of main channel to discharge of flood plain in compound channel. The relationship was established between the ratios and the flow depth, as a result it gave a straight line relationship. Here it was seen that the relation between ratio and flow depth was independent of bed slope but dependent on channel geometry. Equations were generated which describes the relationship of ratio and depth for smooth compound channel. It was seen that at lower depths, the traditional methods overestimated the full main channel carrying capacity and underestimated at higher depths, while floodplain flow capacity was always underestimated for both higher and lower depths. He suggested the need for methods of compound channel analysis which can accurately model flow proportion in floodplain and main channel for both higher as well lower depths.

Stephenson and Kolovopoulos (1990) studied and discussed four different methods to evaluate the discharge prediction method by considering variation of the shear stress between main channel and flood plain with respect to different flow condition. Based on the previously published data, they predicted discharge and ended with a conclusion that their 'area method' was the most reliable method in predicting discharge and that Prinos-Townsend (1984) equation gave better results for apparent shear stress at junction region of floodplain and main channel in a compound channel.

Shiono and Knight (1988, 1991) studied and discussed the flow of water in straight open channels with different cross section. an analytical model for predicting depth averaged velocity and boundary shear stress for trapezoidal channels was derived and then for any shape an analytical model was developed by discretizing the channel boundary in to linear elements. For this they developed the mathematical equations influencing the shear layer between a main channel and its floodplains based on a dimensionless eddy viscosity and secondary current model. They considered three dimensionless parameters such as turbulence, lateral shear turbulence and secondary flows for their model and their effects of bed-generated were studied.

Ackers (1992, 1993) developed a design formula for straight compound channels by taking into account the effects of flow interaction between floodplain and main channel. He proposed a parameter which keeps the consistency between the hydraulic condition of floodplain and main channel zones. The formulations were tested in previously published experimental data set.

Myers and Lyness (1997) reported a study on the behavior of two discharge ratios, namely total to bank full discharge and main channel to floodplain discharge in compound channels for smooth and homogeneously roughened channels of various scales. It showed that the total to bank full discharge ratio was independent of bed slope and scale and was fully dependent upon cross section geometry. The other ratio was also found to be independent of bed slope and scale but was affected by the lateral bed slope of the flood plain. The coefficients and exponents in the equations relating to flow ratios to flow depths were being evaluated.

Pang (1998) undertook experiments on the straight compound channel under in flow and over bank flow conditions. It was observed that the sharing of discharge between the main channel and floodplain was in according to the flow energy loss, which can be expressed in the form of coefficient of flow resistance. In general, Manning's roughness coefficient n not only indicated the characteristics of channel roughness, but also influenced the loss of energy in the flow. Depending upon the variation in water depth manning’s n also varies for same surface roughness in a compound channel. Though the surface of the main channel and flood plain are same but as the depth of water in both main channel as well as in the flood plain are different so manning’s n value is also different for the section.

Bousmar and Zech (1999) proposed a 1D model known as the exchange-discharge model (EDM) which is suitable for prediction of stage-discharge relationship as well as simulations of practical water-surface profile. The momentum transfer is calculated multiplying the velocity gradient at the interface with the mass discharge exchanged through this interface generated from the effect turbulence. They ended up with a conclusion that the model predicts the stage-discharge for both the experimental as well as natural river data. their models is being used for flow prediction in a prototype River named as Sambre in Belgium and it works in a good manner.

Ervine *et. al.* (2000) proposed a practical method for predicting depth-averaged velocity and boundary shear stress in straight over bank flows. An analytical solution to the depth-integrated turbulent form of the RANS equation was proposed, in which lateral shear and secondary flows in addition to bed friction were considered. The obtained analytical solution is applied to number of channels at both field and laboratory, and the results were compared with SKM and the lateral distribution method (LDM).

Patra and Kar (2000) presented the test results related to the boundary shear stress, flow velocity, shear force and discharge characteristics of a compound channel comprises of a rectangular main channel and one or two floodplains present to its adjacent sides. Five dimensionless channel variables were used to form equations which give the total shear force percentage carried by the adjacent floodplains. A study was carried out on a set of smooth and rough sections with aspect ratio varying from 2 to 5. Apparent shear forces on the anticipated vertical, diagonal, and horizontal interface plains were found to be dissimilar. At low depths of flow apparent shear force varies from zero and with increase in depth over floodplain the sign changes. They suggested a variable-inclined interface where apparent shear force was considered to be zero. Empirical equations were proposed for predicting of discharge carried by both the main channel and floodplain.

Thrnton *et. al.* (2000) carried out eight numbers of experiments in a physical model of a compound channel to estimate the apparent shear stress at the junction region of main channel and the flood plain for both vegetated and un-vegetated floodplain flow condition. Data are being analyzed by using a method based on turbulence for calculating the apparent shear stress as a

function of variation in velocities in the compound channel. They gave an empirical relationship for the calculation of the apparent shear stress at the main channel floodplain junction region which was dependent upon the bed shear stress, depth averaged velocity, depth of flow, and the blockage developed due to vegetation present over the floodplain.

Liu and James (2000) predicted discharge in a meandering compound channel using artificial neural networks. This tool is having a flexible structure, capable of establishing a non-linear relationship between the input and output data. They have showed that between predicted and the measured discharge there is up to 15% inconsistency exist.

Myers *et. al.* (2001) used FCF data and presented the results for both fixed and mobile main channel boundaries together with two types of flood plain roughness compound channel. On the basis of mathematical modeling, the velocity and discharge ratio relationships was being proposed which was useful for discharge estimation in over-bank flows and their results were compared with the data of a prototype natural compound river channel. Two different graphs were plotted, one was between the ratios of main channel to floodplain average velocities and discharge obtained by using laboratory data and second was between ratios of main channel to floodplain average velocities and discharge obtained by using the natural river data.it was observed that first graph showed the logarithmic relationship whereas the second graph gave the linear relationship. The Divided channel method overestimated the discharge in all cases and showed good accuracy when it is applied to laboratory data with smooth floodplains, but significant errors of 35% for rough floodplain data, and up to 27% for river data had been found in this method. Compound discharge for all cases for low flow depths was being underestimated by single channel method (SCM), but for the smooth boundary laboratory data as well as the river data it became more accurate at larger depths.

Atabay and Knight (2002) established some stage discharge relationship for symmetrical compound channel section using the experimental results of the Flood Channel Facility (FCF). The effect of flood plain width and main channel aspect ratio to the stage discharge relationship was being examined. Simple empirical relationships between stage and total discharge, and stage and zonal discharge for uniform roughness and varying flood plain width ratio were being derived. They verified broad effects on the stage –discharge relationship due to flood plain width ratio.

Ozbek and Cebe (2003) preferred to use experimental results of the FCF at Wallingford, for calculating apparent shear stress and also for estimating discharge in symmetrical compound channels with varying floodplain widths. Three vertical, horizontal, and diagonal interface planes between the main channel and the floodplain subsections were considered for calculation of apparent shear stresses across the interfaces. The discharge values for the whole cross-section as well as for each sub-section of the channel were computed. It was shown that the performance of these computation methods depend on their ability to predict apparent shear stress accurately. They had shown that as compare to vertical division method, the diagonal and horizontal division methods gave better results.

Weber and Menéndez (2003) presented the scope of 2D-Horizontal and 1D-Lateral models for lateral velocity distribution is addressed, and their relative and absolute performances are tested by making comparisons between their predictions, on the one side, and experimental and field velocity data, on the other side. The models considered are: the Divided Channel Method (DCM), the Lateral Distribution Method (LDM) and a 2D Horizontal hydrodynamic finite-element model (RMA2).

Tominaga and Knight (2004) carried out numerical simulation for better understanding of secondary flow effect on the lateral momentum transfer by linking a standard k-ε model with a given secondary flow. The typical linear distribution of momentum transfer term was being reproduced due to the simulation. The simulated secondary flow was responsible for decrease of bed shear in main channel and increase of bad shear in flood plain shear.

Jin *et. al.* (2004) developed a semi analytical model to predict boundary shear distribution in straight open channels. A simplified stream wise vorticity equation was being used for developing the model, where the secondary Reynolds stress terms were involved. By applying the momentum transfer model, the model incorporated the shear stresses. For computing the effect of the channel boundary on shear stresses an empirical model was generated. To calculate boundary shear distribution trapezoidal open channels the final equation was used the model predictions were giving good agreement with experimental data.

Prooijen *et. al.* (2005) presented the effect of momentum transfer on prediction of discharge. This process results in the so-called “kinematic effect,” a lowering of the total discharge capacity

of a compound channel compared to the case where the channel and the floodplain are considered separately. The mechanisms responsible for the momentum exchange are considered. The transverse shear stress in the mixing region is modeled using a newly developed effective eddy viscosity concept, that contains: (1)the effects of horizontal coherent structures moving on an uneven bottom, taking compression and stretching of the vortices into account and (2) the effects of the three-dimensional bottom turbulence. The model gives a good prediction of the transverse profiles of the stream wise velocity and the transverse shear stress of the flood channel facility experiments.

Guo and Julien (2005) proposed an analytical solution for finding out the values of bed shear stress in an open channel for constant eddy viscosity without secondary currents. After solving the continuity and momentum equations the average bed and sidewall shear stresses can be determined in smooth rectangular open-channel flows. When the width–depth ratio became large, it slightly overestimated the average bed shear stress measurements and underestimated the average sidewall shear stress by 17% when it was compared with experimental data set. Therefore they generated a new formula after introducing two empirical correction factors. The second formula gave good agreement with experimental measurements over a wide range of width–depth ratios, with an average relative error less than 6%.

Othman and Valentine (2006) studied the uniform flow in compound channels in terms of a numerical model, called the NKE model. The model uses the three dimensional Navier-Stokes equations in conjunction with the non-linear *k*-ε turbulence model. The latter is used for the calculation of the Reynolds stress components responsible for the generation of the secondary currents. This model is based on the SIMPLE technique, and computes the six parameters *U*, *V*, *W*, *P*, k, and ε using wall functions on a Cartesian grid. The NKE model was used to simulate the compound open channel flows of the UK Flood Channel Facility run 080301 (*Shiono* and *Knight*, 1989). The Reynolds Stress Model (RSM) of FLUENT was also used as a comparison. The results obtained have shown that the NKE and RSM models can reasonably predict the primary mean velocity and secondary currents.

Proust *et. al.* (2006) had done the experimental investigation on the flow in an asymmetrically compound channel transition reach with an abrupt floodplain contraction (mean angle 22°). To know whether the models developed for straight and slightly converging channels are equally

valid to their geometry they compared three 1D models and one 2D simulation to their experimental data. It was shown that the due to lateral mass transfer, error on the level of water is moderated, but it results in increase the error of discharge distribution in the sub-areas. They recommended for further work for better understanding of the phenomena of severe mass transfers in non-prismatic compound channels.

Knight *et. al.* (2007) offers a new approach to calculating the lateral distributions of depth-averaged velocity and boundary shear stress for flows in straight prismatic channels. It accounts for bed shear, lateral shear, and secondary flow effects via 3 co-efficient (f ,λ and Γ)thus incorporating some key 3D flow feature into a lateral distribution model for stream wise motion. The SKM incorporates the effects of secondary flows by specifying an appropriate value for the _ parameter depending on the sense of direction of the secondary flows, commensurate with the derivative of the term $H(UV)_d$.

Huthoff *et. al.* (2008) proposed a new method to calculate flow in compound channels. The interacting divided channel method (IDCM), based on a new parametrization of the interface stress between adjacent flow compartments, at the junction of the main channel and floodplain of a two-stage channel. This expression is motivated by scaling arguments and allows for a simple analytical solution of the average flow velocities in different compartments. Good agreement is found between the analytical model results and previously published experimental data.

Khatua (2008) reported a study on flow of energy where it is stated that distribution of energy an important aspect needs attention adequately. From the variation of the resistance factors Manning's n, Chezy's C, and Darcy –Weisbach's f it is come to know that the energy distribution is responsible for these variations. Channel resistance coefficients and the Stage-discharge relationship ranging from in-bank to the over-bank flow were found out. It is stated that due to interaction mechanism as well as with sinuosity flow distribution becomes more complicated.

Mamak (2008) carried out a comparison study on different conveyance method for compound channels. Here he has investigated on three 1D models named as COHM (Acker), EDM and SKM for computing the discharge capacity of the compound channel. These methods are being validated by using the previously published experimental data. It is shown that EDM is giving

more accurate result than other 1D models considered here even it is giving less error than 2D SKM model for the data analyzed here.

Khatua (2008) presented equations to predict the section discharge carried by straight channels. The laboratory test results related to the boundary shear stress, shear force, and discharge characteristics of compound straight river sections composed of a rectangular main channel and floodplains are presented. Dimensionless parameters are used to form equations representing the total shear force percentage carried by floodplains. He proposed a curved interface for understanding the important flow interaction for which apparent shear force is calculated as zero. The equations give good agreement with the experimental discharge data. Using the proposed area method, the error between the measured and calculated discharges for the meandering compound sections is found to be the minimum when compared with that using other interfaces.

Seckin *et. al.* (2008) reviewed and applied two-dimensional (2-D) formulae for estimating discharge capacity of straight compound channels for overbank flows in straight fixed and mobile bed compound channels. The 2D formulae were generally influenced by bed shear, lateral shear and secondary flow via three coefficients *f*, λ and Γ so by using these variables discharge prediction was done. But then they ignored the secondary current in the new developed 2D formula. Results of both formulae were compared with the experimental result and they found 2-D formulae almost give practically the same results for the same data when the secondary flow term is ignored.

Tang & Knight (2009) propose a method for predicting the depth-averaged velocity in compound channels with partially vegetated floodplains, based on an analytical solution to the depth-integrated Reynolds-Averaged Navier-Stokes equation with a term included to account for the effects of vegetation. The vegetation is modelled via an additional term in the momentum equation to account for the additional drag force. The method includes the effects of bed friction, drag force, lateral turbulence and secondary flows, via four coefficients *f*, *C*D, λ & Γ respectively.

Khatua (2009) conducted experiments to measure the boundary shear around the wetted perimeter of a two-stage compound channel and to quantify the momentum transfer in terms of apparent shear stress along the assumed interfaces originating at the junction of main channel

and flood plain of the compound channel, which is helpful for deciding the appropriate interface plains for prediction of accurate stage-discharge relationship for a compound channel of all geometry.

Zahiri and Dehghani (2009) estimated flow discharge in compound channels by taking nearly 400 laboratory and field data sets of geometry and flow rating curves from 30 different straight compound sections and also by using artificial neural networks (ANNs). For predicting discharge through ANN he used 13 dimensionless input parameters such as relative depth, relative roughness, relative width, aspect ratio, bed slope, main channel side slopes, flood plains side slopes and berm inclination and flow discharge as one output variable. The ANN results were compared with the results of traditional method (DCM) and it was found that ANN results shows more accurate value than that of DCM.

Tang, Sterling & Knight (2010) presents a method for predicting the depth-averaged velocity distribution in compound channels with either emergent or submerged vegetation. A general analytical solution to the depth integrated Reynolds-Averaged Navier-Stokes (RANS) equation has been given.. the effects of bed friction, drag force, lateral turbulence and secondary flows, via four coefficients f, CD, λ & Γ respectively are included in this method. The analytical solution gives better predictions of lateral velocity distribution when compared with the experimental data of vegetated channels with submerged vegetation and with the experimental data of emergent vegetation. By predicting the depth averaged velocity and bed shear stress distributions, flood conveyance and sediment transport in channels with vegetation can be calculated.

Knight, Tang and Sterling (2010) proposed a model which is based on the Shiono & Knight method (SKM) of analysis that takes into account certain 3-D flow features that are often present in many types of watercourse during either in-bank or overbank flow conditions. He demonstrates the use of this model to predict lateral distributions of depth-averaged velocity and boundary shear stress, stage-discharge relationships, as well as indicating how to deal with some vegetation, sediment and ecological issues. Here they suggested the use of the software named as conveyance estimation system which is largely based on the SKM, through a number of case studies.

Beaman (2010) undertook numerical modeling for both inbank and overbank flows regarding the channels under various depth and width ratio values. The values of three calibration constants f, λ & Γ of SKM (1988) model were derived through large eddy simulation technique for application in the numerical model named as Conveyance Estimation System (CES). This model has been employed by the Environment Agency (EA) for England and Wales for estimation of river conveyance across Europe.

Absi (2011) presented an ordinary differential equation for velocity distribution in open channel flows based on an analytical solution of the Reynolds-Averaged Navier-Stokes equations and a log-wake modified distribution of eddy viscosity. The proposed equation helps in predicting the maximum velocity below the free surface. Here he presented two different degrees of approximations one is semi-analytical solution of the proposed ordinary differential equation, i.e. the full dip-modified-log-wake law and second one is simple dip-modified-log-wake law. Numerical solution of the ordinary differential equation and velocity profiles of the two laws are compared with the previously published experimental data. In this study it is shown that the dip correction is not sufficient for an accurate prediction as it requires larger value of the dip correction parameter. The simple dip-modified-log-wake law shows reasonable agreement and seems to be an interesting tool of intermediate accuracy. The full dip-modified-log-wake law, with a parameter for dip-correction obtained from an estimation of dip positions, provides accurate velocity profiles.

Khatua and Patra (2012) carried out a series of laboratory tests for both smooth and rigid compound channels and a mathematical equation was developed using dimension analysis for evaluating the roughness coefficients. Velocity, hydraulic radius, viscosity, gravitational acceleration, bed slope, sinuosity, and aspect ratio were considered as the important variables which were affecting the stage-discharge relationship in a compound channel.

Khatua *et. al.* (2012) gave a modified expression to predict the boundary shear distribution in compound channels and it is found to provide significant improved results. The practical method to predict the stage-discharge relationship uses the one-dimensional (1D) approach by taking due care of the momentum transfer. The proposed approach is tested for its validity using available experimental data. Error statistics including standard error and coefficient of determination (R^2) are applied to ascertain the effectiveness of the model.

Fernandes, Leal and Cardoso (2012) stated that the momentum transfer generates a complex 3D flow due to velocity difference between the main channel and the flood plain flows at extreme flood condition which makes the discharge prediction difficult. They took comparison study on prediction of discharge by using several models and their accuracy was measured. They took four different flow conditions corresponding to uniform flows for relative depths of 0.15 and 0.3 for smooth and rough floodplains. The effect of relative depth and roughness of the flood plain evaluated and the flow characteristics were shown. Their study included the longitudinal velocity distribution in lateral direction and Reynolds stresses in horizontal plane.

Yang et al (2014) proposed a new method for the discharge distribution and estimating the stage-discharge relationship in a compound channels by considering the flow interaction between the upper and lower main channel and that between the upper main channel and its adjoining floodplain data from the laboratory channels and three natural rivers were being tested and it was shown that the proposed method made a good agreement with the experimental as well as with the field data. The computed results showed that apart from predicting discharge distribution of flood plain and the whole main channel the presented method was well capable of predicting the discharge distributions in the inbank flow condition.

EXPERIMENTAL SETUP AND PROCEDURE

3.1.1. Introduction

Generally, experimentation on open channel models is bit difficult in a laboratory in practical point of view if the scaling of the prototype is properly done and for this case only a model should be designed according to the prototype so that the hydraulic characteristics can be studied in a laboratory and the different improvement techniques can be implemented. Discharge means rate of flow per unit duration of time and measurement of discharge in a channel is the most important work in river engineering study. Prediction of discharge is required to establish the stage discharge relationship which is helpful for river engineers who are working on sediment transport, bank protection, erosion of bed and flood forecasting. To predict the discharge there are various methods being developed by the researchers from last decades. But all the methods do not give satisfactory results. Some of the methods overestimate the discharge and some of them underestimate it, but still with the development of technology there are new standard methods are being developed with give better result and apart from discharge estimation these methods are truly useful for velocity measurement and boundary shear stress calculation for that channel for a given flow condition. To predict Stage-Discharge relationships in straight channel is easier but till date no hydraulic model is good enough which can give accurate discharge value. So in our present work a comparison study is being done where discharge being calculated using different numerical as well as computational methods and the obtained results are compared with the experimental results by conducting experiment on a straight rectangular prismatic channel in hydraulic engineering laboratory, NIT Rourkela. So for comparison study a straight open channel model has been constructed and flow conditions are studied by varying the flow depth. According the requirement the construction of the channel is done as follows.

3.1.2. Design and construction of channel

For carrying out study in straight channels, experimental setup was built in Fluid mechanics and Hydraulics Laboratory of NIT, Rourkela. Experiments was conducted in prismatic compound channels made of concrete having dimension as 15m×.95m×0.55m (Bandita Channel).The width ratio of the channel is $\alpha>1.8$ and the aspect ratio is $\delta>5$. The channel is made up of cement concrete. The main channel was rectangular in shape having bottom width 0.5m,

depth 0.1m with a vertical side slope, and the flood plains were having bottom width 0.2m and also having vertical side walls (Fig shows the overall view of the channel.) Fig.3.1 shows the schematic diagram of experimental setup and fig 3.2 and fig 3.3 represent the dimensions of channel with test section respectively). By the help of centrifugal pump (15Hp) the water is supplied to the flume from an underground sump via an overhead tank. This water is re circulated through the downstream volumetric tank fitted with closure valves for calibration purpose. Water entered the channel through bell mouth section via an upstream rectangular notch specifically built to measure discharge in such a wide laboratory channel. At the downstream end an adjustable tail gate was provided to control the flow depth and maintain a uniform flow in the channel. . A movable bridge was provided across the flume for both span wise and stream wise movements over the channel area so that each location on the plan of compound channel could be accessed for taking measurements. The broad parameters of this channel are aspect ratio of main channel (δ), width ratio (α). In all the experimental channels, the flow has been maintained uniform i.e. the water surface is parallel to bed of channel.

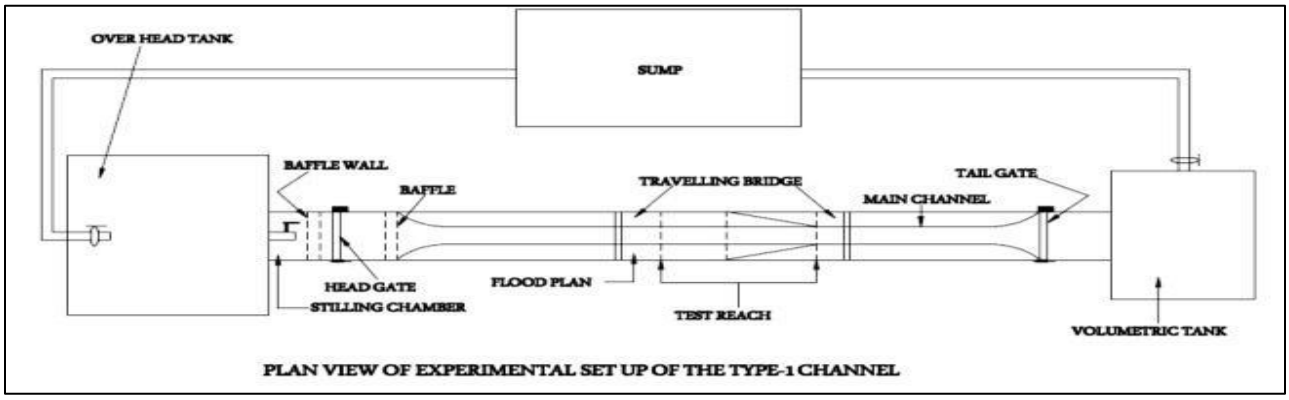

Fig.3.1.1 Schematic diagram of Experimental compound channels with setup

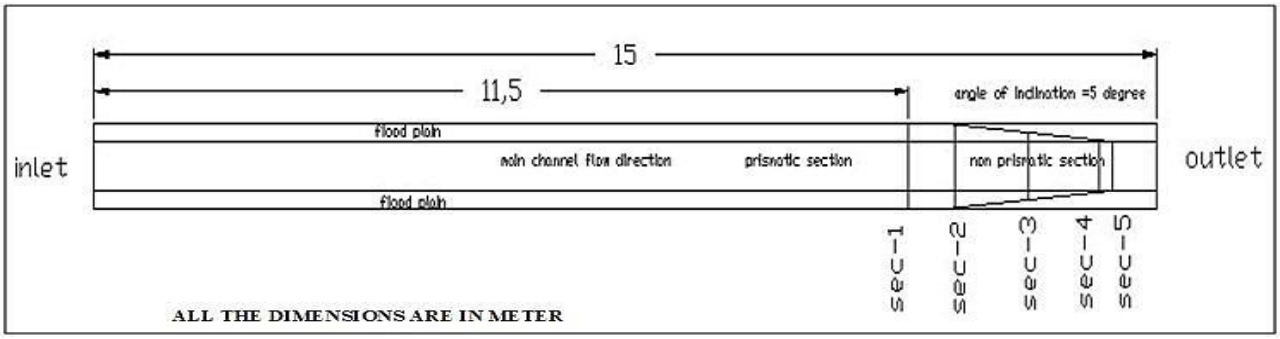

Fig.3.1.2 Longitudinal dimension of the compound channel

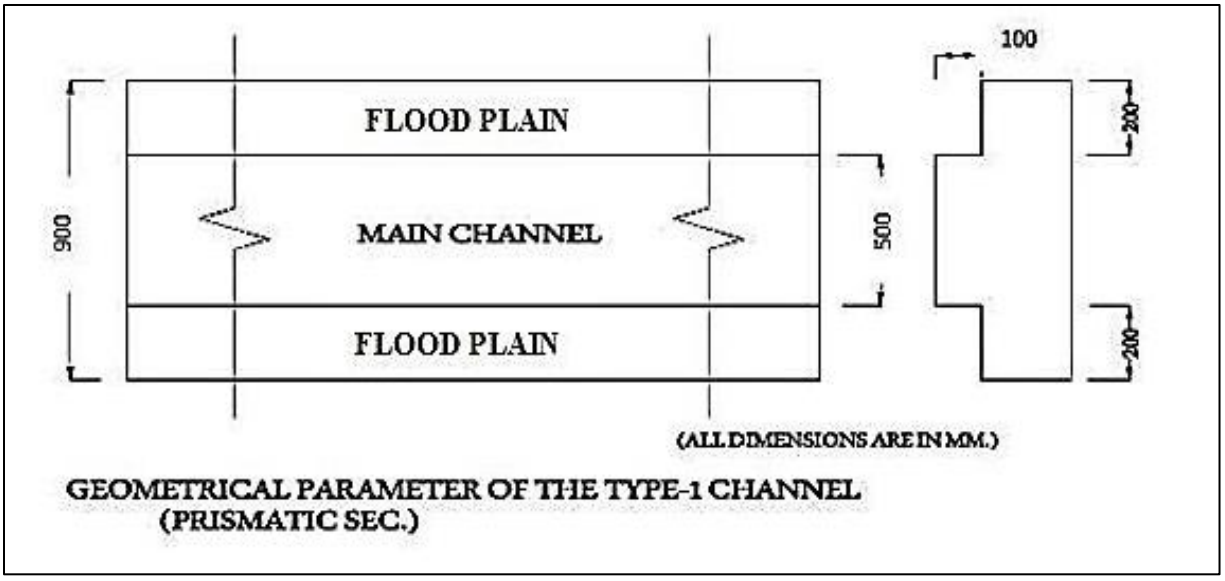

Fig.3.1.3. Top view and Cross sectional dimensions of the compound channel.

3.1.3. Apparatus & equipment used

For this study measuring devices such as a pointer gauge having least count of 0.1 mm, rectangular notch, one pitot tubes having 4.6 mm external diameter and one manometer were used in the experiments. These measuring devices are used to measure longitudinal velocity in the direction of flow within the channels. In the experiments structures like baffle walls, travelling bridge, sump, tail gate, volumetric tank, overhead tank arrangement, water supply devices, two parallel pumps etc. are used. The proper arrangement of the measuring equipment and the devices were done to carry out experiments in the channels.

(i) Overhead tank

(ii) Baffle wall at the Inlet of the channel

(iii) Point gauge and Pitot tube measuring velocity

(iv) Series of manometer used for measuring pressure

Fig.3.1.4 (i to iv): Apparatus used in experimentation in the rectangular compound channel

3.1.4. Experimental procedure

All the observations are recorded at section 1 of the compound channel. Point velocities were measured along verticals spread across the main channel as well as flood plain so as to cover the width of entire cross section. Also at a number of horizontal layers in each vertical for both main channel as well as flood plain, point velocities were measured. Measurements were thus taken from left edge point to the right edge of the main channel as well as for the flood plain bed and side vertical walls. The lateral spacing of grid points over which measurements were taken was kept 5cm inside the main channel and also Pitot tube is moved from the bottom of the channel to upwards by 0.2H, 0.4H, 0.6H, 0.8H (H=total depth of flow of water)(Fig.3.5 shows the grid diagram used for experiments). Velocity measurements are taken by Pitot static tube (outside diameter 4.77mm) and two piezometers fitted inside a transparent fiber block fixed to a wooden board and hung vertically at the edge of flume. The ends of which were open to atmosphere at one end and the other end connected to total pressure hole and static hole of Pitot tube by long transparent PVC tubes. Before taking the readings the Pitot tube along with the long tubes measuring about 5m were to be properly immersed in water and caution was exercised for complete expulsion of any air bubble present inside the Pitot tube or the PVC tube. Even the presence of a small air bubble inside the static limb or total pressure limb could give erroneous

readings in piezometers used for recording the pressure. Steady uniform discharge was maintained in each run of the experiment and the differences in pressure were measured at each allocated points.

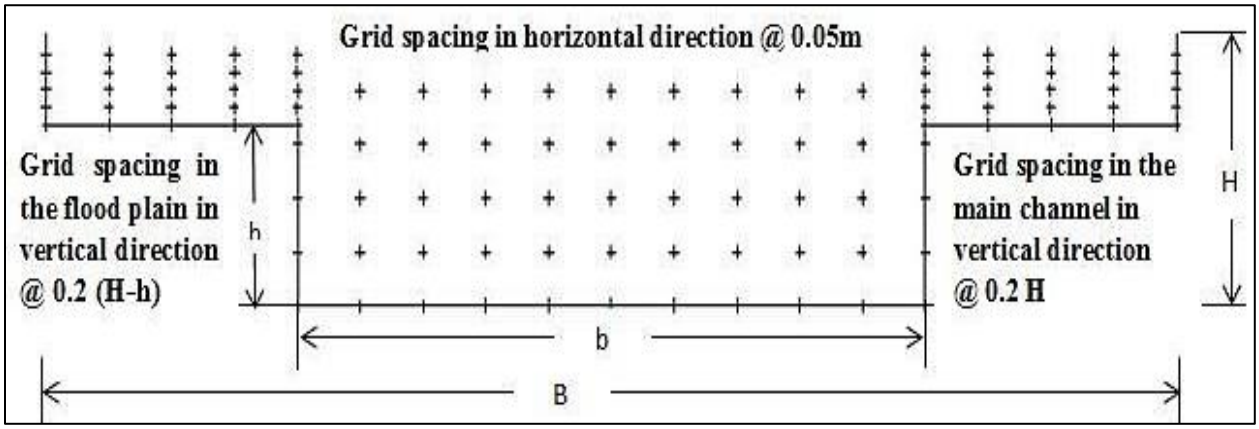

Fig.3.1.5: Typical grid showing the arrangement of velocity measurement points along horizontal and in vertical direction at the test section for the rectangular compound channel.

3.1.5. Experimental channels

The main channel is constructed of 500 mm wide at bottom, having a full bank level of 100 mm with a vertical wall. Two symmetrical flood plains are constructed of 200mm width with side vertical walls along both side of the main channel. Channel has the width ratio of 1.8, and having aspect ratio of 5. For better information the details of geometrical parameters for the experimental channels are tabulated below (Table 3.1) and also fig.3.6 shows details overview of compound channels.

Fig 3.1.6: Compound channel inside the concrete flume with measuring equipment.

Table 3.1.1: Details of Geometrical parameters of the experimental runs

Sl No	Item description	Present Experimental Channels
1	Channel Type	Straight compound channel
2	Flume size	15m×.95m×0.55m
3	Geometry of Main channel section	Rectangular with vertical side wall
4	Geometry of Flood plain section	Rectangular with vertical side wall
5	Main channel width (*b*)	0.5m
6	Flood plain width	0.2m
7	Top width of the channel along with the flood plain (*B*)	0.9m
8	Bed Slope of the channel	0.001
8	Bank full depth of channel (*h*)	0.1m

3.1.6. Measurement of bed slope

There are several methods exists for the measuring the bed slope of the flume, which are used depending upon the practical conditions and interest of the researcher. In the present work the bed slope is measured by the help of water level piezometric tube. So at first with reference to the bed of the channel the water level in piezometric tube was maintained at the upstream side as well as in the downstream side of the compound channel at a distance of 15m. Piezometric tube was properly leveled at both the sides. Vertical distance between the water level and the bottom of the bed excluding the thickness of the Perspex sheet is measured at both upstream as well as in the downstream referred points. The channel bed slope was calculated by simply dividing difference between the leveled heights measured at the two ends with the distance between the two referred points of the given channel (15m). For getting better and accurate result this procedure was repeated for three times and then by averaging slope of the channel was found to be 0.001.

3.1.7. Measurement of depth of flow and discharge

Pointer gauge is being used above the bed of the channel for the measurement of depth of flow for all the series of experiments. A vernier caliper is fitted with the point gauge with least count of 0.1 mm and the total measuring device is fitted with the movable bridge and it was operated manually. For measuring the discharge in the channel, the construction of rectangular notch is provided at the upstream side. At the downstream side of channel a volumetric tank was constructed to receive the incoming water flowing through the channels. For each run the discharge '*Qactual*' is calculated as the equation given below.

$$Q_{actual=}C_d \frac{2}{3} L\sqrt{2g}\ H_n^{2/3} \qquad (3.1.1)$$

Where, Q_{actual} is the actual discharge, C_d is known as coefficient of discharge obtained from notch calibration, L is the length of the notch, Hn is the height of water flowing above the notch and g is acceleration due to gravity.

3.1.8. Measurement of longitudinal velocity

Generally energy loss occurs in the open channel when water flows from one point to another point. The total energy depends upon kinetic energy, potential energy and pressure energy. Among all kinetic energy affects the total energy more especially in case of open channel flow condition. Kinetic energy is the ratio of square of the velocity to twice of acceleration due to gravity. So it is required to find out the mean velocity of the fluid flowing in the channel. In the present study, by the help of Pitot tube and manometer, total pressure head as well as static pressure head readings were taken and their differences were calculated. From these observed data corresponding velocities at each point within the channel were calculated. Normally Pitot tube was placed with in the channel in the direction of flow and then allowed to move along a plane parallel to the bed to get the longitudinal velocity with respect to bed along lateral direction. At required interval pitot tube was placed and kept it their until the head difference obtained in manometer remained constant. To measure the magnitude of point velocity vector a simple formula was being used i.e. $v=2gh$, where g is the acceleration due to gravity. Here the tube coefficient is taken as unit and the error due to turbulence considered was being neglected at the time of measuring velocity. Velocities were being calculated in main channel as well as in flood plains at the given grid points at an interval of 0.05m in horizontal direction. Apart from this velocities were measured in the vertical direction at an interval of 0.2H, 0.4H, 0.6H, 0.8H for

main channel and *0.2(H-h), 0.4(H-h), 0.6(H-h), 0.8(H-h)* for flood plain depending upon the depth of flow in the compound channel. Each experimental runs of the channel are conducted by maintaining the water surface slope parallel to the bed slope of the channel to achieve the steady and uniform flow conditions.

3.1.9. Measurement of boundary shear stress

Shear stress is the stress develops between the two layers of water at flowing condition. Boundary shear stress is the stress that is developed between the water flowing in the channel and its bed as well as wall of the channel. Generally it is denoted by the symbol τ. Boundary shear develops due to resistance offered by the channel upon the fluid flowing through the channel. Due to this shears stress there is a reduction in velocity occurs. So it's a parameter which is required to find out. So for finding out the boundary shear stress there are few formula existing. Patel's formula (1965) is most common formula which is being used for finding out the boundary shear stress. There are three equations are proposed by patel's to find out the shear stress depending upon the range of the Reynolds number.

$$y^* = 0.5x^* + 0.037 \quad (3.1.2)$$

When $y^*<1.5$, $u_\tau d/2\nu < 5.6$

$$y^* = 0.8287 - .1381x^* + 0.1437x^{*2} - 0.0060x^{*3} \quad (3.1.3)$$

When $1.5< y^*<3.5$, $5.6 < u_\tau d/2\nu < 55$

$$x^* = y^* + 2\, log_{10}(1.95y^* + 4.10) \quad (3.1.4)$$

When $3.5< y^*<5.3$, $55 < u_\tau d/2\nu < 800$

Where $x^* = log_{10}(\frac{\Delta p d^2}{4\rho\nu^2})$ and $y^* = log_{10}(\frac{\tau_w d^2}{4\rho\nu^2})$

Here τ_w is the wall shear stress, d is the diameter of the pitot tube, ρ is the density of water, ν is the kinematic viscosity of water at standard temperature which is equal to 0.801×10^{-6}, Δp is the pressure difference between the total pressure and the static pressure at the wall which is measured by the pitot tube. So by using pitot tube boundary shear stress can be calculated along

the cross section as well as wall of the channel at different point if the pressure difference of that point is known.

Apart from this the shear stress at each point of the channel can also be calculated by using depth averaged velocity or mean velocity of the channel if the co-efficient friction of the fluid is known. The equation for finding shear stress is given below.

$$\tau_w = \frac{f\rho U_d^2}{8} \tag{3.1.6}$$

Where

u_d and f are mean velocity and co-efficient of friction of the channel respectively.

DESCRIPTION OF DISCHARGE PREDICTION APPROACHES

3.2.1. Introduction

During floods, part of the river discharge is carried by the main channel and the rest is carried by the adjacent flood plains. Once water in the river overtops the banks, the cross sectional geometry of flow goes on changing. The channel section becomes compound and the flow structure for such section is affected by large shear layers generated by the difference in velocities of water in the main channel and the floodplain due to the transfer of momentum between them. In a compound channel formation of vortices at the junction of main channel and flood plain was first shown by Sellin [1964] and Zheleznvakov [1965]. Wormleaton *et. al.* (1982) have stated that the total draging force on the main channel flow due to floodplain flow at the interfaces is equal to the accelerating force on the flood plain flow due to the main channel flow due to which transfer of momentum occurs. At lower depths of flow over the floodplain, momentum transfer takes place from the main channel to the floodplain resulting in decrement of the main channel velocity and discharge, while its floodplain components are being increased and at higher depths of flow over the floodplains the process of momentum transfer is reversed, i.e. the momentum is supplied to the main channel from the floodplain and this momentum transfer makes the discharge prediction difficult. The effect of flow interaction between the floodplain and main channel for various depths of flow over floodplain should adequately take care while calculating discharge in the compound channel. There are various traditional methods through which discharge can be predicted. Patra (1999), and Patra and Kar (2000) proposed a variable interface plane of separation of compound channel which nullify the momentum transfer for a better estimate of discharge in straight compound river sections. Ackers (1992) proposed a method by making some correction to the DCM named as coherence method (COHM). Huthoff *et. al.* (2008) parameterized the interface stress in terms of velocity of the main channel and floodplains. Later Khatua *et.al* (2012) quantified momentum transfer in terms of interface length which makes discharge prediction more accurate. Apart from these one dimensional mathematical models, there is some 1D software such as HEC-RAS, ANN, MIKE 11, and CES which also do better discharge prediction in a compound channel.

The traditional discharge prediction models such as SCM, DCM fail to give accurate discharge as they don't consider the effect of momentum transfer. Therefore some new models are developed which does discharge prediction more accurately by considering the effect of momentum transfer. This chapter includes discharge computation by numerical models such as SCM, DCM, IDCM, MDCM, SKM as well as computational methods such as CES and ANN.

3.2.2. Numerical methods for computation of discharge

3.2.2.1. Single Channel Method:-

It treats the channel cross-section as a whole channel without division to subsections. This method usually fails to give a good estimate of the stage-discharge relationship, as it over estimates the discharge.

$$Q = \frac{1}{n} * R^{2/3} S_o^{1/2} \tag{3.2.1}$$

Where *Q*= discharge

R=Hydraulic Radius

S_o=Bed slope of the channel

3.2.2.2. Divide Channel Method:-

This classical method employs division of the compound channel to two subsections i.e. the main channel (bank full) and floodplains (berms).The conveyance is calculated for each sub sections considering the interfaces. Again, this method is modified into a few versions distinguishing each other by the way how they consider verticals dividing the compound channel into sub-sections. This includes horizontal interface, vertical interface, diagonal interface, curved interface, variable interface (Fig. 3.2.1). However vertical interface and diagonal interface are the two methods which are commonly used. Discharge for each sub-section can be calculated by using the Eq.(3.2.1) given below.

$$Q = \sqrt{S_o}\left[\frac{1}{n_{mc}} A_{mc}^{\frac{5}{3}} {P_{mc}}^{-\frac{2}{3}} + \frac{1}{n_{fp}} A_{fp}^{\frac{5}{3}} {P_{fp}}^{-\frac{2}{3}}\right] \tag{3.2.2}$$

Where *Q* = Discharge through the compound channel, A_{mc} & A_{fp}= Area of the main channel and floodplain respectively, P_{mc} & P_{fp}= perimeter of the main channel and floodplain respectively, S_0= Bed slope of the channel, n_{mc} & n_{fp}= manning's co-efficient for main channel and flood plain respectively.

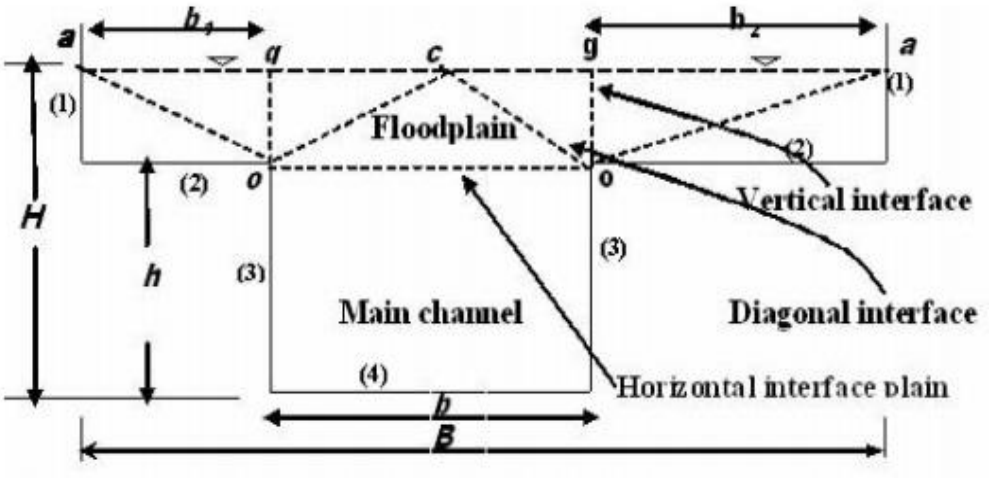

Fig.3.2.1: The vertical, horizontal, diagonal interface of a prismatic compound channel.

3.2.2.2.1. Vertical interface method

In this method the flood banks are separated from the main channel by means of vertical interface (Fig. 3.2.1), but the interface length is not included in the calculation of wetted perimeter of either of the over bank flow or main channel flow as this interface is considered as a surface of zero shear stress and no momentum transfer takes place through junction of main channel and flood plain.

3.2.2.2.2. Diagonal Interface method

In this method a diagonal interface is considered from the top of the main channel bank to the centerline of the water surface. This interface is considered to be the surface of zero shear stress and due to that the length is not included in the calculation of wetted perimeter of the over bank flow and main channel flow. The problem with both the methods is, they overestimate the discharge to some extent.

3.2.2.3. Interacting Divide Channel Method

This method developed by Fredrik Huthoff in the year 2007. Here the channel is divided in to two parts by vertical interfaces and the effect of momentum transfer occurring at the junction of main channel and flood plain is considered in terms of interface stress (τ_{int}).

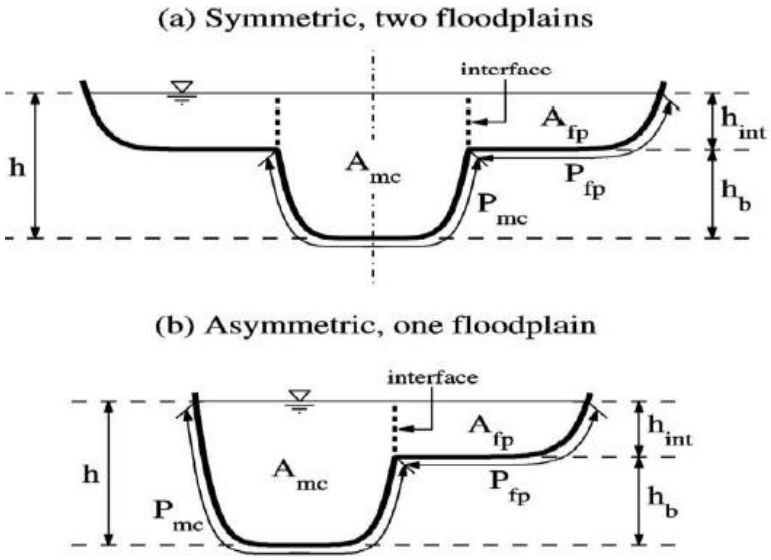

Fig.3.2.2: Cross section of a two-stage channel: (a) symmetric with two identical floodplains. (b) Asymmetric with one side floodplain. (Hutoff 2007)

The following equations have been developed to find out the velocity of the main channel as well as flood plain given as

$$\tau_{int} = \frac{1}{2}\gamma\rho\left(U_{mc}^2 - U_{fp}^2\right) \tag{3.2.3}$$

$$U_{mc}^2 = U_{mc,0}^2 - \frac{\frac{1}{2}\gamma N_{fp}\varepsilon_{mc}\left(U_{mc,0}^2 - U_{fp,0}^2\right)}{1+\frac{1}{2}\gamma\left(N_{fp}\varepsilon_{mc}+\varepsilon_{fp}\right)} \tag{3.2.4}$$

$$U_{fp}^2 = U_{fp,0}^2 + \frac{\frac{1}{2}\gamma\varepsilon_{fp}\left(U_{mc,0}^2 - U_{fp,0}^2\right)}{1+\frac{1}{2}\gamma\left(N_{fp}\varepsilon_{mc}+\varepsilon_{fp}\right)} \tag{3.2.5}$$

Where U_{mc} & U_{fp} are the velocities of main channel and the flood-plain respectively assumed steady and longitudinally uniform, γ= co-efficient of interface. N_{fp}= number of flood plains. $U_{mc,0}$ & $U_{fp,0}$ = velocities of the main channel and flood plain when $\gamma = 0$. τ_{int} = interface stress developed at the interface of the main channel and flood plain. The value of co-efficient of interface

$$\varepsilon_{mc} = \frac{h_{int}}{f_{mc}P_{mc}}, \varepsilon_{fp} = \frac{h_{int}}{f_{fp}P_{fp}} \tag{3.2.6}$$

$$U_{mc,0}^2 = \frac{gR_{mc}S}{f_{mc}}, U_{fp,0}^2 = \frac{gR_{fp}S}{f_{fp}} \tag{3.2.7}$$

$$R_{mc} = \frac{A_{mc}}{P_{mc}}, R_{fp} = \frac{A_{fp}}{P_{fp}} \tag{3.2.8}$$

Where f_{mc}& $f_{mc}$are co-efficient of friction. P_{mc} & P_{fp} are the perimeter of the main channel and flood plain respectively. A_{mc} & A_{fp} are the area for main channel and flood plain respectively.R_{mc} & R_{fp} are the hydraulic radius of main channel and flood plain respectively. h_{int}=difference between the water depth and the full bank level (Fig.3.2.2).

After finding out the velocities, discharge (Q) of the total section can be predicted through inter acting divided channel method by using equation (3.2.9).

$$Q = A_{mc}U_{mc} + N_{fp}A_{fp}U_{fp} \tag{3.2.9}$$

"The interface stress parameterization yields a set of model equations that is linear in the squared velocities, leading to an analytical solution" is a practical property of IDCM. When generalizing IDCM to compound channels with several numbers of compartments, this property is retained. This generalization is required as the interface co-efficient γ has either a universal value or an explicit dependency on the geometry as well as on the roughness of the nearby compartments. Based on the results from their study, Huthoff *et.al* has recommend a constant value of γ =0 .020.

3.2.2.4. Modified Divided Channel Method

This is another method developed by Khatua *et. al* (2012), which quantified the momentum transfer in terms of interface length. According to Wormleaton *et. al.* (1982), the total dragging force on the main channel flow due to floodplain flow at the interfaces is equal to the accelerating force on the floodplain flow due to the main channel flow due to which transfer of momentum occurs which makes the discharge prediction difficult. So for balancing the force, here the main channel boundary shear to be increased and that of the floodplain decreased suitably to account for main channel and floodplain flow interaction. Let X_{mc}= the interface length for inclusion in the main channel wetted perimeter and X_{fp}= the length of interface to be subtracted from the wetted perimeter of the floodplain termed as interaction length. So according to this method, the value of X_{mc}, X_{fp} are found out from Equation (3.2.10) and Equation (3.2.11).

$$X_{mc} = \frac{100P_{mc}}{(100-\%S_{fp})[1+(\alpha-1)\beta]} - P_{mc} \tag{3.2.10}$$

$$X_{fp} = P_{fp} - \frac{100(\alpha-1)\beta}{(\%S_{fp})[1+(\alpha-1)\beta]}P_{fp} \tag{3.2.11}$$

Where α = width ratio = *B/b*; β = relative depth = $\frac{H-h}{H}$, b = width of main channel bottom; B = total width of compound channel; h = bank full depth; and H = total depth of flow. $\%S_{fp}$= percentage of shear force in the flood plains. Knowing $\%S_{fp}$ and the channel geometry, the interface lengths X_{mc} and X_{fp} are evaluated. Next, the discharges for the main channel and floodplain are calculated using Manning's equation and added together to give total discharge as

$$Q = \sqrt{S_o}\left[\frac{1}{n_{mc}} A_{mc}^{\frac{5}{3}}(P_{mc}+X_{mc})^{-\frac{2}{3}} + \frac{1}{n_{fp}} A_{fp}^{\frac{5}{3}}\left(P_{fp}+X_{fp}\right)^{-\frac{2}{3}}\right] \quad (3.2.12)$$

Where S_o = bed slope of both main channel and floodplain (assumed to be the same in 1D models) and n_{mc}, n_{fp} = manning's co-efficient of main channel and floodplain subsections respectively. For rectangular channel and floodplains having homogeneous roughness (i.e., Manning's *n* value is equal for both the main channel and floodplains). $\%S_{fp}$ is calculated from the equation (3.2.13), developed by Khatua & Patra(2012).

$$\%S_{fp} = 4.105\left[\frac{100\beta(\alpha-1)}{1+\beta(\alpha-1)}\right]^{0.6917} \quad (3.2.13)$$

So by putting the value of %S*fp*, the value of X_{mc} and X_{fp} can be calculated. After finding out the values of interface length the discharge of the straight compound channel can be estimated.

3.2.2.5. Shiono knight Method

The SKM is based on a depth averaged form of Navier-Stokes equation, expressed for steady flow as

$$\rho g S_o H - \rho \frac{f}{8}\sqrt{1+s^2}U_d^2 + \frac{\partial}{\partial y}\left[\rho\lambda H^2\sqrt{\frac{f}{8}}U_d\frac{\partial U_d}{\partial y}\right] = \frac{\partial}{\partial y}\left[H(\rho VU)_d\right] \quad (3.2.14)$$

Where ρ=density, g=acceleration due to gravity, S_o= longitudinal slope, H= depth of water flowing, s= lateral slope, f=co-efficient of friction, U_d=depth averaged velocity in longitudinal direction, V_d=depth averaged velocity in lateral direction, λ= dimensionless eddy viscosity, y= lateral direction co-ordinate.

Here in the equation the 1st left hand side term is gravitational term for a uniform flow, the second term is bed shear stress and the third term is the Reynolds's shear stress and the term which is present in the right hand side is the secondary current. The given equation is dependent upon depth averaged velocity, bed shear stress and Reynolds's stress, but these parameters are influenced by three calibration co-efficient *f, λ, Γ*, which are related to local bed friction, Reynolds's stress and the secondary flow respectively.

Shiono and Knight proposed an analytical solution to find out depth averaged velocity as well as boundary shear stress by considering the effect of secondary current. From their experimental results they conclude that the depth averaged velocity varies linearly in y direction therefore they replaced the right hand side term in the equation by a constant, *Γ*. The derivation (Rezai 2006) is given below.

$$\Gamma = \frac{\partial}{\partial y}[H(\rho UV)_d] \tag{3.2.15}$$

$$\rho g S_o H - \rho \frac{f}{8}\sqrt{1+s^2}U_d^2 + \frac{\partial}{\partial y}\left[\rho \lambda H^2 \sqrt{\frac{f}{8}} U_d \frac{\partial U_d}{\partial y}\right] = \Gamma \tag{3.2.16}$$

For a flatbed region or when there is no lateral slope the above equation (3.2.16) can be written as

$$\rho g S_o H - \rho \frac{f}{8}U_d^2 + \frac{\partial}{\partial y}\left[\rho \lambda H^2 \sqrt{\frac{f}{8}} U_d \frac{\partial U_d}{\partial y}\right] = \Gamma \tag{3.2.17}$$

Here Γ, λ are assumed to be constant in each channel sub section.

$$\left(\boldsymbol{U_d \frac{\partial U_d}{\partial y} = \frac{1}{2}\frac{\partial}{\partial y}U_d^2} \;, \Rightarrow\; \boldsymbol{\frac{\partial}{\partial y}\left(U_d \frac{\partial U_d}{\partial y}\right) = \frac{1}{2}\left(\frac{\partial^2}{\partial y^2}U_d^2\right)}\right)$$

So we can write the equation (3.2.17) in the following form

$$\rho g S_o H - \rho \frac{f}{8}U_d^2 + \left[\frac{\rho \lambda H^2}{2}\sqrt{\frac{f}{8}}\frac{\partial^2 {U_d}^2}{\partial y^2}\right] - \Gamma = 0 \tag{3.2.18}$$

Let $A = \frac{\rho \lambda H^2}{2}\sqrt{\frac{f}{8}}$, $B = \rho \frac{f}{8}$, $C = \rho g S_o H - \Gamma$, $X_d = U_d^2$

So we can rewrite the above equation in terms of A, B, C.

$$A\frac{\partial^2 X_d}{\partial y^2} - BX_d + C = 0 \tag{3.2.19}$$

$\frac{\partial^2 X_d}{\partial y^2} = \frac{B}{A} X_d - \frac{C}{A}$ (Auxiliary equation)

$D^2 - \frac{B}{A} = 0$

$D = \pm\sqrt{\frac{B}{A}}$

$X_d(y) = A_1 e^{\sqrt{\frac{B}{A}}y} + A_1 e^{-\sqrt{\frac{B}{A}}y} + k$ (3.2.20)

$U_d(y) = \left[A_1 e^{\gamma y} + A_1 e^{-\gamma y} + k \quad \right]^{1/2}$ (3.2.21)

Now $\frac{\partial X_d}{\partial y} = \left(\frac{B}{A}\right)^{1/2} A_1 e^{\sqrt{\frac{B}{A}}y} - \left(\frac{B}{A}\right)^{1/2} A_2 e^{-\sqrt{\frac{B}{A}}y}$

$\frac{\partial^2 X_d}{\partial y^2} = \frac{B}{A} A_1 e^{\sqrt{\frac{B}{A}}y} + \frac{B}{A} A_2 e^{-\sqrt{\frac{B}{A}}y}$

Putting the value of $\frac{\partial^2 X_d}{\partial y^2}$ and X_d in equation (3.2.18) we can get

$\Rightarrow A\left(\frac{B}{A} A_1 e^{\sqrt{\frac{B}{A}}y} + \frac{B}{A} A_2 e^{-\sqrt{\frac{B}{A}}y}\right) - B\left(A_1 e^{\sqrt{\frac{B}{A}}y} + A_1 e^{-\sqrt{\frac{B}{A}}y} + k\right) + C = 0$

$\Rightarrow -Bk + C = 0$

$\Rightarrow k = \frac{C}{B}$ (3.2.22)

$C = \rho g S_o H - \Gamma,\ B = \frac{\rho f}{8}$

$\frac{C}{B} = \frac{(\rho g S_o H - \Gamma)}{\left(\frac{\rho f}{8}\right)}$

$\Rightarrow \frac{8\rho g S_o H - 8\Gamma}{\rho f} = \frac{8 g S_o H}{f} - \frac{8\Gamma}{\rho f}$

$\Rightarrow \frac{8 g S_o H}{f}\left[1 - \frac{\Gamma}{\rho g S_o H}\right]$

$K = \frac{8 g S_o H}{f},\ \beta = \frac{\Gamma}{\rho g S_o H}$

Again *(B/A)* can be simplified

$$\frac{B}{A} = \left(\rho \frac{f}{8}\right) * \frac{1}{\left(\frac{\rho \lambda H^2}{2}\sqrt{\frac{f}{8}}\right)}$$

$$\frac{B}{A} = \left(\frac{f}{8}\right)^{1/2}\left(\frac{2}{\lambda}\right)\left(\frac{1}{H^2}\right)$$

$$\left(\frac{B}{A}\right)^{1/2} = \left(\frac{f}{8}\right)^{1/4}\left(\frac{2}{\lambda}\right)^{1/2}\left(\frac{1}{H}\right) = \gamma$$

So the general solution for depth averaged velocity for a rectangular channel can be written as

$$U_d(y) = \left[A_1 e^{\gamma y} + A_1 e^{-\gamma y} + k \quad \right]^{1/2} \tag{3.2.23}$$

Where $\gamma = \left(\frac{f}{8}\right)^{\frac{1}{4}}\left(\frac{2}{\lambda}\right)^{\frac{1}{2}}\left(\frac{1}{H}\right)$

$$k = K(1-\beta) \tag{3.2.24}$$

$$K = \frac{8 g S_o H}{f}$$

$$\beta = \frac{\Gamma}{\rho g S_o H}$$

The cross section of a prismatic compound channel is then divided into number of panels, in which the three calibration co-efficient *f, λ, Γ* are calculated and then U_d & τ_b can be evaluated within each panel as a function of *y*.

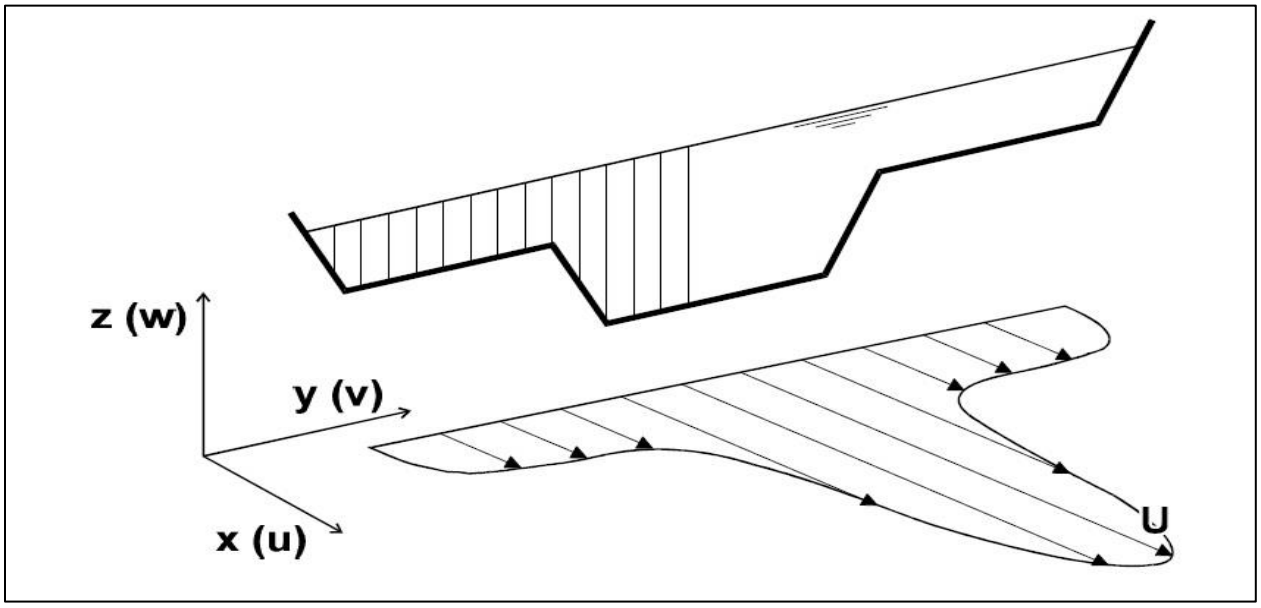

Fig.3.2.3: Lateral distribution of longitudinal velocity (Bousmar 2002)

Boundary condition

1. $(U_d)_i = (U_d)_{i+1}$, Continuity of depth averaged velocity.
2. $\left(\frac{\partial U_d}{\partial y}\right)_i = \left(\frac{\partial U_d}{\partial y}\right)_{i+1}$, Continuity of the lateral gradient of the depth averaged velocity
3. The boundary condition for a rigid side wall (No slip condition) may be written as $U_i = 0$

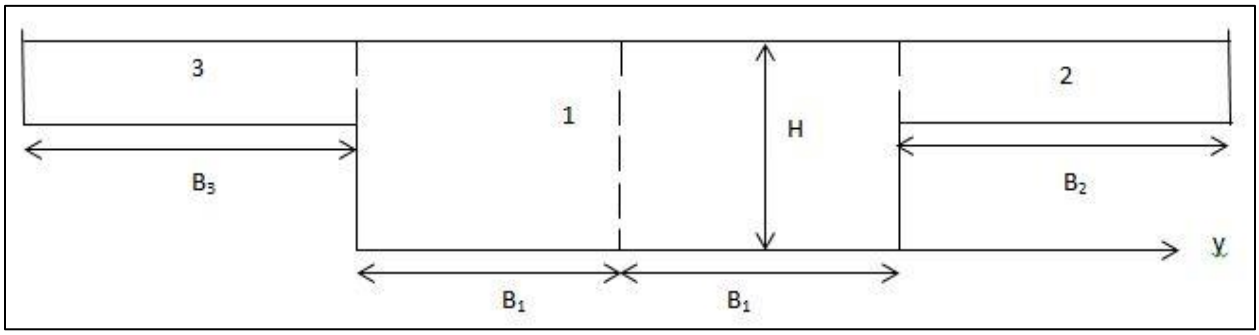

Fig.3.2.4: The partition of rectangular compound channel by taking the center as origin

Here the compound channel is divided into 3 panels

Applying boundary condition to 1st and 2nd pannel

$$A_1 e^{\gamma_1 B_1} + A_2 e^{-e^{\gamma_1 B_1}} + k_1 = A_3 e^{\gamma_2 B_1} + A_4 e^{-e^{\gamma_2 B_1}} + k_2 \quad (3.2.25)$$

$$\gamma_1 A_1 e^{\gamma_1 B_1} - \gamma_1 A_2 e^{-\gamma_1 B_1} = \gamma_2 A_3 e^{\gamma_2 B_1} - \gamma_2 A_4 e^{-\gamma_2 B_1} \quad (3.2.26)$$

$$A_3 e^{\gamma_2 (B_1 + B_2)} + A_4 e^{-\gamma_2 (B_1 + B_2)} + k_2 = 0 \quad (3.2.27)$$

Likewise boundary condition applied to 1st and 3rd panel

$$A_1 e^{-\gamma_1 B_1} + A_2 e^{\gamma_1 B_1} + k_1 = A_5 e^{-\gamma_3 B_1} + A_6 e^{\gamma_3 B_1} + k_3 \quad (3.2.28)$$

$$\gamma_1 A_1 e^{-\gamma_1 B_1} - \gamma_1 A_2 e^{\gamma_1 B_1} = \gamma_3 A_5 e^{-\gamma_3 B_1} - \gamma_3 A_6 e^{\gamma_3 B_1} \quad (3.2.29)$$

$$A_5 e^{-\gamma_3 (B_1 + B_3)} + A_6 e^{\gamma_3 (B_1 + B_3)} + k_3 = 0 \quad (3.2.30)$$

In all the above equations the $A_1, A_2, \ldots A_6$ are the six unknowns which can be found out by using elimination method or by matrix method (Rezai 2006).

Elimination method is quite lengthy as well as complex to get the values of unknowns so here we are using matrix method for finding out the values of $A_1, A_2, \ldots A_6$.

$$\begin{bmatrix} e^{\gamma_1 B_1} & e^{-\gamma_1 B_1} & -e^{\gamma_2 B_1} & -e^{-\gamma_2 B_1} & 0 & 0 \\ \gamma_1 e^{\gamma_1 B_1} & -\gamma_1 e^{\gamma_1 B_1} & -\gamma_2 e^{\gamma_2 B_1} & \gamma_2 e^{\gamma_2 B_1} & 0 & 0 \\ 0 & 0 & e^{\gamma_2 (B_1+B_2)} & e^{-\gamma_2 (B_1+B_2)} & 0 & 0 \\ e^{-\gamma_1 B_1} & e^{\gamma_1 B_1} & 0 & 0 & -e^{-\gamma_3 B_1} & -e^{\gamma_3 B_1} \\ \gamma_1 e^{-\gamma_1 B_1} & -\gamma_1 e^{-\gamma_1 B_1} & 0 & 0 & -\gamma_3 e^{-\gamma_3 B_1} & \gamma_3 e^{-\gamma_3 B_1} \\ 0 & 0 & 0 & 0 & e^{-\gamma_3 (B_1+B_3)} & e^{\gamma_3 (B_1+B_3)} \end{bmatrix} * \begin{bmatrix} A_1 \\ A_2 \\ A_3 \\ A_4 \\ A_5 \\ A_6 \end{bmatrix} = \begin{bmatrix} k_2 - k_1 \\ 0 \\ -k_2 \\ k_3 - k_1 \\ 0 \\ -k_3 \end{bmatrix}$$

From this matrix method the values of unknowns can be found out which will be useful for finding out the depth averaged velocity, bed shear stress and discharge for that particular depth can be found out.

3.2.3. Computational method for discharge calculation

3.2.3.1. Conveyance Estimation System

The **Conveyance and Afflux Estimation System (CES/AES**) is a software tool which is used for estimation of flood and drainage water levels in the rivers, watercourses and drainage channels. This software is being developed by the hydraulic engineers of United Kingdom.

This software helps in estimation of hydraulic roughness, water levels corresponding to channel conveyance, flow for a given slope, sectional averaged velocity as well as spatial velocities, backwater profiles of a known flow-head control like weir (steady), afflux at upstream of bridges and culverts, uncertainties of input and out data etc.

The CES software involves roughness advisor, conveyance generator, uncertainty estimator, backwater module, afflux estimator etc. The **roughness advisor** carries the information regarding the roughness values for a range of natural and man-made roughness types along with description and photographs related to that roughness. . The roughness values are obtained from over 700 references (River Habitat Survey) and it also contain aquatic vegetation, crops, grasses, hedges, trees, substrates, bank protection and irregularities. The Roughness Advisor has also the information regarding seasonal variations in vegetation roughness, cutting and recommended regrowth patterns following the cutting. Based on the roughness information and cross section geometry the **conveyance generator** estimates the conveyance of the channel. By the help of lateral distribution method the conveyance is calculated. Here unit flow rate is calculated at 100 points across the channel section and then by integrating the flow rate across the section over all flow is found out. Water level, flow, rating curves, velocity, area, perimeter, Froude Number, Reynolds Number etc. are the available outputs with respect to given depth. Spatial distributions

of velocity, boundary shear and shear velocity can also be obtained across the section. The **uncertainty estimator** gives some measure of the uncertainty associated with each predicted water level. The upper and lower values of the uncertainty estimator depend upon the upper and lower roughness values estimated from the roughness advisor. Backwater module consists of a modest calculation for forming a backwater profile at upstream with known stage and flow value. This is based on the concept of balancing the energy between the upstream and downstream and it has an option to include the velocity head term. For gradually varied flow condition a code is used which is called as **afflux generator**. This code is helpful in finding out the afflux at upstream of the bridge and culvert at high flow condition. This code also provides longitudinal water surface profile.

Apart from these main tools, there is another tool named as **afflux advisor** which helps in quick calculation of afflux at simple culvert and bridge in a uniform flow condition. Like afflux generator, here also calculation is based on laboratory data as well as on field data but the problem with afflux advisor is it cannot provide longitudinal water surface profile.

The CES software tools help in calculating water levels, flows and velocities for rivers for given flow condition. It provides upper and lower uncertainty situations regarding the flow. It helps in measuring the flood at high water levels and requirement of channel reconstruction or management option. It evaluates the influence of timing and type of cutting of vegetation. It shows the impact of blockage generated from unwanted vegetation and debris. Now a days it provides guidance for channel preservation and performance.

Along with all above advantages there are some limitations of this software. It can only work with steady flow condition. It cannot work for sluice gates, weirs etc. Except within bridge and culvert it cannot consider super critical flow conditions.

3.2.3.2. Artificial Neural Network

Artificial neural network (ANN) is a soft computing tool, which is attempting to signify low-level intelligence in natural organisms. This tool is having a flexible structure, capable of establishing a non-linear relationship between the input and output data. Here multilayer perceptron network (MLP) based on back propagation rule were used. The MLP network is also called as Back Propagation (BP) network. It involves three layers, like wise input layer, hidden layer and output layer. The data values were received by input nodes and input nodes pass them

to the nodes of first hidden layer. Each hidden layer collects the input from all input nodes after multiplying a weight with each input value, attaches a bias to this sum, and the results were passed through a nonlinear transformation like the sigmoid transfer function. This helps in forming the input either for the second hidden layer or it forms an output layer that operates same to the hidden layer. The subsequent transformed output generated from each output node is the network output. The network required to be trained by using a training algorithm such as back propagation, conjugate gradient, cascade correlation etc.

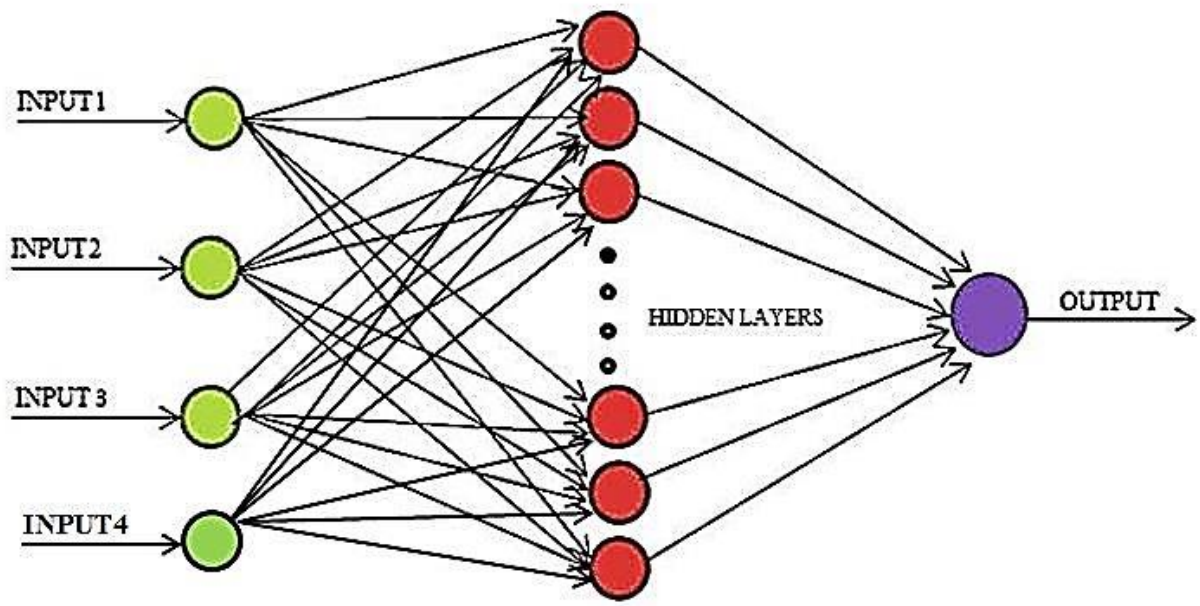

Fig. 3.2.5: Multilayer perceptron neural network

The main motive of training the patterns is to decrease the global error, which can be found out by using the formula given below.

$$\sum_{i=1}^{n_i} \sum_{j=1}^{n_j} \left(T_{ij} - O_{ij}\right)^2$$

Where T_{ij} is *the* j^{th} element of the target output associated to the i^{th} pattern, O_{ij} is the computed output of j^{th} neuron linked to the i^{th} pattern, n_p is the number of patterns and n_o is the number of neurons in the layer of output.

Previously Liu and James (2000) predicted discharge in a meandering compound channel using ANN and they have showed that between predicted and the measured discharge there is up to 15% inconsistency exist. But still now a days ANN has wide applications in prediction of

sediment concentration in the rivers, modeling of river flow, modelling of rainfall and runoff. It helps in simulation of stage discharge relationship in rivers and computation of flow resistance in smooth channels.

Flow pattern and momentum transfer between the flood plain and main channel in straight compound channels is governed by geometric and hydraulic variables significantly. Here the important dimensionless geometric ratios are taken as input parameters for ANN model. For this analysis four dimensionless parameters and one output variable are chosen.

The input dimensionless variables are area ratio, perimeter ratio, width ratio, slope and discharge ratio is considered as a output dimensionless parameter.

3.2.3.2.1. Input parameters

1. The area ratio defines the ratio between area of the compound channel to the area of main channel at full bank flow condition.

$$A_r = \frac{A_{total}}{A_{full\ bank}} \tag{3.2.31}$$

2. The perimeter ratio defines the ratio between perimeter of the compound channel to the perimeter of main channel at full bank flow condition.

$$P_r = \frac{P_{total}}{P_{full\ bank}} \tag{3.2.32}$$

3. The width ratio defines the ratio between width of the compound channel to the bottom width of main channel.

$$W_r = \frac{W_{total}}{W_{full\ bank}} \tag{3.2.33}$$

4. The bed slope (S_o) of the channel which is already a dimensionless quantity.

3.2.3.2.2. Output Parameter

The discharge ratio is the only one dimensionless output parameter which is used in this ANN model. Flow discharge ratio can be expressed as the ratio of the total observed discharge to the bank full flow discharge.

$$Q_r = \frac{Q_{total}}{Q_{full\ bank}} \tag{3.2.34}$$

3.2.4. Source of data collection:-

Experimental discharge data have been collected from FCF (Large scale Flood channel facility created at Wallingford UK) series data(*S-1, S-2, S-3, S-8, S-10*), Kinght & Demetriou (1983) (K&D-1, K&D-2, K&D-3), Atbay (2002), Rezai (2006) & NIT Rourkela Hydraulic lab data with varying width ratio α (B/b).

Table 3.2.1: Geometrical parameters of FCF channel

Series name	S_o	W_{mc} (m)	W_{fp} (m)	N_{fp}	S_{mc}	W_{total} (m)	h (m)	H (m)	S_{fp}
FCF Series-1	0.001027	1.5	4.1	2	1	10	0.15	0.15899	1
	0.001027	1.5	4.1	2	1	10	0.15	0.16519	1
	0.001027	1.5	4.1	2	1	10	0.15	0.17563	1
	0.001027	1.5	4.1	2	1	10	0.15	0.18656	1
	0.001027	1.5	4.1	2	1	10	0.15	0.19881	1
	0.001027	1.5	4.1	2	1	10	0.15	0.21411	1
	0.001027	1.5	4.1	2	1	10	0.15	0.21443	1
	0.001027	1.5	4.1	2	1	10	0.15	0.25012	1
FCF Series-2	0.001027	1.5	2.25	2	1	6.3	0.15	0.15649	1
	0.001027	1.5	2.25	2	1	6.3	0.15	0.16873	1
	0.001027	1.5	2.25	2	1	6.3	0.15	0.1699	1
	0.001027	1.5	2.25	2	1	6.3	0.15	0.17784	1
	0.001027	1.5	2.25	2	1	6.3	0.15	0.18676	1
	0.001027	1.5	2.25	2	1	6.3	0.15	0.18695	1
	0.001027	1.5	2.25	2	1	6.3	0.15	0.19796	1
	0.001027	1.5	2.25	2	1	6.3	0.15	0.21355	1
	0.001027	1.5	2.25	2	1	6.3	0.15	0.24855	1
	0.001027	1.5	2.25	2	1	6.3	0.15	0.28795	1

Series name	S_o	W_{mc} (m)	W_{fp} (m)	N_{fp}	S_{mc}	W_{total} (m)	h (m)	H (m)	S_{fp}
FCF Series -3	0.001027	1.5	0.75	2	1	3.3	0.15	0.158	1
	0.001027	1.5	0.75	2	1	3.3	0.15	0.16627	1
	0.001027	1.5	0.75	2	1	3.3	0.15	0.17712	1
	0.001027	1.5	0.75	2	1	3.3	0.15	0.18779	1
	0.001027	1.5	0.75	2	1	3.3	0.15	0.19804	1
	0.001027	1.5	0.75	2	1	3.3	0.15	0.21454	1
	0.001027	1.5	0.75	2	1	3.3	0.15	0.2477	1
	0.001027	1.5	0.75	2	1	3.3	0.15	0.2484	1
	0.001027	1.5	0.75	2	1	3.3	0.15	0.29922	1
	0.001027	1.5	0.75	2	1	3.3	0.15	0.30014	1
FCF Series -8	0.001027	1.5	2.25	2	*v*	6	0.15	0.15796	1
	0.001027	1.5	2.25	2	*v*	6	0.15	0.167	1
	0.001027	1.5	2.25	2	*v*	6	0.15	0.17653	1
	0.001027	1.5	2.25	2	*v*	6	0.15	0.18757	1
	0.001027	1.5	2.25	2	*v*	6	0.15	0.20008	1
	0.001027	1.5	2.25	2	*v*	6	0.15	0.21483	1
	0.001027	1.5	2.25	2	*v*	6	0.15	0.25022	1
	0.001027	1.5	2.25	2	*v*	6	0.15	0.29973	1
FCF Series -10	0.001027	1.5	2.25	2	2	6.6	0.15	0.15803	1
	0.001027	1.5	2.25	2	2	6.6	0.15	0.1666	1
	0.001027	1.5	2.25	2	2	6.6	0.15	0.17654	1
	0.001027	1.5	2.25	2	2	6.6	0.15	0.18701	1
	0.001027	1.5	2.25	2	2	6.6	0.15	0.20033	1
	0.001027	1.5	2.25	2	2	6.6	0.15	0.20051	1
	0.001027	1.5	2.25	2	2	6.6	0.15	0.21481	1
	0.001027	1.5	2.25	2	2	6.6	0.15	0.2493	1
	0.001027	1.5	2.25	2	2	6.6	0.15	0.2797	1

Table 3.2.2: Geometrical parameters of Knight & Demetriou channel

Series Name	S_o	W_{mc} (m)	W_{fp} (m)	N_{fp}	S_{mc}	W_{total} (m)	h (m)	H (m)	S_{fp}
Knight & Demetriou -1	0.000966	0.152	0.076	2	*v*	0.304	0.076	0.0855	*v*
	0.000966	0.152	0.076	2	*v*	0.304	0.076	0.09453	*v*
	0.000966	0.152	0.076	2	*v*	0.304	0.076	0.10026	*v*
	0.000966	0.152	0.076	2	*v*	0.304	0.076	0.11343	*v*
	0.000966	0.152	0.076	2	*v*	0.304	0.076	0.12583	*v*
	0.000966	0.152	0.076	2	*v*	0.304	0.076	0.1511	*v*
	0.000966	0.152	0.076	2	*v*	0.304	0.076	0.08746	*v*
Knight & Demetriou -2	0.000966	0.152	0.152	2	*v*	0.456	0.15	0.09608	*v*
	0.000966	0.152	0.152	2	*v*	0.456	0.15	0.10093	*v*
	0.000966	0.152	0.152	2	*v*	0.456	0.15	0.11209	*v*
	0.000966	0.152	0.152	2	*v*	0.456	0.15	0.125	*v*
	0.000966	0.152	0.152	2	*v*	0.456	0.15	0.14931	*v*
	0.000966	0.152	0.152	2	*v*	0.456	0.15	0.08501	*v*
Knight & Demetriou -3	0.000966	0.152	0.228	2	*v*	0.608	0.15	0.095597	*v*
	0.000966	0.152	0.228	2	*v*	0.608	0.15	0.102151	*v*
	0.000966	0.152	0.228	2	*v*	0.608	0.15	0.114286	*v*
	0.000966	0.152	0.228	2	*v*	0.608	0.15	0.127303	*v*
	0.000966	0.152	0.228	2	*v*	0.608	0.15	0.153846	*v*

Table 3.2.3: Geometrical parameters of Atbay channel

Series Name	S_o	W_{mc} (m)	W_{fp} (m)	N_{fp}	S_{mc}	W_{total} (m)	h (m)	H (m)	S_{fp}
Atbay's Data	0.002024	0.398	0.407	2	*v*	0.805	0.05	0.0538	*v*
	0.002024	0.398	0.407	2	*v*	0.805	0.05	0.0596	*v*
	0.002024	0.398	0.407	2	*v*	0.805	0.05	0.0641	*v*
	0.002024	0.398	0.407	2	*v*	0.805	0.05	0.0682	*v*
	0.002024	0.398	0.407	2	*v*	0.805	0.05	0.0713	*v*
	0.002024	0.398	0.407	2	*v*	0.805	0.05	0.0686	*v*
	0.002024	0.398	0.407	2	*v*	0.805	0.05	0.0733	*v*
	0.002024	0.398	0.407	2	*v*	0.805	0.05	0.0764	*v*
	0.002024	0.398	0.407	2	*v*	0.805	0.05	0.0788	*v*
	0.002024	0.398	0.407	2	*v*	0.805	0.05	0.0846	*v*
	0.002024	0.398	0.407	2	*v*	0.805	0.05	0.0876	*v*
	0.002024	0.398	0.407	2	*v*	0.805	0.05	0.0923	*v*
	0.002024	0.398	0.407	2	*v*	0.805	0.05	0.0946	*v*
	0.002024	0.398	0.407	2	*v*	0.805	0.05	0.0980	*v*

Table 3.2.4: Geometrical parameters of Rezai channel

Series Name	S_o	W_{mc} (m)	W_{fp} (m)	N_{fp}	S_{mc}	W_{total} (m)	h (m)	H (m)	S_{fp}
Rezai's Data	0.002003	0.398	0.1	2	*v*	0.598	0.05	0.0528	*v*
	0.002003	0.398	0.1	2	*v*	0.598	0.05	0.05556	*v*
	0.002003	0.398	0.1	2	*v*	0.598	0.05	0.058824	*v*
	0.002003	0.398	0.1	2	*v*	0.598	0.05	0.0603	*v*
	0.002003	0.398	0.1	2	*v*	0.598	0.05	0.0625	*v*
	0.002003	0.398	0.1	2	*v*	0.598	0.05	0.0667	*v*
	0.002003	0.398	0.1	2	*v*	0.598	0.05	0.0718	*v*
	0.002003	0.398	0.1	2	*v*	0.598	0.05	0.0762	*v*
	0.002003	0.398	0.1	2	*v*	0.598	0.05	0.08	*v*
	0.002003	0.398	0.1	2	*v*	0.598	0.05	0.08333	*v*
	0.002003	0.398	0.1	2	*v*	0.598	0.05	0.0852	*v*
	0.002003	0.398	0.1	2	*v*	0.598	0.05	0.0933	*v*
	0.002003	0.398	0.1	2	*v*	0.598	0.05	0.1015	*v*
	0.002003	0.398	0.1	2	*v*	0.598	0.05	0.1077	*v*

Table 3.2.5: Geometrical parameters of NIT Rourkela channel

Series Name	S_o	W_{mc} (m)	W_{fp} (m)	N_{fp}	S_{mc}	W_{total} (m)	h (m)	H (m)	S_{fp}
NIT Rourkela Data 2013-2014	0.001	0.5	0.2	2	*v*	0.9	0.1	0.1111	*v*
	0.001	0.5	0.2	2	*v*	0.9	0.1	0.1147	*v*
	0.001	0.5	0.2	2	*v*	0.9	0.1	0.117647	*v*
	0.001	0.5	0.2	2	*v*	0.9	0.1	0.125	*v*
	0.001	0.5	0.2	2	*v*	0.9	0.1	0.128	*v*
	0.001	0.5	0.2	2	*v*	0.9	0.1	0.1334	*v*
	0.001	0.5	0.2	2	*v*	0.9	0.1	0.137	*v*
	0.001	0.5	0.2	2	*v*	0.9	0.1	0.142857	*v*
	0.001	0.5	0.2	2	*v*	0.9	0.1	0.15	*v*
	0.001	0.5	0.2	2	*v*	0.9	0.1	0.16667	*v*
	0.001	0.5	0.2	2	*v*	0.9	0.1	0.2	*v*

All the channels taken here are smooth and symmetrical type. All FCF channels are having main channel trapezoidal shape but some of their flood plains are rectangular and some of them are trapezoidal, whereas all others channels are rectangular in shape for both main channel and in the flood plain.

RESULTS

4.1 Introduction

In chapter 3 the experimental procedures as well as discharge predicting methods have been described. Eleven sets of data are presented in that chapter. The geometrical parameters of those data sets which are influencing the discharge are tabulated in there. In this chapter the results of experiments conducted in NIT Rourkela will be presented in terms of local velocity distribution, stage discharge relationship, and boundary shear stress distribution. Apart from this a comparison study is being done between five different methods and their results are compared with the experimental results and percentage of error is found out.

4.2. Stage Discharge Results

Stage discharge relationship is one of the most important relationships for a River Engineer which is required for design and flood management purposes. From the stage-discharge data, it is possible to capacity of the channel and to predict the discharge. In order to understand the influence of the momentum transfer on discharge prediction five different methods are used for predicting the discharge at different flow conditions on eleven numbers of data sets. To achieve uniform flow the gate was adjusted to get *M1* and *M2* profiles. The depth related to this tailgate setting was then considered as the normal depth. This procedure was repeated for every single experiment in order to obtain accurate stage discharge relationships for the meandering channels.

In the present work stage discharge relationship is achieved by maintaining steady uniform flow in the prismatic part of the experimental channel (sec-1) shown in the fig 3.2. in chapter 3. From the experiment it was found that the discharge is influenced the hydraulic parameters and the geometrical parameters of the experimental channel. It was tried to maintain the water surface profile parallel to the valley slope. Discharge is measured for 16 different depth of flow, out of them 9 numbers are in bank flow depths and rest is over bank flow. Initially the rate of flow was less but as the depth of flow goes on increasing the rate of flow also increasing subsequently. The stage discharge curve is given in fig.4.1.

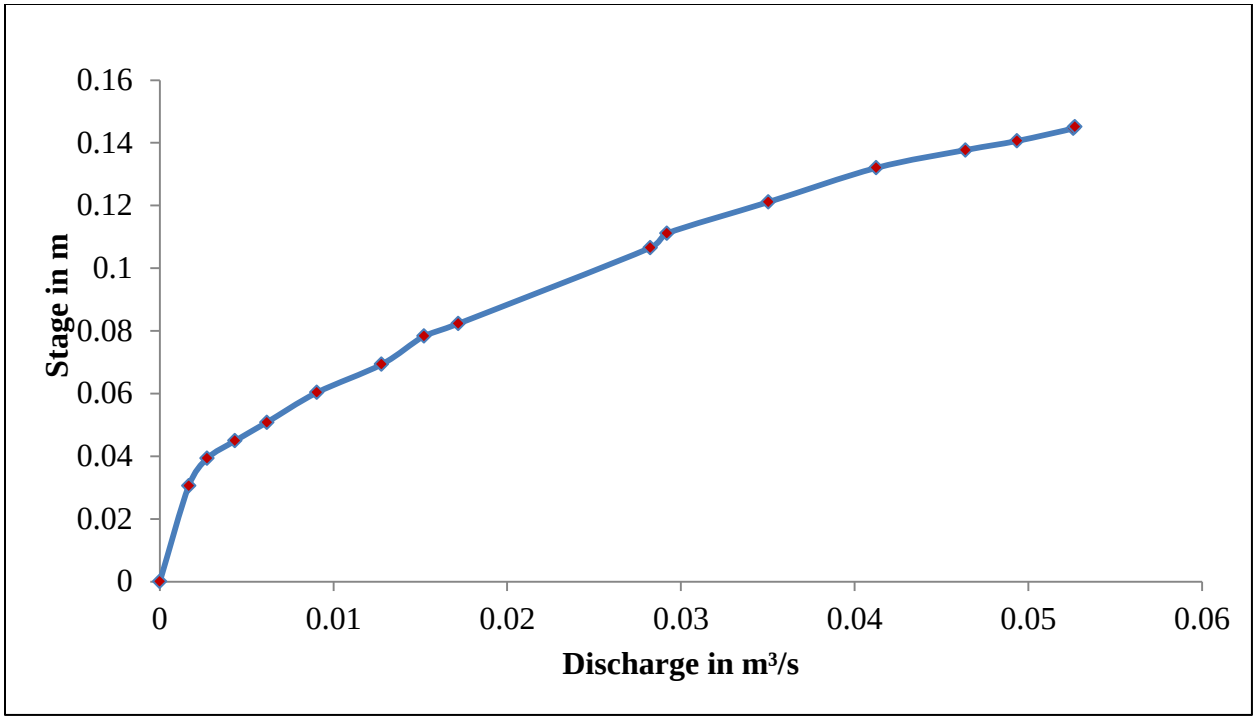

Fig.4.1: Stage discharge curve for the straight channel at section 1

4.3. Distribution of Longitudinal Velocity Results:-

In order to find out the local velocities and to determine the discharge, a velocity measuring device commonly used is the Pitot tube. The Pitot tube is connected to a U-tube manometer by the help of two pipes. Among these two pipes one gives static pressure and another gives the total pressure. The static and total pressure values are measured in the U-tube manometer. The difference between these reading gives the dynamic pressure of the moving fluid. The velocity of any point of the moving fluid is related to the dynamic pressure of that point. The velocity can be found out by using the equation 4.1 given below.

$$V = C\sqrt{2gh} \qquad (4.1)$$

Where V = the velocity of flow

h = the difference between the total pressure and static pressure or the dynamic pressure.

g = acceleration due to gravity

C = the non-dimensional constant.

The non-dimensional constant *C* is dependent upon the degree of imperfection in the Pitot tube, and on method of using the Pitot tube. The Pitot tube also helps in calculating the discharge in the channel but for this it is required to have sufficient velocity measurements. Depending upon the nature of velocity distribution across the channel, the local velocity measurements are taken. If the flow pattern is complex then more number of velocity measurements is required. The depth averaged velocity is required to be found out over a small area. Once the depth averaged velocity with respect to its area is found out, the discharge of the channel can be calculated by numerical integration.

The pitot tube which is used in the experiment has outside diameter as 4.6mm. The pitot tube is fixed to a trolley which helps in the movement of the pitot tube in both horizontal and vertical direction. Adequate care should be taken while taking the reading as there is always a chance of formation of air bubbles in the tube if it is exposed to air. The longitudinal velocities at specified points are taken by pitot tube at section 1 of the straight channel, which is prismatic. Velocity distributions along lateral direction are taken for 4 different depths. The points where the velocity is measured is shown in the fig 3.5 in chapter three. The velocity distribution of both main channel and flood plain along lateral direction are shown in fig 4.2.(i)-4.2.(viii), apart from this the velocity contours are also presented in the fig4.3.(i)-4.3.(iv).

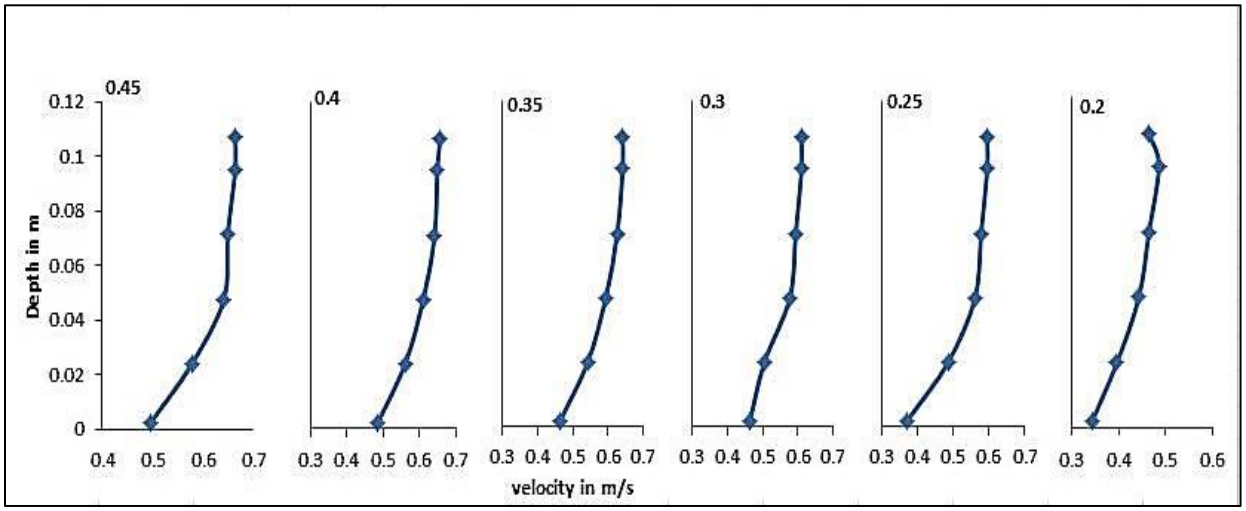

Fig.4.2.(i): Longitudinal velocity distribution along lateral direction in the main channel for relative depth of 0.15

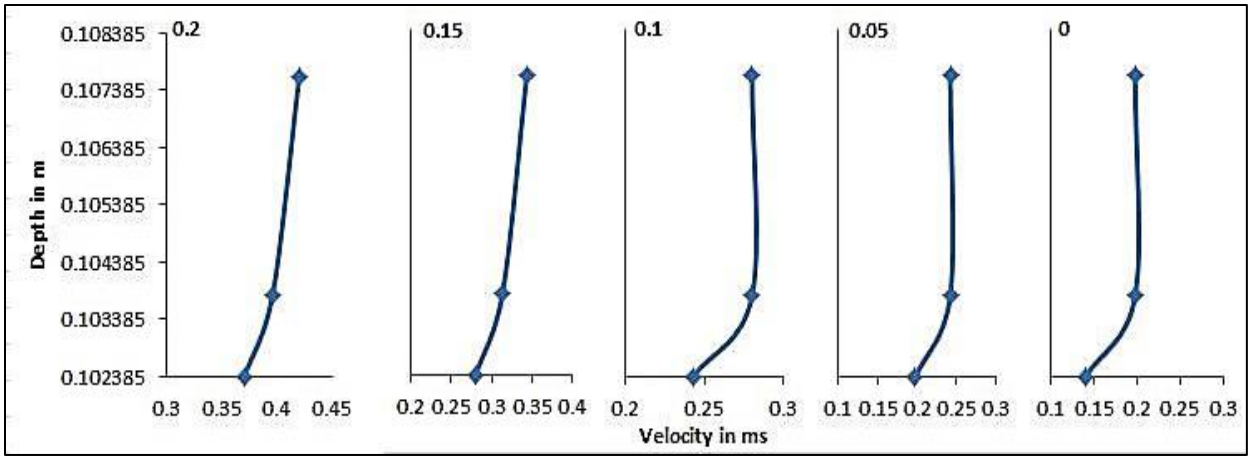

Fig.4.2.(ii): Longitudinal velocity distribution along lateral direction in the Flood plain for relative depth of 0.15

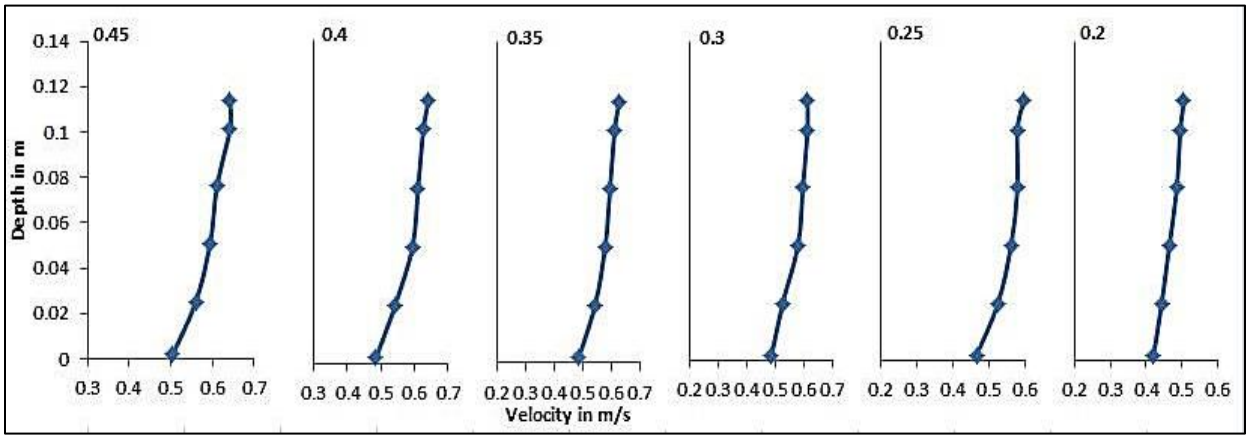

Fig.4.2.(iii): Longitudinal velocity distribution along lateral direction in the main channel for relative depth of 0.2

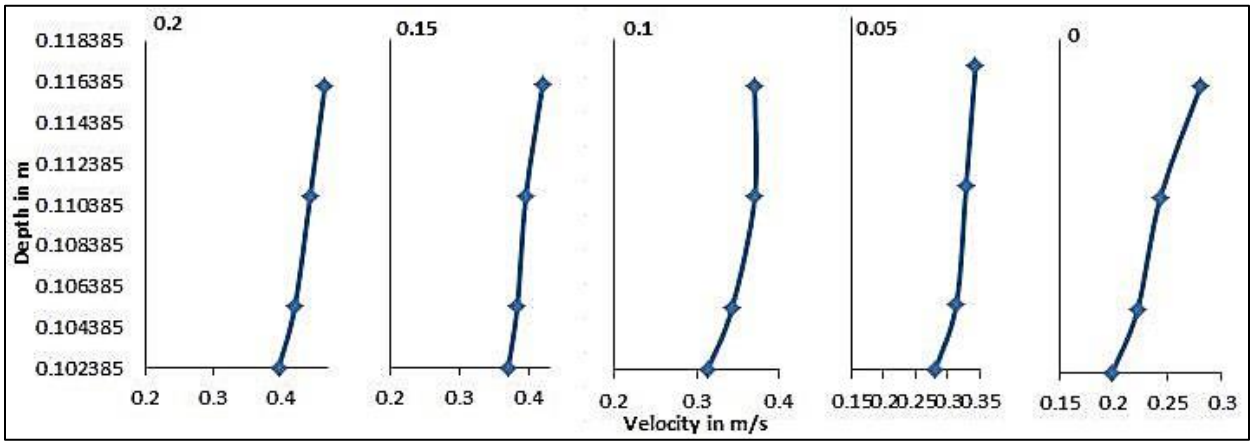

Fig.4.2.(iv): Longitudinal velocity distribution along lateral direction in the Flood plain for relative depth of 0.2

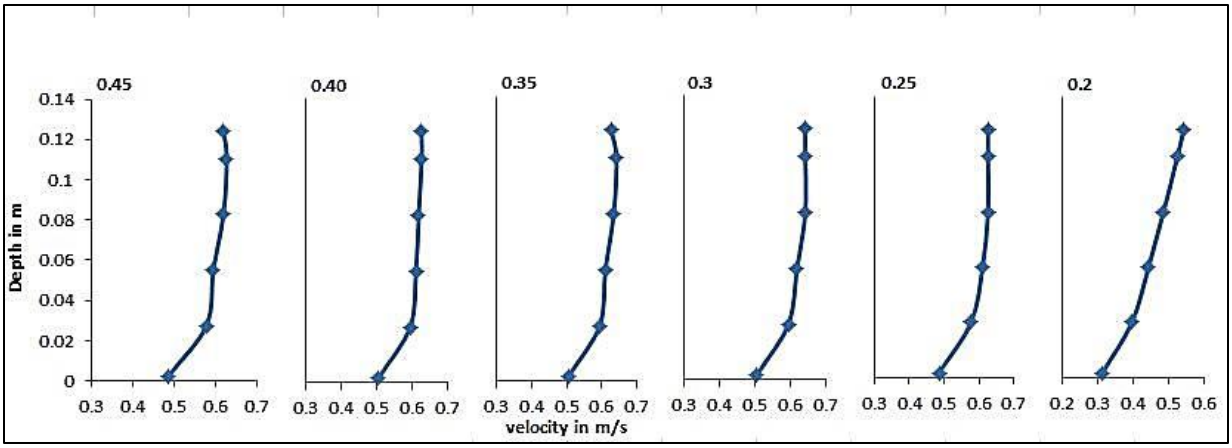

Fig.4.2.(v): Longitudinal velocity distribution along lateral direction in the main channel for relative depth of 0.25

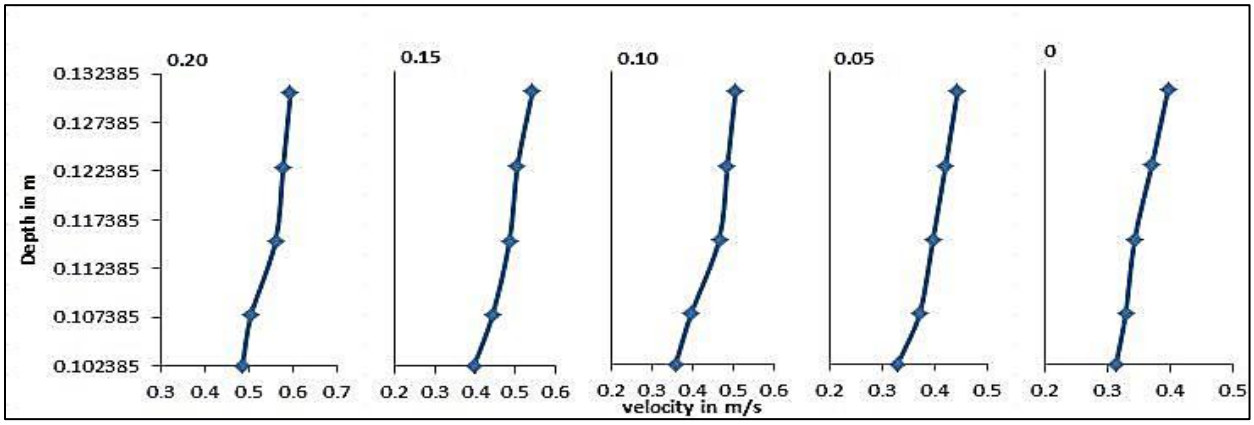

Fig.4.2.(vi): Longitudinal velocity distribution along lateral direction in the Flood plain for relative depth of 0.25

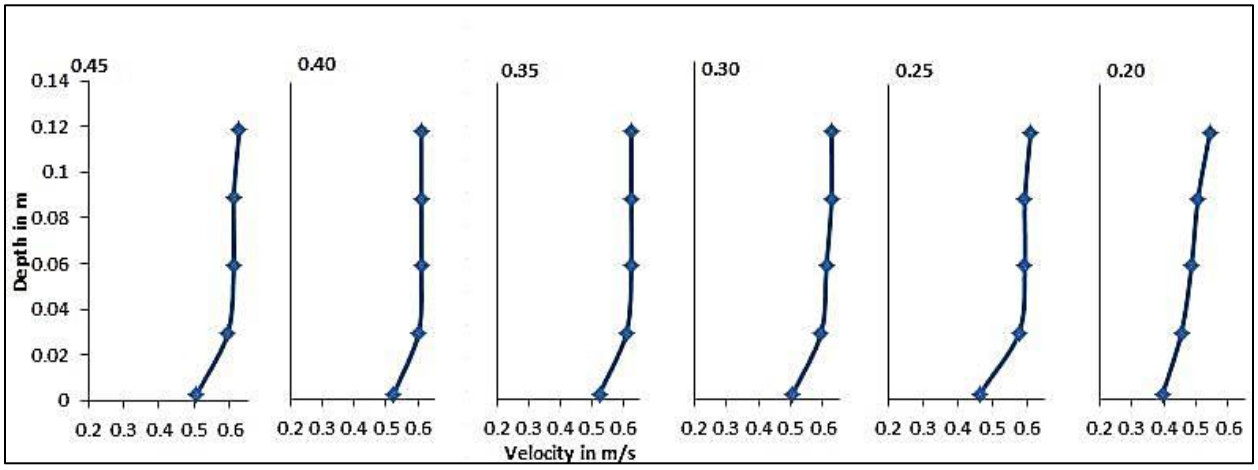

Fig.4.2.(vii): Longitudinal velocity distribution along lateral direction in the main channel for relative depth of 0.3

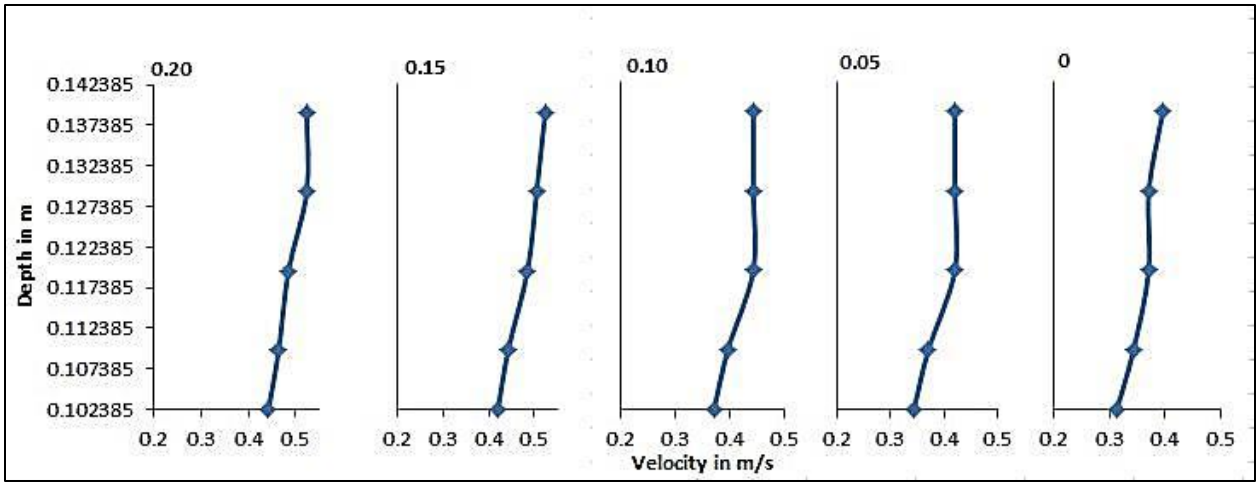

Fig.4.2.(viii): Longitudinal velocity distribution along lateral direction in the Flood plain for relative depth of 0.3

From this velocity profile it is seen that velocity is increasing as the depth goes on increasing. Most of the case it is seen that height value occurs at 0.8H depth from the bottom for the main channel. Likewise for the flood plain height value of the velocity occurs at the top point where the velocity measurements are taken. Most of the cases the highest value occurs at *0.6(H-h)* from the bottom of the flood plain depending upon the depth of water flowing over the flood plain and the condition of the pitot tube.

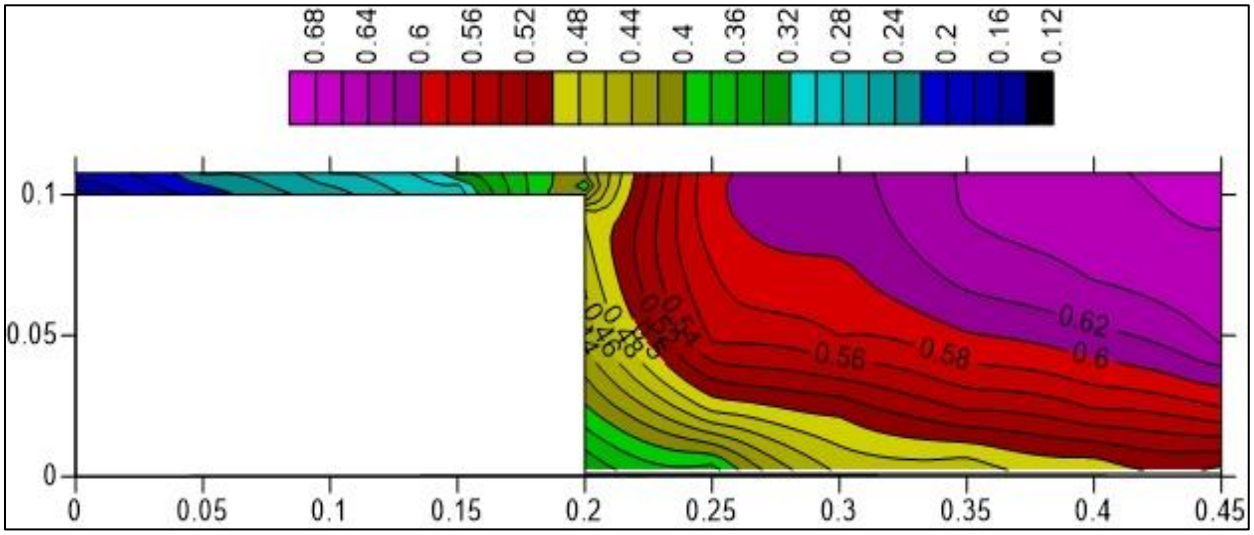

Fig.4.3.(i): Longitudinal velocity Contour for half portion of the section for relative depth of 0.15

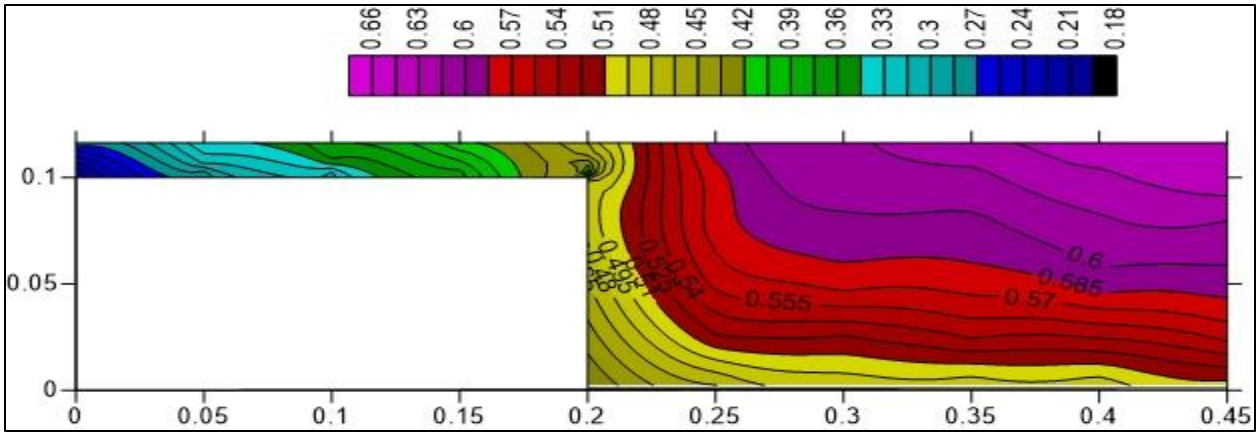

Fig.4.3.(ii): Longitudinal velocity Contour for half portion of the section for relative depth of 0.2

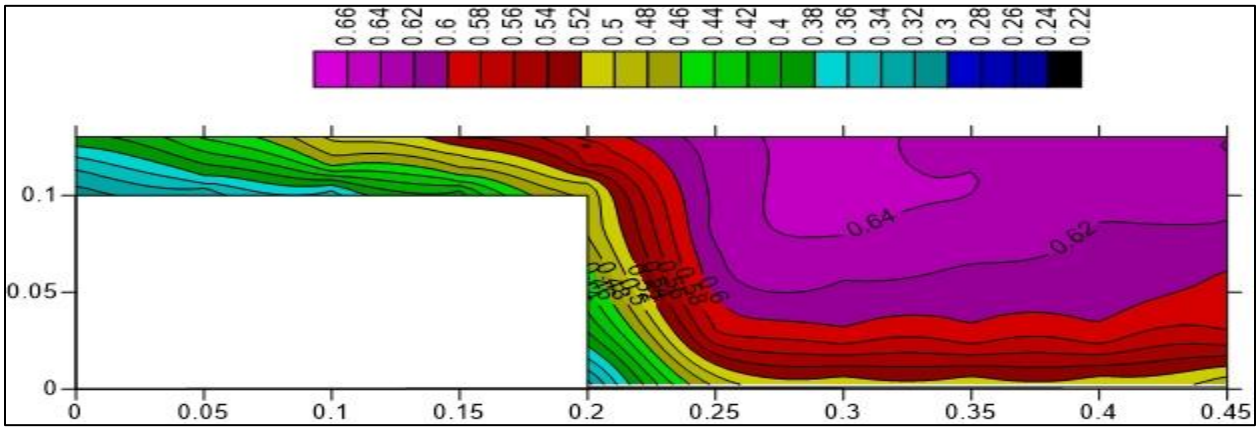

Fig.4.3.(iii): Longitudinal velocity Contour for half portion of the section for relative depth of 0.25

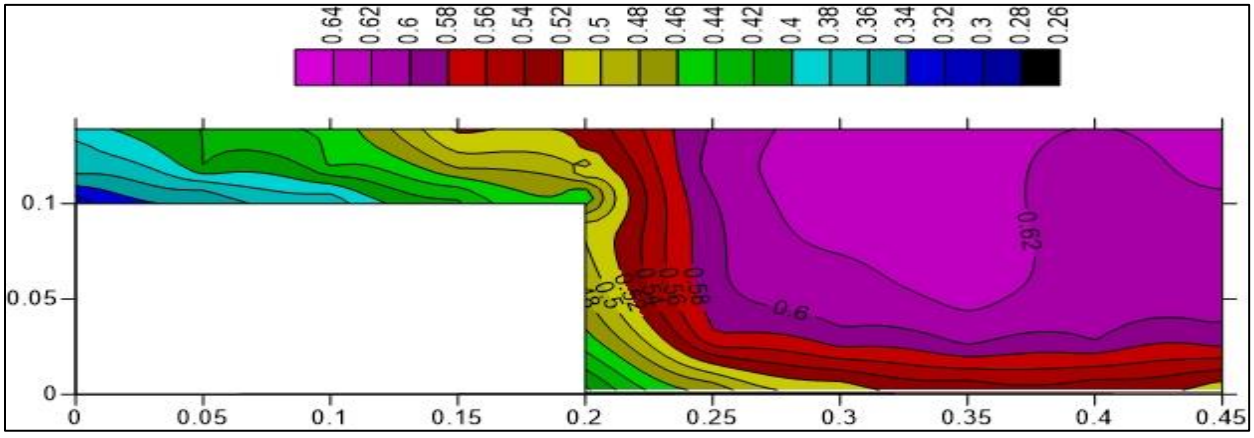

Fig.4.3.(iv): Longitudinal velocity Contour for half portion of the section for relative depth of 0.3

The velocity contours shows that maximum velocity occurs either at the center of the main channel or just adjacent to it. For lower depth of flow maximum velocity is occurred at the

center but as the depth of flow goes higher the maximum velocity is occurred just adjacent to the center position of the channel, this is clearly visible for the relative depth of 0.3.

4.4. Distribution of Longitudinal depth averaged Velocity Results

The depth averaged longitudinal velocity for the section 1 along lateral direction is measured for 4 different depth of flow and presented in the fig.4.4.(i)-4.4(iv). It is required to know the average velocity of flow at each specified section of the channel which is helpful in calculating the discharge.

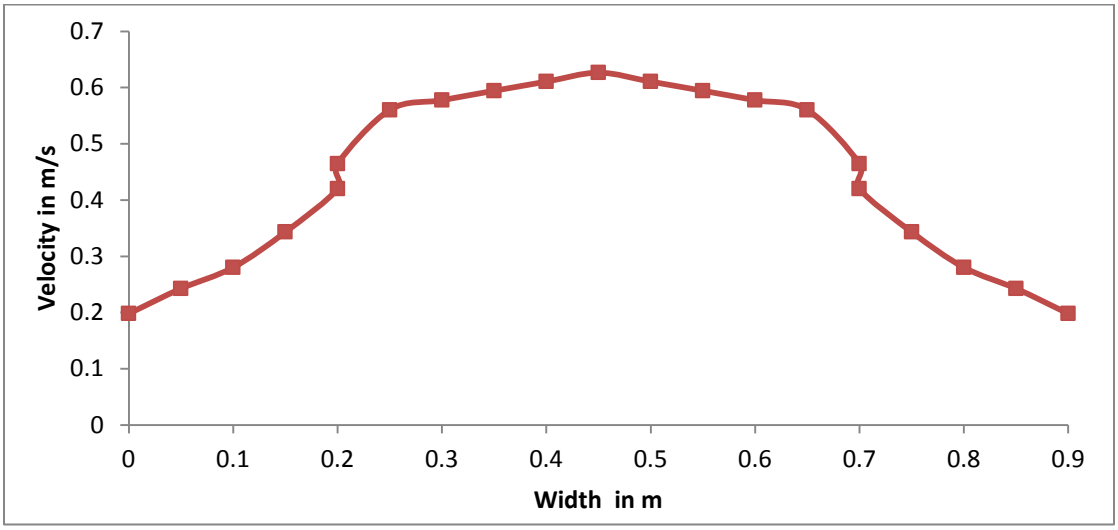

Fig.4.4.(i): Distribution of depth averaged velocity for the relative depth of 0.15

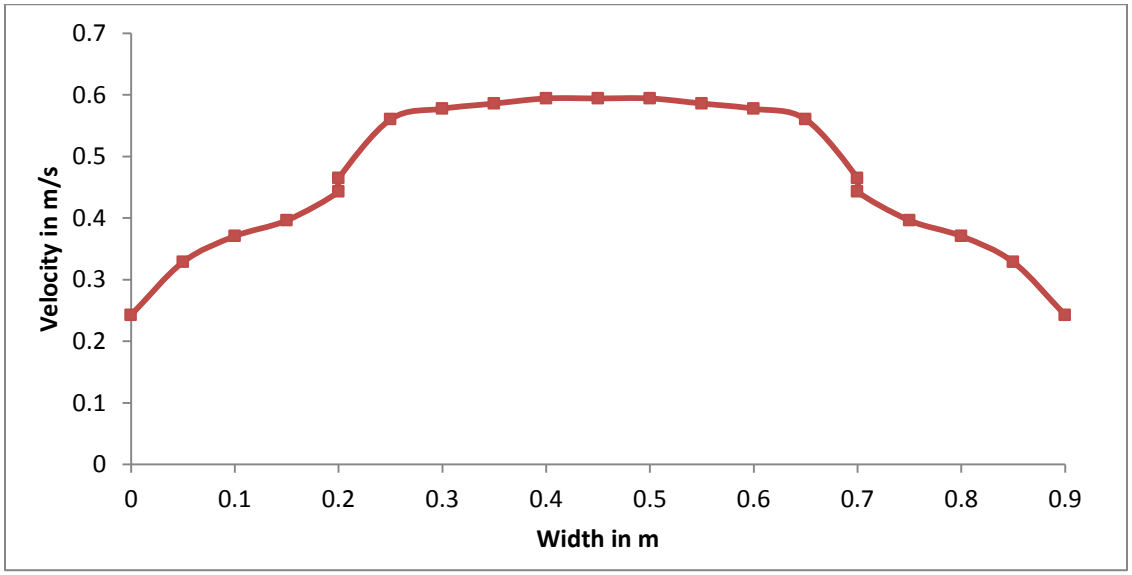

Fig.4.4.(ii): Distribution of depth averaged velocity for the relative depth of 0.2

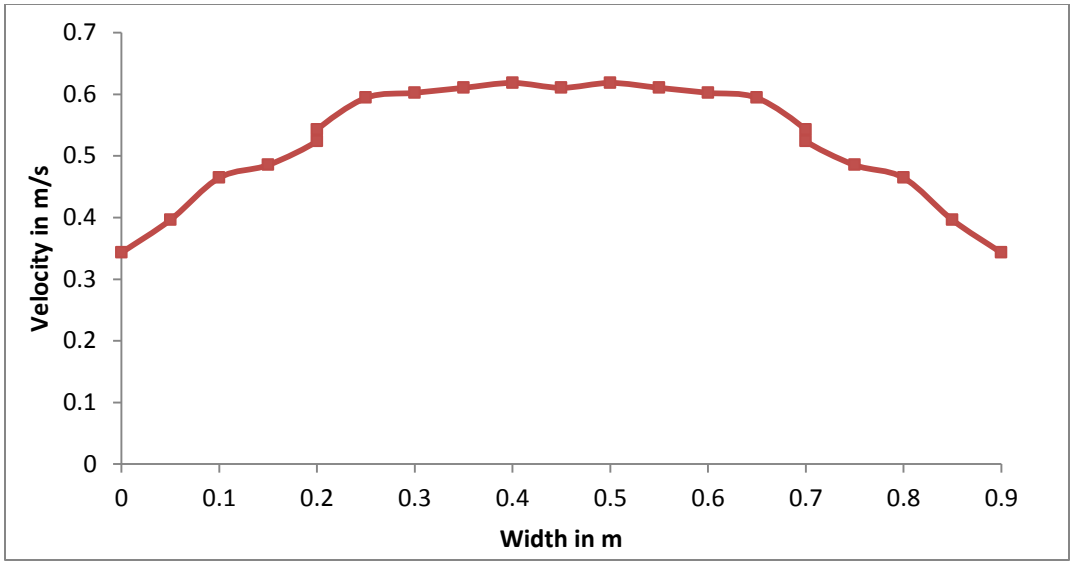

Fig.4.4.(iii): Distribution of depth averaged velocity for the relative depth of 0.25

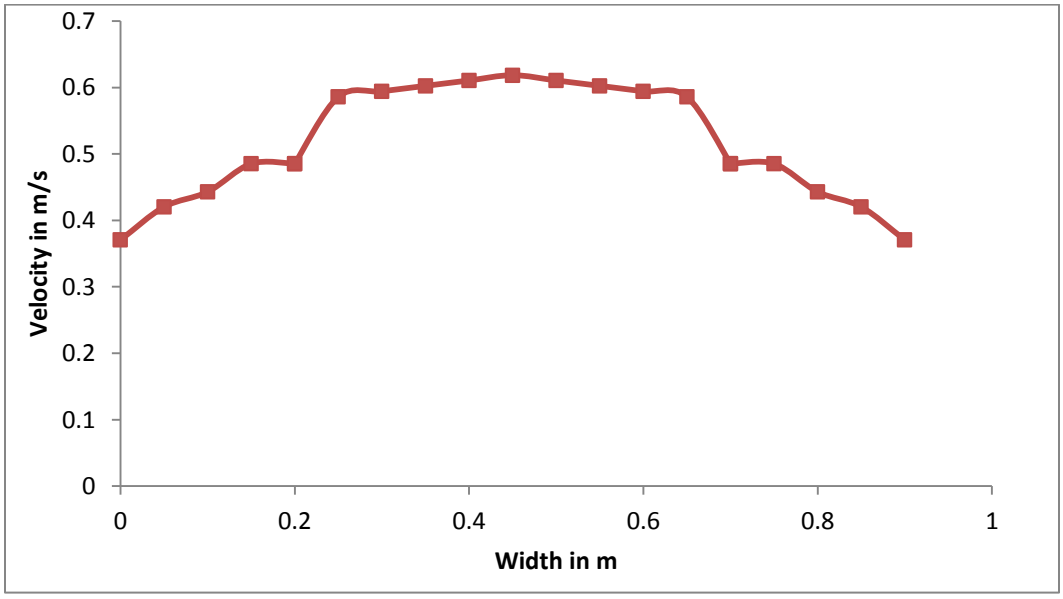

Fig.4.4.(iv): Distribution of depth averaged velocity for the relative depth of 0.3

4.5. Distribution of boundary shear stress Results

Shear stress distribution along the cross section of the channel is required to find out to know the variation of shear stress along the bed and it is also helpful in finding out the apparent shear stress in the channel section. In general Patel's equation is used to find out the shear stress develop at the bed and wall of the channel. Boundary shear stress at the bed and wall of the main channel and the flood plain are presented in the fig4.5.(i)-fig.4.5(iv).

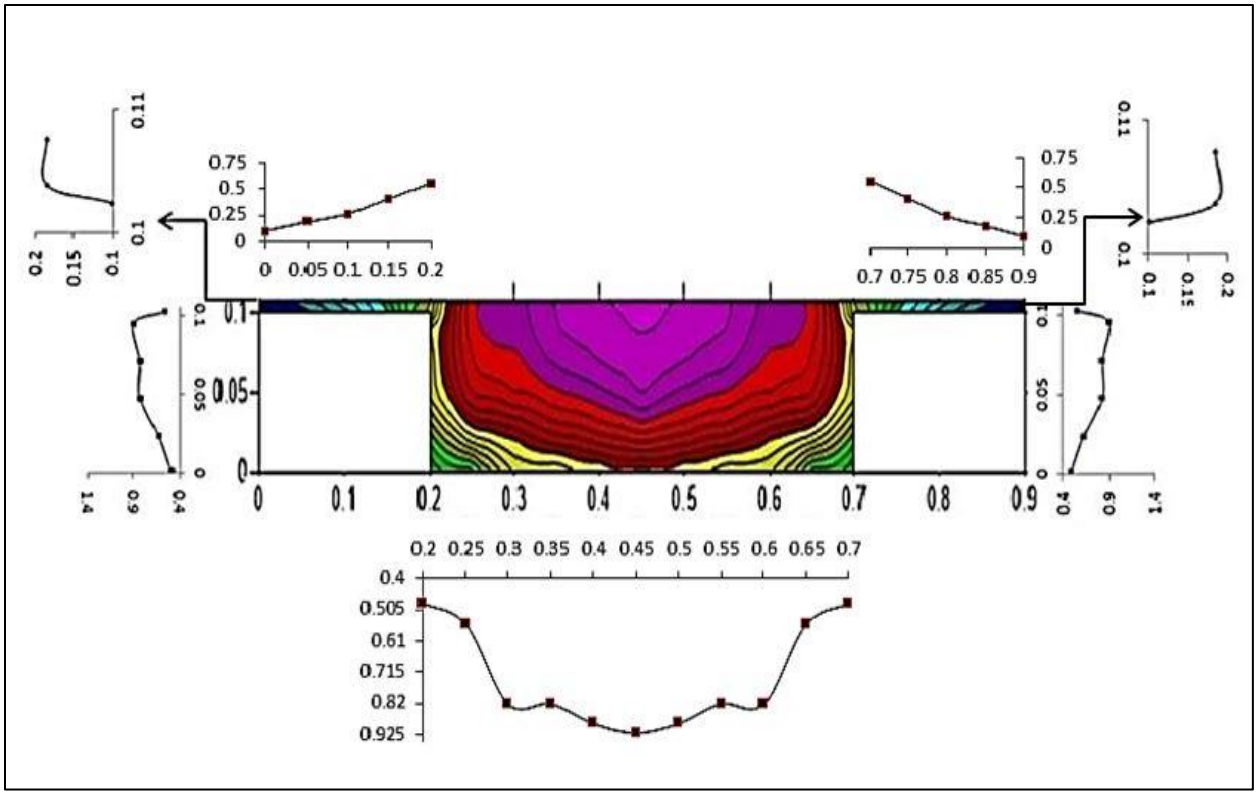

Fig.4.5.(i): Boundary shear stress distribution of section 1 of the straight channel for relative depth 0.15

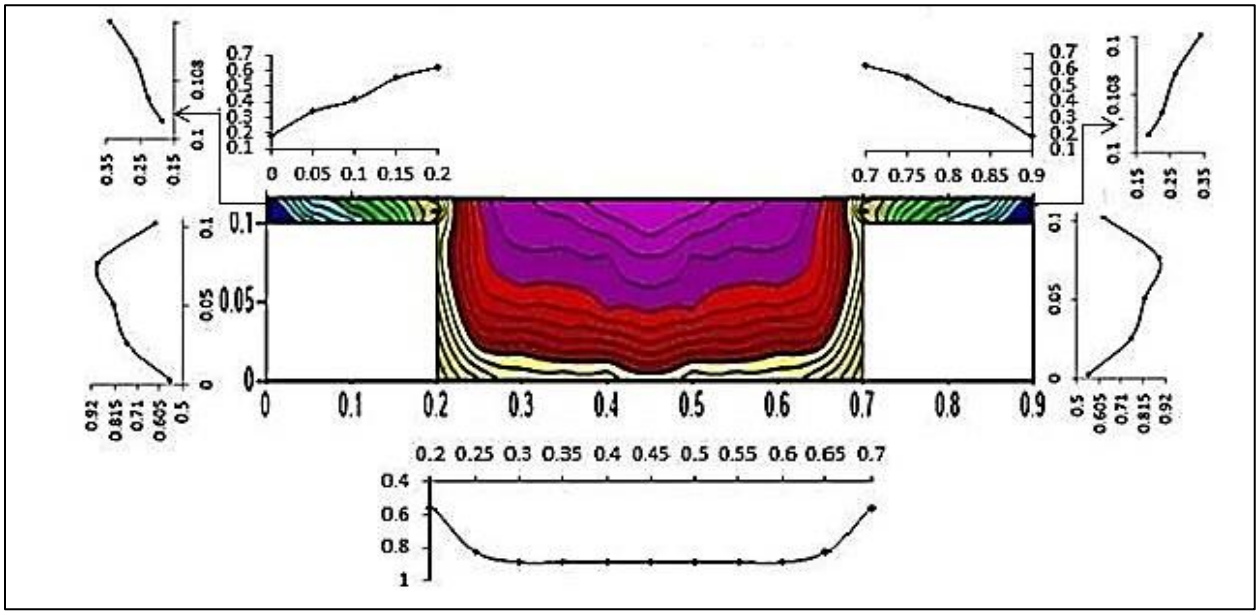

Fig.4.5.(ii): Boundary shear stress distribution of section 1 of the straight channel for relative depth 0.2

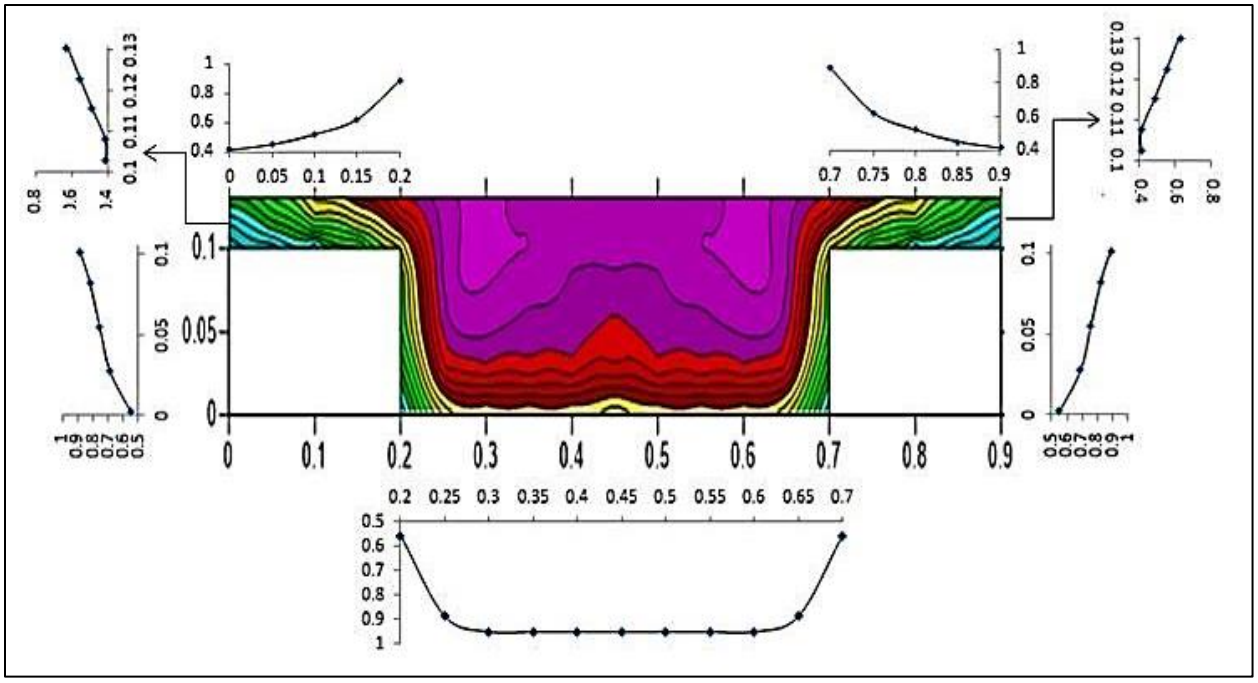

Fig.4.5.(iii): Boundary shear stress distribution of section 1 of the straight channel for relative depth 0.25

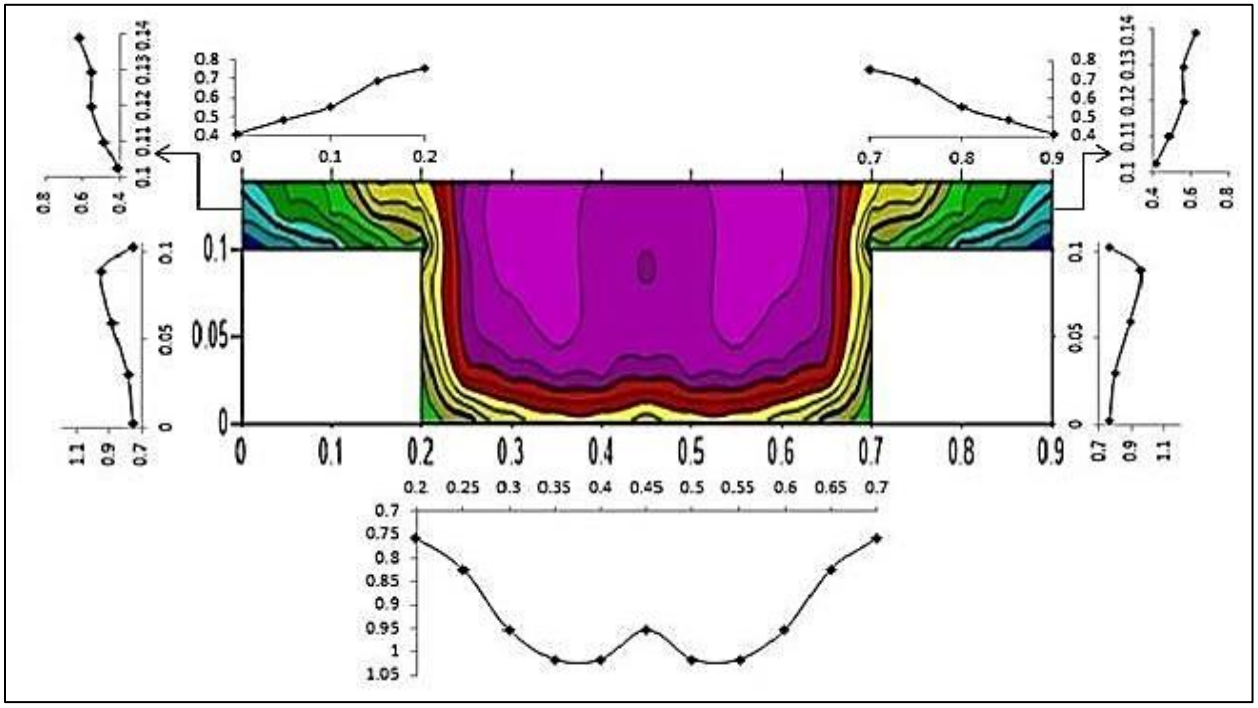

Fig.4.5.(iv): Boundary shear stress distribution of section 1 of the straight channel for relative depth 0.3

4.6. Comparison of experimental results with SKM

Shiono Knight Method is one of the methods which include three important parameters while calculating the discharge. The three important parameters are frictional resistance, eddy viscosity and lastly secondary current. This method uses RANS equation for predicting discharge. The analytical solution is already described in the chapter 3. A MATLAB code being written for calculating the depth averaged velocity and boundary shear stress through SKM, but the limitation with this code is, it is valid for rectangular compound channel only. So here we need to compare the experimental result with the results obtained from SKM.

The results of depth averaged velocity of both experimental as well as SKM are presented in the fig 4.6.(i)-4.6.(iv). Experimental results as well as results of SKM for boundary shear distributions are shown in the fig.4.7(i)-4.7(iv). The discharge results for both experimental and SKM are tabulated in the table 4.1 and the percentage of error between the actual discharge and the discharge obtained from SKM are calculated there.

4.6.1. Comparison of Depth averaged velocity with SKM

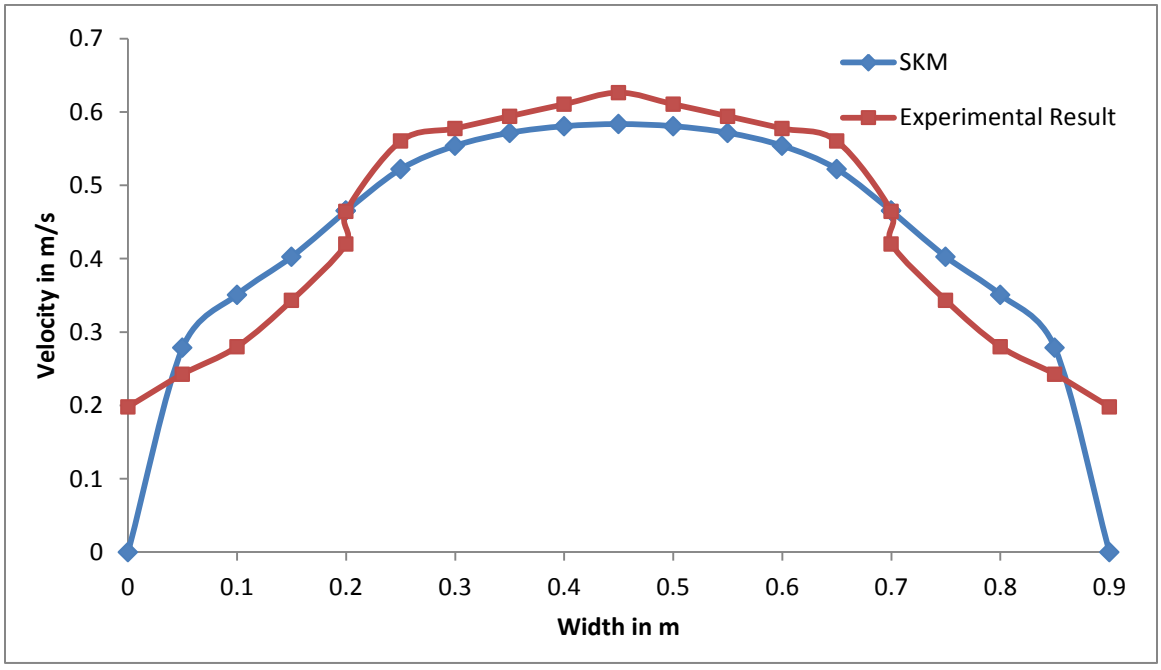

Fig.4.6.(i): Distribution of depth averaged velocity for the relative depth of 0.15

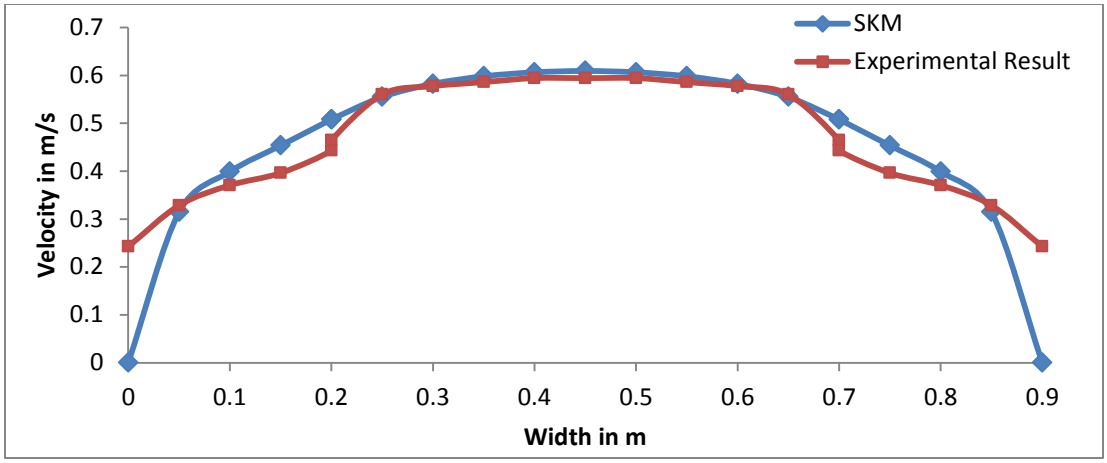

Fig.4.6.(ii): Distribution of depth averaged velocity for the relative depth of 0.2

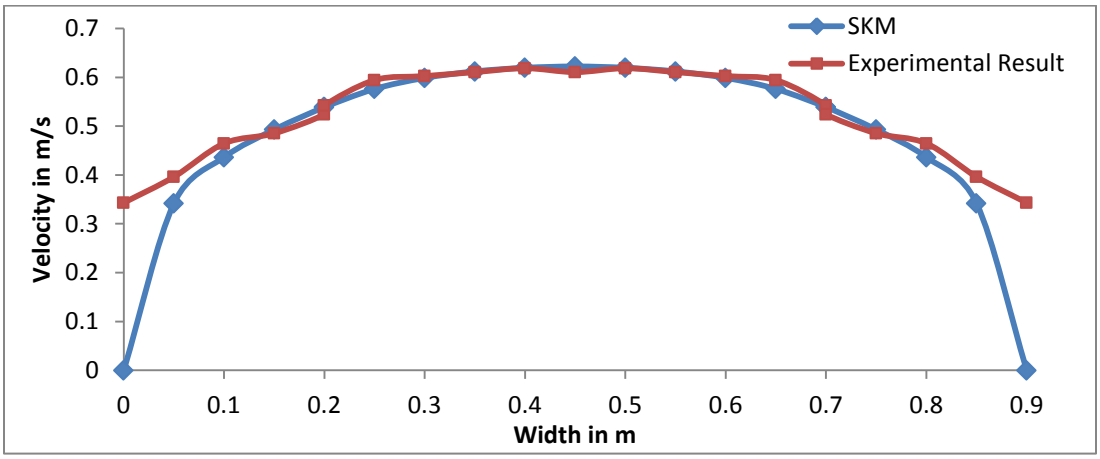

Fig.4.6.(iii): Distribution of depth averaged velocity for the relative depth of 0.25

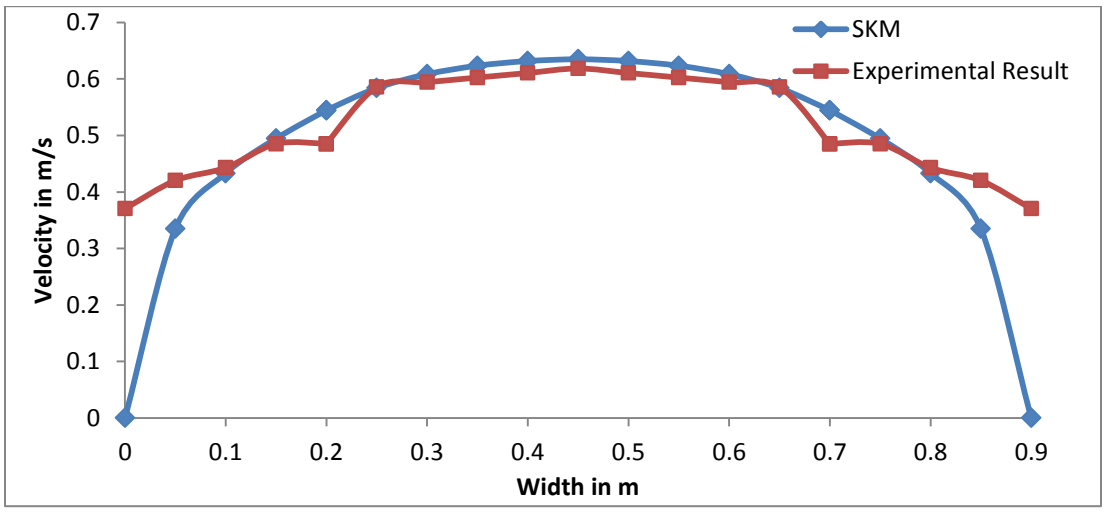

Fig.4.6.(iv) Distribution of depth averaged velocity for the relative depth of 0.3

4.6.2. Comparison of Boundary Shear Stress with SKM

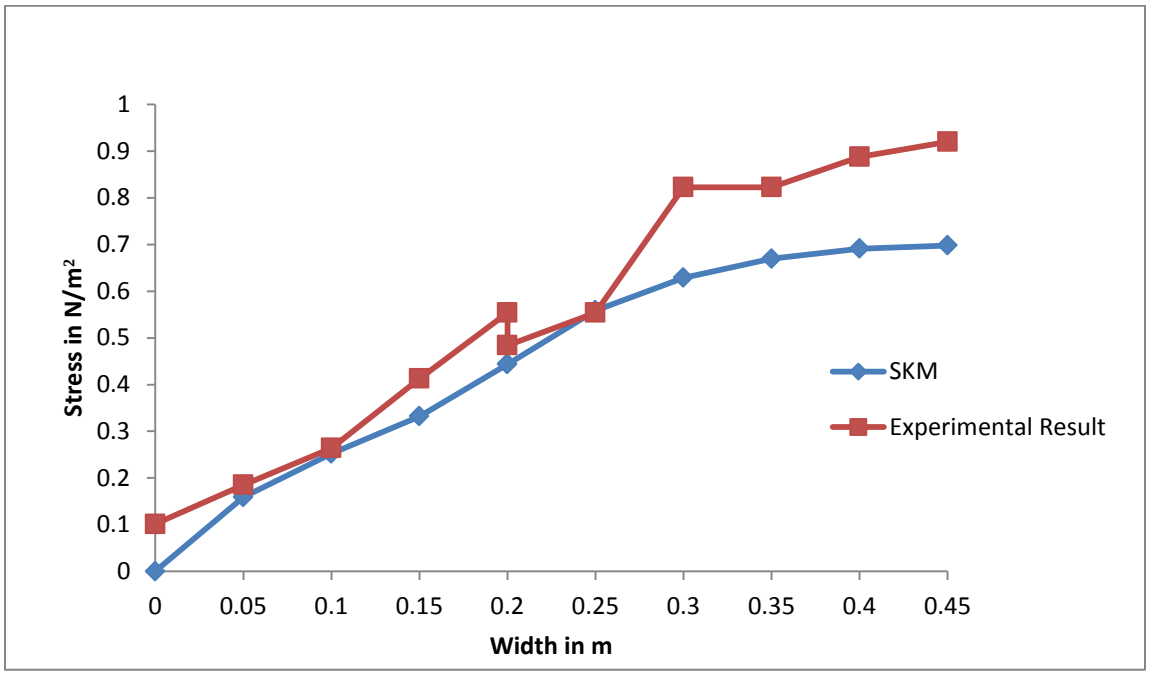

Fig.4.7.(i): Boundary shear distribution of section 1 of the straight channel for relative depth 0.15

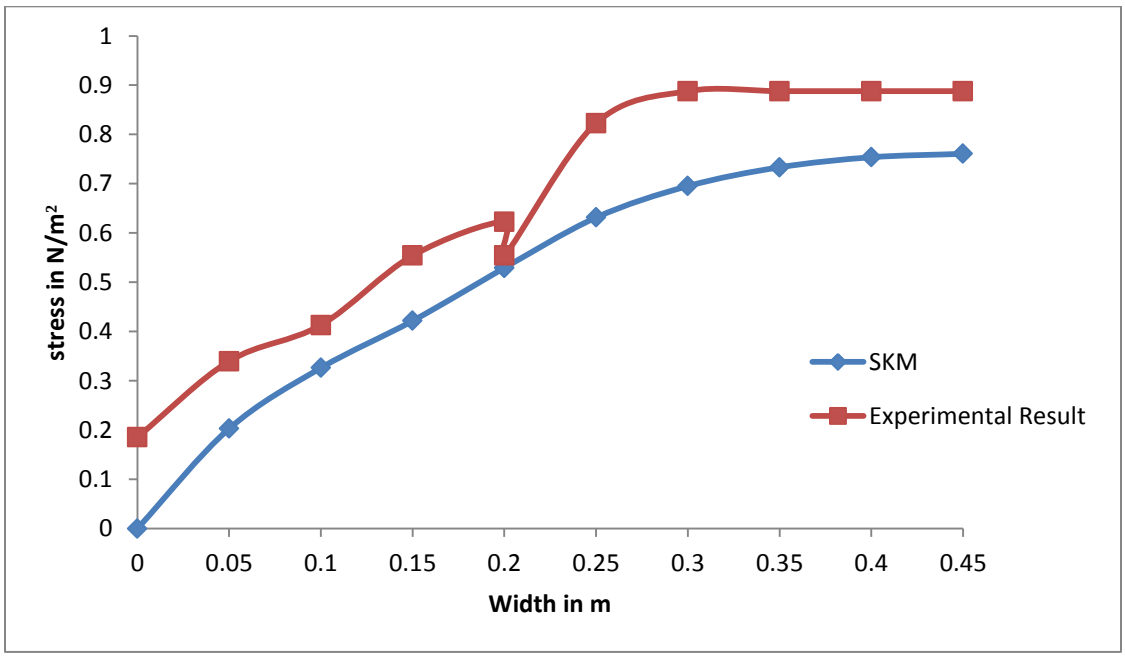

Fig.4.7.(ii): Boundary shear distribution of section 1 of the straight channel for relative depth 0.2

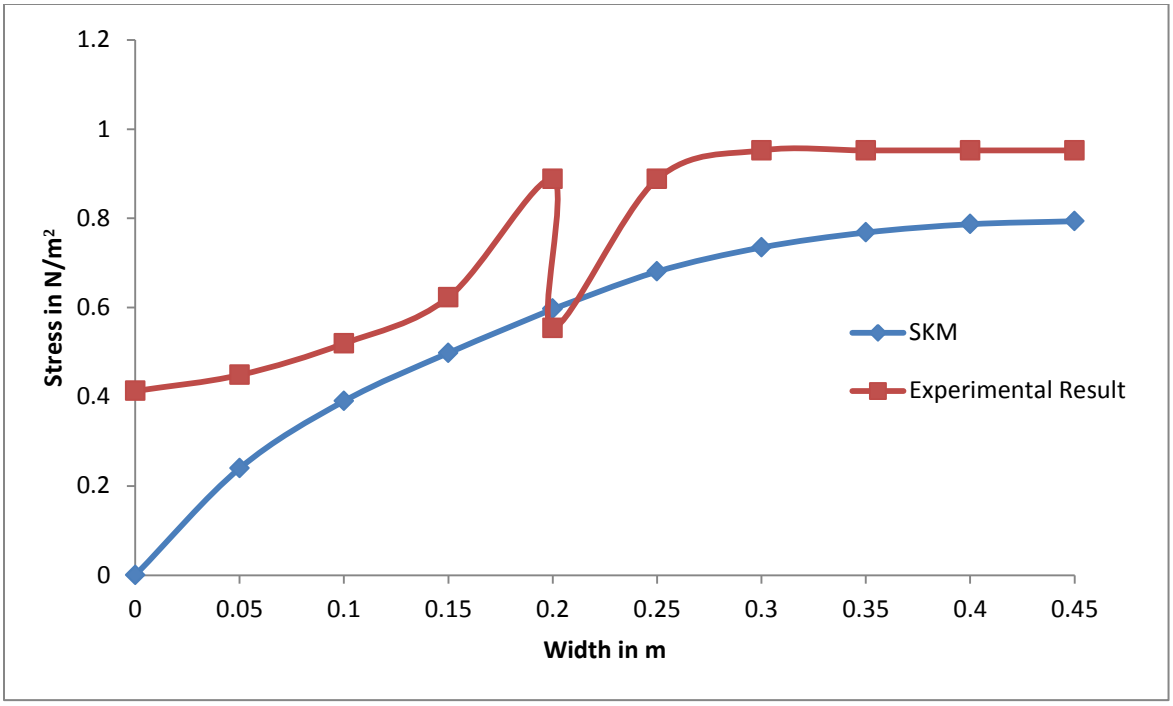

Fig.4.7.(iii): Boundary shear distribution of section 1 of the straight channel for relative depth 0.25

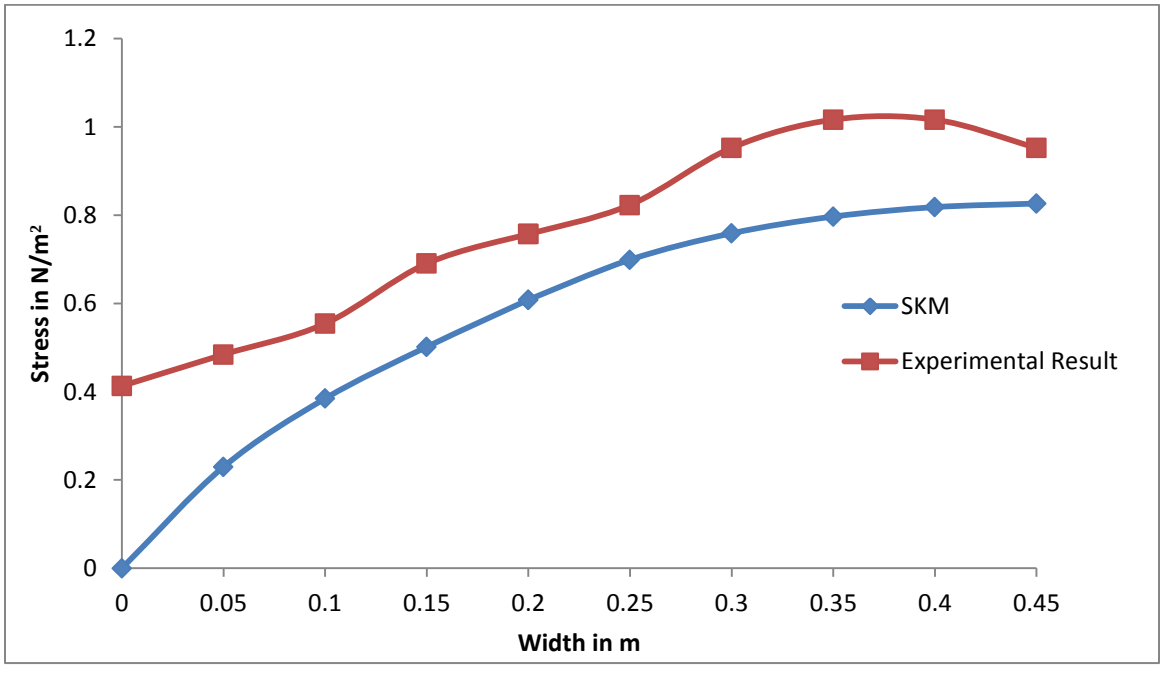

Fig.4.7.(iv): Boundary shear distribution of section 1 of the straight channel for relative depth 0.3

4.6.3. Comparison of Discharge with SKM

Table 4.1: Percentage of error in discharge through SKM

Depth of flow (m)	α	β	Observed discharge (m^3/s)	Discharge obtained from SKM (m^3/s)	% of error
0.119	1.8	0.15	0.037594	0.03516	-6.47426
0.127	1.8	0.20	0.039444	0.040672	3.113372
0.138	1.8	0.25	0.04618	0.04708	1.950242
0.149	1.8	0.30	0.052165	0.052774	1.167085

Here the percentage of error in discharge is found out and the graph (Fig 4.8) is plotted between percentage of error and the relative depths of the channel.

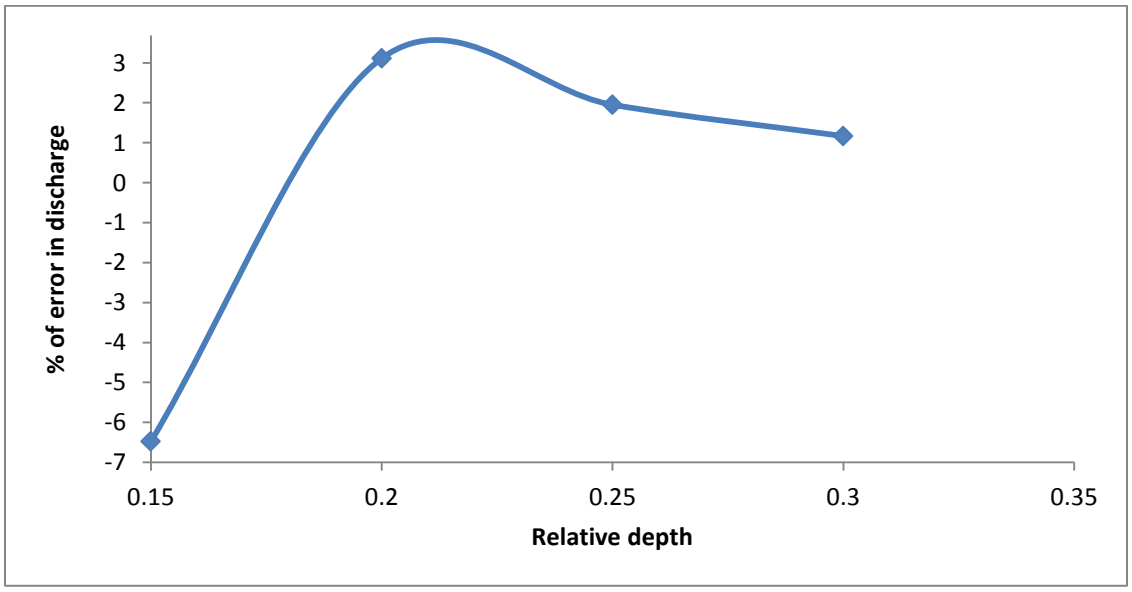

Fig.4.8: Error in discharge through SKM

From the error analysis the average percentage of error is found to be 3%.

4.7 Comparison of discharge prediction approaches

In the early years discharge prediction was done by single channel method. In this method, it considers the channel section as a single channel and discharge is predicted by using manning's formula. This method gives good result for simples channels but when it is used for compound channel it over estimated the discharge for which it could not be in river flow analysis. After this Divided Channel method was developed where it divided the channel in both horizontal and vertical interfaces and depending upon the division the discharge was estimated. Though it gives better discharge prediction than Single channel method but it over estimated the discharge for the main channel and under estimated the discharge for the flood plain. This was happened both the method did not quantify the momentum transfer. So many researchers worked on this, they developed some new models where they quantified the momentum transfer. Modified divided channel method, Interacting Divided channel method are two hydraulic model where the momentum exchange is quantified by interface length and shear stress respectively, due to which these models are able to predict the discharge in a better manner than divided channel method and single channel method. But Interacting divided channel method is limited to straight channels. Apart from these numerical methods some software are being developed which also do discharge prediction. Conveyance estimation system software developed by hydraulic engineers of United Kingdom which gives output in terms of discharge, water level, water surface profile, boundary shear stress, depth average d velocity, spatial velocity etc. Artificial neural network is the mathematical tool which can also be used to predict the discharge by using multilayer programming or back propagation technique. This method is reliable if the number of hidden layers is more so that number of iteration will be more.

Therefore we consider divided channel method, modified divided channel method, interacting divided channel method, CES and ANN for a comparison study on prediction of discharge. So here eleven sets of data of varying cross sections are being presented in the table 4.2.(i)-4.2(xi) where actual discharge and predicted discharge obtained through all these methods are tabulated. The percentage of error calculation is done for each of the method so that we can know that which methods are good in predicting discharge and which method is giving best discharge prediction result among these numerical as well as computational methods.

Table 4.2(i)

Series Name	observed discharge	MDCM	% of error	IDCM	% of error	DCM	% of error	CES	% of error	ANN	% of error
Series-1 FCF data	0.2082	0.213	2.405	0.233	11.688	0.237	13.807	0.252	20.897	0.187	-9.998
	0.2337	0.240	2.622	0.258	10.408	0.265	13.431	0.282	20.859	0.233	-0.353
	0.2852	0.298	4.566	0.316	10.726	0.327	14.662	0.347	21.799	0.324	13.779
	0.3535	0.373	5.626	0.389	10.172	0.405	14.452	0.429	21.471	0.353	-0.094
	0.4511	0.472	4.634	0.486	7.792	0.505	12.011	0.536	18.719	0.326	-27.630
	0.6001	0.614	2.328	0.626	4.358	0.650	8.239	0.690	14.924	0.596	-0.629
	0.6046	0.617	2.093	0.629	4.100	0.653	7.967	0.690	14.104	0.607	0.444
	1.0145	1.021	0.658	1.030	1.528	1.061	4.603	1.113	9.663	1.464	44.294

Table 4.2(ii)

Series Name	observed discharge	MDCM	% of error	IDCM	% of error	DCM	% of error	CES	% of error	ANN	% of error
Series-2 FCF data	0.225	0.214	-4.959	0.220	-2.409	0.224	-0.665	0.242	7.458	0.187	-17.117
	0.241	0.235	-2.589	0.241	-0.097	0.248	3.010	0.267	10.528	0.205	-15.168
	0.268	0.268	-0.033	0.273	1.910	0.284	6.243	0.304	13.759	0.230	-13.914
	0.303	0.304	0.163	0.308	1.484	0.323	6.471	0.345	13.869	0.258	-14.839
	0.332	0.341	2.757	0.344	3.570	0.362	9.025	0.387	16.459	0.287	-13.579
	0.392	0.408	4.102	0.409	4.190	0.431	9.909	0.458	16.711	0.339	-13.542
	0.558	0.562	0.760	0.556	-0.290	0.586	5.085	0.624	11.925	0.463	-16.979
	0.558	0.566	1.353	0.560	0.275	0.590	5.675	0.628	12.519	0.466	-16.488
	0.836	0.847	1.356	0.825	-1.291	0.867	3.667	0.925	10.599	0.710	-15.035
	0.835	0.853	2.157	0.830	-0.540	0.872	4.450	0.931	11.544	0.715	-14.307

Table 4.2(iii)

Series Name	observed discharge	MDCM	% of error	IDCM	% of error	DCM	% of error	CES	% of error	ANN	% of error
Series -3 FCF data	0.225	0.214	-4.959	0.220	-2.409	0.224	-0.665	0.242	7.458	0.187	-17.117
	0.241	0.235	-2.589	0.241	-0.097	0.248	3.010	0.267	10.528	0.205	-15.168
	0.268	0.268	-0.033	0.273	1.910	0.284	6.243	0.304	13.759	0.230	-13.914
	0.303	0.304	0.163	0.308	1.484	0.323	6.471	0.345	13.869	0.258	-14.839
	0.332	0.341	2.757	0.344	3.570	0.362	9.025	0.387	16.459	0.287	-13.579
	0.392	0.408	4.102	0.409	4.190	0.431	9.909	0.458	16.711	0.339	-13.542
	0.558	0.562	0.760	0.556	-0.290	0.586	5.085	0.624	11.925	0.463	-16.979
	0.558	0.566	1.353	0.560	0.275	0.590	5.675	0.628	12.519	0.466	-16.488
	0.836	0.847	1.356	0.825	-1.291	0.867	3.667	0.925	10.599	0.710	-15.035
	0.835	0.853	2.157	0.830	-0.540	0.872	4.450	0.931	11.544	0.715	-14.307

Table 4.2(iv)

Series Name	observed discharge	MDCM	% of error	IDCM	% of error	DCM	% of error	CES	% of error	ANN	% of error
Series-8 FCF data	0.186	0.186	0.132	0.197	6.261	0.201	8.209	0.208	12.123	0.208	11.864
	0.206	0.212	2.829	0.225	8.799	0.232	12.263	0.254	23.125	0.219	6.258
	0.238	0.248	4.252	0.260	9.122	0.270	13.476	0.296	24.319	0.244	2.644
	0.284	0.298	4.927	0.308	8.493	0.322	13.266	0.355	25.023	0.295	3.989
	0.344	0.363	5.608	0.371	7.991	0.388	12.813	0.432	25.717	0.383	11.398
	0.427	0.451	5.517	0.457	6.864	0.476	11.426	0.526	23.187	0.512	19.841
	0.690	0.703	1.798	0.702	1.645	0.726	5.169	0.804	16.470	0.771	11.776
	1.103	1.142	3.492	1.127	2.101	1.155	4.649	1.241	12.506	1.230	11.463

Table 4.2(v)

Series Name	observed discharge	MDCM	% of error	IDCM	% of error	DCM	% of error	CES	% of error	ANN	% of error
Series-10 FCF data	0.237	0.226	-4.432	0.239	1.114	0.243	2.675	0.277	16.795	0.236	-0.244
	0.263	0.257	-2.075	0.272	3.613	0.279	6.380	0.312	18.826	0.258	-1.911
	0.301	0.303	0.675	0.317	5.618	0.329	9.299	0.364	21.189	0.292	-2.787
	0.351	0.359	2.077	0.373	6.027	0.387	10.216	0.427	21.642	0.344	-2.065
	0.429	0.440	2.653	0.452	5.469	0.471	9.882	0.518	20.776	0.439	2.248
	0.429	0.442	2.880	0.454	5.688	0.473	10.111	0.519	21.032	0.440	2.550
	0.522	0.541	3.619	0.551	5.483	0.574	9.897	0.629	20.418	0.574	9.988
	0.807	0.824	2.087	0.827	2.418	0.858	6.303	0.932	15.432	0.874	8.303
	1.094	1.119	2.336	1.114	1.804	1.151	5.235	1.238	13.170	1.094	0.038

Table 4.2(vi)

Series Name	observed discharge	MDCM	% of error	IDCM	% of error	DCM	% of error	CES	% of error	ANN	% of error
K&D-2	0.005	0.005	-6.621	0.005	-6.372	0.005	-1.451	0.006	11.538	0.005	-12.981
	0.006	0.006	-5.803	0.006	-5.999	0.006	-0.506	0.007	15.625	0.005	-15.673
	0.007	0.007	-5.956	0.007	-6.195	0.007	-0.840	0.009	16.753	0.006	-17.201
	0.009	0.009	-5.021	0.009	-5.280	0.009	-0.256	0.011	19.481	0.008	-17.023
	0.012	0.011	-4.702	0.011	-5.055	0.012	-0.165	0.014	20.598	0.010	-14.829
	0.017	0.016	-6.341	0.016	-7.142	0.017	-2.039	0.020	19.298	0.016	-8.355

Table 4.2(vii)

Series Name	observed discharge	MDCM	% of error	IDCM	% of error	DCM	% of error	CES	% of error	ANN	% of error
K&D-3	0.007	0.007	2.64	0.007	3.498	0.007	8.79	0.008	23.522	0.007	4.25
	0.008	0.008	-1.85	0.008	-1.131	0.008	3.45	0.010	19.006	0.008	-0.53
	0.011	0.011	-5.55	0.011	-4.860	0.011	-1.46	0.013	15.695	0.011	-3.67
	0.015	0.014	-7.90	0.014	-7.176	0.014	-4.64	0.017	13.531	0.015	-1.30
	0.023	0.021	-9.18	0.021	-8.482	0.022	-6.66	0.026	12.650	0.029	24.01

Table 4.2(viii)

Series Name	observed discharge	MDCM	% of error	IDCM	% of error	DCM	% of error	CES	% of error	ANN	% of error
K&D-4	0.008	0.007	-1.135	0.008	0.126	0.008	4.789	0.009	20.667	0.010	29.918
	0.009	0.009	1.400	0.009	2.434	0.010	6.379	0.011	24.286	0.012	31.768
	0.014	0.013	-2.906	0.013	-2.005	0.014	0.502	0.016	19.259	0.017	29.304
	0.018	0.018	-0.620	0.018	0.294	0.018	1.979	0.022	21.944	0.022	24.380
	0.029	0.029	-0.756	0.029	0.090	0.030	0.964	0.035	19.694	0.031	6.963

Table 4.2(ix)

Series Name	observed discharge	MDCM	% of error	IDCM	% of error	DCM	% of error	CES	% of error	ANN	% of error
Atbay	0.012	0.012	-0.236	0.012	-0.564	0.012	1.441	0.010	-17.670	0.012	-0.487
	0.015	0.016	1.075	0.015	-1.902	0.016	1.545	0.013	-17.911	0.016	7.020
	0.018	0.019	4.392	0.018	0.323	0.019	4.245	0.015	-16.726	0.020	10.935
	0.021	0.022	5.791	0.021	1.272	0.022	5.287	0.018	-16.003	0.023	11.476
	0.024	0.025	3.387	0.024	-1.128	0.025	2.731	0.020	-18.059	0.026	8.131
	0.024	0.022	-5.639	0.022	-9.688	0.022	-6.111	0.021	-11.186	0.024	-0.665
	0.027	0.027	-1.334	0.026	-5.651	0.027	-2.034	0.024	-13.236	0.028	2.795
	0.030	0.030	-1.128	0.028	-5.411	0.029	-1.910	0.025	-15.401	0.031	2.724
	0.034	0.032	-6.777	0.031	-10.753	0.032	-7.554	0.032	-8.333	0.033	-3.053
	0.040	0.038	-4.518	0.037	-8.382	0.038	-5.363	0.033	-17.992	0.040	0.367
	0.045	0.042	-7.554	0.040	-11.180	0.041	-8.381	0.037	-17.333	0.044	-2.269
	0.050	0.047	-5.854	0.045	-9.356	0.047	-6.696	0.040	-21.041	0.050	-0.331
	0.055	0.050	-9.341	0.048	-12.627	0.049	-10.149	0.043	-22.470	0.053	-4.352
	0.060	0.054	-9.783	0.052	-12.930	0.054	-10.578	0.045	-24.996	0.057	-5.459

Table 4.2(x)

Series Name	observed discharge	MDCM	% of error	IDCM	% of error	DCM	% of error	CES	% of error	ANN	% of error
Rezai	0.012	0.014	12.617	0.014	16.344	0.014	13.662	0.013	4.250	0.012	-3.664
	0.013	0.015	15.193	0.015	20.138	0.015	15.654	0.014	13.490	0.013	-0.022
	0.014	0.016	18.098	0.017	23.806	0.016	17.951	0.016	16.296	0.014	3.450
	0.015	0.017	13.334	0.018	18.966	0.017	12.997	0.018	19.553	0.015	-0.436
	0.015	0.018	17.420	0.019	23.406	0.018	16.839	0.017	8.260	0.016	3.523
	0.018	0.021	14.687	0.022	20.651	0.020	13.857	0.020	13.296	0.018	1.724
	0.021	0.024	12.396	0.025	18.246	0.023	11.429	0.023	11.000	0.021	0.502
	0.024	0.026	10.067	0.028	15.757	0.026	9.048	0.026	8.583	0.024	-0.712
	0.027	0.029	7.240	0.030	12.743	0.029	6.199	0.029	5.696	0.026	-2.359
	0.029	0.031	7.902	0.033	13.404	0.031	6.814	0.031	6.221	0.029	-0.811
	0.030	0.033	8.602	0.034	14.121	0.032	7.481	0.032	6.853	0.030	0.431
	0.035	0.039	10.149	0.040	15.685	0.038	8.875	0.038	8.057	0.037	5.078
	0.040	0.045	12.698	0.047	18.335	0.044	11.203	0.044	10.276	0.045	11.939
	0.045	0.050	10.967	0.053	16.517	0.049	9.318	0.049	8.371	0.052	14.328

Table 4.2(xi)

Series Name	observed discharge	MDCM	% of error	IDCM	% of error	DCM	% of error	CES	% of error	ANN	% of error
NIT Rourkela Data 2013-2014	0.029	0.029	-2.053	0.029	-0.490	0.030	3.129	0.035	21.104	0.032	10.220
	0.033	0.030	-0.080	0.031	-0.068	0.032	-0.028	0.039	0.193	0.033	0.014
	0.034	0.032	-0.073	0.032	-0.063	0.034	-0.019	0.041	0.204	0.035	0.005
	0.039	0.036	-0.081	0.036	-0.075	0.038	-0.027	0.047	0.199	0.038	-0.043
	0.041	0.038	-0.073	0.038	-0.068	0.040	-0.018	0.046	0.136	0.039	-0.049
	0.044	0.041	-0.061	0.041	-0.058	0.044	-0.007	0.054	0.230	0.041	-0.061
	0.046	0.044	-0.057	0.044	-0.055	0.046	-0.003	0.055	0.198	0.043	-0.070
	0.049	0.043	-0.117	0.048	-0.027	0.050	0.026	0.062	0.274	0.026	-0.464
	0.052	0.052	0.006	0.052	0.006	0.055	0.061	0.069	0.322	0.050	-0.047
	0.059	0.065	0.109	0.065	0.108	0.068	0.167	0.086	0.460	0.060	0.025

Table 4.2(i)-4.2(xi): Percentage of error calculation for discharge through hydraulic models

4.8 Determination of average absolute error

The by averaging the percentage of error in discharge for all sets of data average absolute error is found out. The average absolute error value is shown in the table 4.4 and it is shown in the form of bar chart in the fig4.9.

Table 4.3: Average absolute error value

Average Absolute error	MDCM	IDCM	DCM	CES	ANN
	4.070955	5.782871	6.549618	14.50004	9.11942

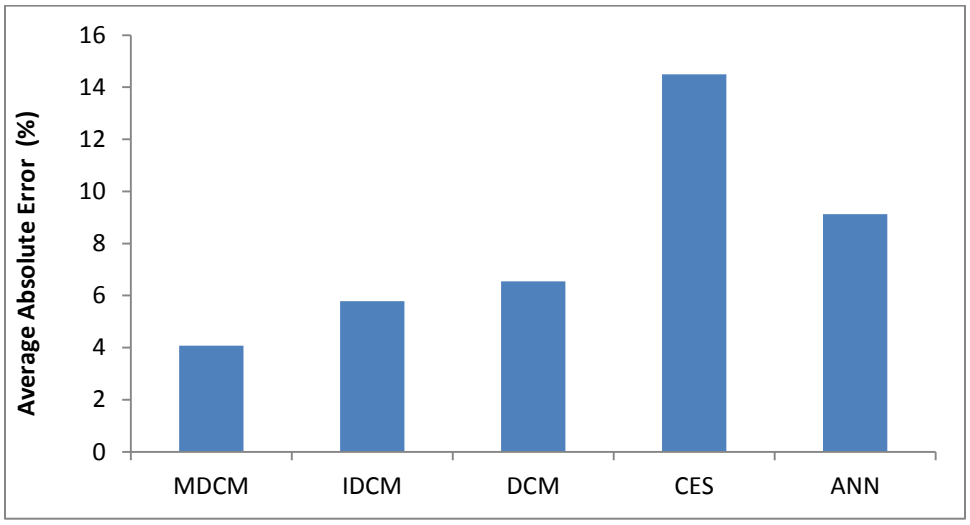

Fig4.9: average absolute error in all five methods.

In all the above numerical methods the value of n is kept constant with respect to the surface roughness. Historically both the Chézy and the Manning coefficients were expected to be constant and functions of the roughness only. But it is now well known that these coefficients are only constant for a range of flow rates. Though surface roughness is most influencing factor but it is seen that there are some other factors which influence the value of manning's *n*. Therefore it is required to know how it affects the discharge if the value of *n* is changed. The variation of *n* value with flow rate is required to be studied and discharge is predicted by varying *n* values. But before that the other hydraulic parameters of the channels has to be found out to know flow characteristics.

4.9 Determination of hydraulic parameters of collected data set

Discharge prediction is one of the most uncertain area of hydraulic engineering as it is influenced by both geometrical parameter as well as hydraulic parameters. As geometrical parameters we can consider the relative depth, width ratio and shape of the channel etc. and as hydraulic parameter channel roughness, Reynolds number, Froude's number etc. So it is required to find out these parameters.

The channel roughness is commonly known as manning's n. The channel roughness is required to find out to know the type of bed material is available.. Generally the value of manning's n is depends upon various factors such as surface roughness, channel shape, type of vegetation, the depth of flow etc. many researchers have given the range of n value for open channels depending upon the surface characteristics. Manning's n can be found out using the equation given below

$$n = \frac{1}{\mathrm{Q}} \mathrm{AR}^{\frac{2}{3}} \mathrm{S}_{\mathrm{o}}^{\frac{1}{2}} \tag{4.2}$$

Where *Q*= discharge of the channel

A= total cross sectional area of the channel

R= Hydraulic radius of the channel

S_o= bed slope of the channel

Reynolds number is the ratio of inertia force to viscous force. By the help of Reynolds number, whether the fluid flowing in the channel is laminar or turbulent is known. As we know if the Reynolds number values is less than 500, the flowing fluid is considered to be laminar, if its value is greater than 2000 then it comes under turbulent flow category and if its values lies in between 500 to 2000 then it comes under transition zone. So to understand this we need to find out the Reynolds number for each experimental run. The Reynolds number can be calculated using the formula given below for open channel.

$$\rho = \frac{VR}{\nu} \tag{4.3}$$

Where ρ= density of flowing fluid

V= mean velocity of the flowing fluid

R= hydraulic radius of the channel

ν= kinematic viscosity of the flowing fluid

Darcy-Weisbach co-efficient of friction is required to find out to evaluate the shear stress at the boundary. So to understand the effect of shear stress or effect of friction on fluid flowing through the channel it is required to find out by using the formula given below

$$f = \frac{8gn^2}{R^{1/3}} \tag{4.4}$$

Where *f*= co-efficient of friction of the channel

g= acceleration due to gravity

R= hydraulic radius of the channel

n= manning's n for the channel

To know the profile of the channel it is required to find out the Froude's number. By knowing the values of Froude's number we can conclude that whether the flow type is subcritical or supercritical. The Froude's number is calculated by using the formula given below.

$$F_r = \frac{V}{\sqrt{gD}} \tag{4.5}$$

Where F_r = Froude's number

V= mean velocity of the flowing fluid

g= acceleration due to gravity

D= hydraulic depth of the channel

Chezy's C is required to find out the velocity of the channel and it can be found out by using the formulae given below.

$$C = \sqrt{\frac{8g}{f}} \tag{4.6}$$

$$C = \frac{R^{\frac{1}{6}}}{n} \tag{4.7}$$

Where *C* = Chezy's constant

R= hydraulic radius of the channel

g= acceleration due to gravity

n= manning's n for the channel

f= co-efficient of friction of the channel

Here hydraulic parameters of the eleven data sets are presented in the Table 4.4.(i)-4.4(xi).

Table 4.4(i)

Series name	Observed discharge	Area	Radius	mean velocity	Manning's *n*	Chezy's *C*	Darcy's *f*	Reynolds number	Froude's Number
	Q (m3/s)	*A* (m^2)	*R*(m)	*V* (m/s)				(*Re*)	(*Fr*)
FCF Series-1	0.2082	0.3374	0.033416	0.617072	0.005387863	105.3356	0.007073	73642.43	1.073541
	0.2337	0.3994	0.039332	0.585128	0.006334273	92.06483	0.009259	82193.22	0.936205
	0.2852	0.5038	0.049511	0.566098	0.007632992	79.38811	0.012452	100100.1	0.807306
	0.3535	0.6131	0.060123	0.576578	0.008530127	73.37559	0.014577	123806.3	0.746174
	0.4511	0.7356	0.071963	0.613241	0.009041239	71.333	0.015423	157610	0.725413
	0.6001	0.8886	0.086672	0.675332	0.009293644	71.5803	0.015317	209043.4	0.727941
	0.6046	0.8918	0.086978	0.677955	0.009279517	71.73149	0.015252	210597.8	0.729479
	1.0145	1.2487	0.120945	0.812445	0.009646814	72.89777	0.014768	350933.5	0.741371

Table 4.4(ii)

Series name	Observed discharge	Area	Radius	mean velocity	Manning's *n*	Chezy's *C*	Darcy's *f*	Reynolds number	Froude's Number
	Q (m3/s)	*A* (m^2)	*R*(m)	*V* (m/s)				(*Re*)	(*Fr*)
FCF Series-2	0.2123	0.28842	0.0448	0.736056	0.005491928	108.5145	0.006665	117768.3	1.099446
	0.2483	0.36585	0.056564	0.678694	0.006957767	89.0471	0.009897	137105.1	0.901873
	0.2492	0.37326	0.057684	0.66762	0.00716622	86.73981	0.010431	137538.2	0.878463
	0.2821	0.42366	0.065262	0.665853	0.007801516	81.33249	0.011864	155195.3	0.823403
	0.3237	0.48043	0.073731	0.673758	0.008363365	77.42727	0.013091	177417.4	0.783502
	0.32382	0.48165	0.073911	0.672313	0.008394966	77.16715	0.013179	177468.9	0.780862
	0.3832	0.55194	0.084299	0.694268	0.008874445	74.61559	0.014096	209023	0.754562
	0.48	0.65190	0.09889	0.736305	0.009307418	73.06279	0.014702	260047.5	0.738141
	0.763	0.87807	0.131146	0.868944	0.009519845	74.87369	0.013999	406994.6	0.754659
	1.1142	1.13561	0.16665	0.981142	0.009891394	74.99694	0.013953	583956.2	0.753806

Table 4.4(iii)

Series name	Observed Discharge	Area	Radius	mean velocity	Manning's *n*	Chezy's *C*	Darcy's *f*	Reynolds number	Froude's Number
	Q (m3/s)	*A* (m^2)	*R*(m)	*V* (m/s)				(*Re*)	(*Fr*)
FCF Series-3	0.2251	0.273964	0.079616	0.821641	0.00721833	90.865	0.009505	233627.6	0.912658
	0.2412	0.301456	0.08713	0.800118	0.00787184	84.58336	0.01097	248979.1	0.849367
	0.2676	0.337731	0.09688	0.792345	0.008531502	79.43524	0.012437	274150.3	0.797244
	0.3031	0.373635	0.10635	0.811219	0.008867561	77.62206	0.013025	308117.3	0.778492
	0.3323	0.40834	0.115339	0.813783	0.009330969	74.77145	0.014037	335216.7	0.749294
	0.3922	0.464647	0.129591	0.844081	0.009722652	73.16631	0.01466	390662.2	0.73211
	0.5579	0.579455	0.157448	0.962801	0.009705267	75.71505	0.01369	541397.7	0.754989
	0.5581	0.581903	0.158025	0.959095	0.009766554	75.28581	0.013846	541290.7	0.75065
	0.836	0.762193	0.19876	1.096836	0.009950927	76.76998	0.013316	778598	0.760907
	0.8349	0.765504	0.199477	1.090654	0.010031377	76.20001	0.013516	777002.5	0.755174

Table 4.4(iv)

Series name	Observed Discharge	Area	Radius	mean velocity	Manning's *n*	Chezy's *C*	Darcy's *f*	Reynolds number	Froude's Number
	Q (m3/s)	*A* (m^2)	*R*(m)	*V* (m/s)				(*Re*)	(*Fr*)
FCF Series-8	0.1858	0.272823	0.043186	0.681027	0.005792292	102.2603	0.007505	105038.9	1.021033
	0.2064	0.327289	0.051626	0.630635	0.007045634	86.60804	0.010463	116276	0.864531
	0.23815	0.384884	0.060472	0.618758	0.007979313	78.51629	0.01273	133633.3	0.783446
	0.28406	0.451832	0.070653	0.628686	0.008711714	73.80476	0.014408	158636.6	0.736019
	0.34398	0.527988	0.082104	0.651492	0.009292224	70.94818	0.015591	191036.5	0.707022
	0.42726	0.618183	0.095492	0.691155	0.009686959	69.7922	0.016112	235712.9	0.694865
	0.69018	0.836364	0.127118	0.825215	0.009817974	72.22358	0.015045	374640.3	0.717375
	1.1034	1.145799	0.170223	0.962996	0.010221302	72.83333	0.014794	585443.2	0.720921

Table 4.4(v)

Series name	Observed discharge	Area	Radius	mean velocity	Manning's *n*	Chezy's *C*	Darcy's *f*	Reynolds number	Froude's Number
	Q (m3/s)	*A* (m^2)	*R*(m)	*V* (m/s)				(*Re*)	(*Fr*)
FCF Series-10	0.2368	0.323062	0.048303	0.732985	0.005798837	104.0691	0.007246	126448.4	1.059052
	0.2627	0.379836	0.056617	0.691615	0.006832047	90.69987	0.00954	139846.5	0.92277
	0.3006	0.445868	0.066206	0.67419	0.007779209	81.76128	0.01174	159412.7	0.831488
	0.3514	0.515636	0.076246	0.681489	0.00845546	77.01325	0.013232	185573.9	0.782792
	0.429	0.604711	0.088929	0.70943	0.00899988	74.23411	0.014241	225316.3	0.75398
	0.4292	0.605917	0.089099	0.708348	0.00902516	74.04984	0.014312	225404.4	0.7521
	0.522	0.701946	0.102603	0.743647	0.009444787	72.4438	0.014954	272501.5	0.735149
	0.8071	0.93524	0.13471	0.862987	0.009758458	73.37005	0.014579	415189.2	0.742878
	1.0939	1.142842	0.16248	0.957175	0.00996919	74.09803	0.014294	555434	0.748698

Table 4.4(vi)

Series name	Observed discharge	Area	Radius	mean velocity	Manning's *n*	Chezy's *C*	Darcy's *f*	Reynolds number	Froude's Number
	Q (m3/s)	*A* (m^2)	*R*(m)	*V* (m/s)				(*Re*)	(*Fr*)
Knight & Demetriou -1	0.005200	0.01444	0.0304	0.360111	0.008406879	66.45242	0.017772	39097.74	0.527539
	0.006400	0.017184	0.031394	0.372433	0.008304932	67.62974	0.017159	41757.3	0.500131
	0.007300	0.018928	0.034853	0.385668	0.008598712	66.46701	0.017764	48005.66	0.49347
	0.009450	0.022932	0.037517	0.412095	0.008452279	68.4537	0.016748	55215.92	0.479052
	0.011700	0.0267	0.043197	0.438208	0.008731884	67.83705	0.017054	67603.87	0.472095
	0.017100	0.034382	0.048051	0.497347	0.008259656	72.99975	0.014727	85349.67	0.472165
	0.005000	0.015035	0.056718	0.33256	0.013796388	44.92844	0.038879	67364.68	0.477444

Table 4.4(vii)

Series name	Observed discharge	Area	Radius	mean velocity	Manning's *n*	Chezy's *C*	Darcy's *f*	Reynolds number	Froude's Number
	Q (m3/s)	*A* (m^2)	*R*(m)	*V* (m/s)				(*Re*)	(*Fr*)
Knight & Demetriou -2	0.006700	0.020709	0.025017	0.323532	0.008217234	65.81321	0.018119	28906.28	0.484716
	0.008050	0.02292	0.03195	0.351223	0.008910207	63.22048	0.019636	40077.31	0.500178
	0.011150	0.028011	0.03484	0.398057	0.008329064	68.61469	0.01667	49529.89	0.512777
	0.015150	0.033896	0.041181	0.446955	0.008292604	70.86401	0.015628	65736.41	0.523405
	0.023400	0.044982	0.048011	0.520203	0.007892445	76.38575	0.01345	89198.7	0.528809
	0.004900	0.015661	0.059609	0.312877	0.015158495	41.23151	0.046164	66608.21	0.539027

Table 4.4(viii)

Series name	Observed discharge	Area	Radius	mean velocity	Manning's *n*	Chezy's *C*	Darcy's *f*	Reynolds number	Froude's Number
	Q (m3/s)	*A* (m^2)	*R*(m)	*V* (m/s)				(*Re*)	(*Fr*)
Knight & Demetrious -3	0.007500	0.023467	0.029364	0.319594	0.009256137	60.00745	0.021795	33515.87	0.519379
	0.009100	0.027452	0.033795	0.331493	0.009800465	58.01784	0.023315	40009.8	0.498091
	0.013500	0.03483	0.041634	0.3876	0.009632432	61.11838	0.021009	57633.2	0.517042
	0.018000	0.042744	0.049553	0.421108	0.009957231	60.86567	0.021184	74524.97	0.507075
	0.029400	0.058882	0.064304	0.4993	0.009991211	63.35117	0.019555	114667.3	0.512254

Table 4.4(ix)

Series name	Observed discharge	Area	Radius	mean velocity	Manning's *n*	Chezy's *C*	Darcy's *f*	Reynolds number	Froude's Number
	Q (m3/s)	*A* (m^2)	*R*(m)	*V* (m/s)				(*Re*)	(*Fr*)
Atbay's Data	0.012	0.024506	0.01857	0.489684	0.006442751	79.87284	0.012302	32477.37	0.403679
	0.015349	0.031535	0.023689	0.48673	0.007624042	70.29214	0.015883	41179.63	0.401243
	0.018013	0.036989	0.0276	0.486977	0.008437236	65.15544	0.018487	48001.62	0.401447
	0.020953	0.041998	0.031145	0.498911	0.008926331	62.83835	0.019875	55494.78	0.411285
	0.024042	0.045716	0.033748	0.525896	0.008933891	63.63093	0.019383	63386.31	0.433531
	0.023836	0.04246	0.03147	0.561385	0.007988031	70.3411	0.015861	63095.23	0.462787
	0.027085	0.048179	0.035461	0.562173	0.008637713	66.35782	0.017823	71196.28	0.463436
	0.030012	0.051906	0.038031	0.578207	0.008799348	65.90323	0.018069	78535.89	0.476654
	0.034429	0.054837	0.040037	0.627839	0.008386257	69.74444	0.016134	89775.26	0.517569
	0.040052	0.061859	0.044785	0.64747	0.008762814	68.00579	0.016969	103561.5	0.533752
	0.044939	0.065427	0.047167	0.686857	0.008550672	70.29754	0.015881	115704.7	0.566222
	0.050026	0.071169	0.050959	0.702921	0.008797208	69.21363	0.016382	127928.4	0.579464
	0.055037	0.073955	0.05278	0.744192	0.008506145	72.00212	0.015138	140279.9	0.613486
	0.060025	0.078076	0.055452	0.768804	0.008509411	72.56931	0.014902	152255.4	0.633776

Table 4.4(x)

Series name	Observed discharge	Area	Radius	mean velocity	Manning's *n*	Chezy's *C*	Darcy's *f*	Reynolds number	Froude's Number
	Q (m3/s)	*A* (m^2)	*R*(m)	*V* (m/s)				(*Re*)	(*Fr*)
Rezai's Data	0.012	0.021574	0.030663	0.556215	0.007882668	70.9734	0.015966	70761.93	0.458524
	0.01275	0.023225	0.032752	0.54898	0.008345255	67.77966	0.018647	79460.45	0.45256
	0.013758	0.025177	0.03518	0.546457	0.008793296	65.0976	0.020537	86313.07	0.45048
	0.015	0.026059	0.036264	0.575608	0.008518539	67.53793	0.019898	88657.29	0.474511
	0.015472	0.027375	0.037863	0.565187	0.008928778	64.89989	0.021686	100838.7	0.465921
	0.0179	0.029887	0.040862	0.598931	0.008864992	66.20263	0.018495	105852.3	0.493738
	0.021	0.032936	0.044413	0.637592	0.008803085	67.60043	0.017579	118993.9	0.525609
	0.024	0.035568	0.047398	0.674771	0.008686769	69.25248	0.016412	134680	0.556258
	0.027	0.03784	0.049921	0.713531	0.008503854	71.35612	0.015174	155629.8	0.58821
	0.028968	0.039831	0.05209	0.727267	0.00858324	71.19916	0.015728	160363.9	0.599534
	0.03	0.04095	0.053292	0.732608	0.008651215	70.90877	0.016048	170954.5	0.603937
	0.035	0.045793	0.058365	0.764302	0.008810726	70.68828	0.015541	178497.7	0.630065
	0.0399	0.050697	0.063292	0.787029	0.009031288	69.8997	0.015014	199491.9	0.648799
	0.0451	0.054405	0.066885	0.828974	0.008895845	71.62007	0.014003	221806.6	0.683378

Table 4.4(xi)

Series name	Observed discharge	Area	Radius	mean velocity	Manning's *n*	Chezy's *C*	Darcy's *f*	Reynolds number	Froude's Number
	Q (m3/s)	*A* (m^2)	*R*(m)	*V* (m/s)				(*Re*)	(*Fr*)
NIT Rourkela Data 2013-2014	0.02919	0.05999	0.053457	0.486577	0.009222618	66.54987	0.01772	32473.39	0.401117
	0.033	0.06323	0.055985	0.521904	0.008867329	69.75142	0.016131	36478.22	0.43024
	0.034403	0.065882	0.058031	0.522189	0.009077077	68.54841	0.016702	37831.67	0.430474
	0.039207	0.0725	0.063043	0.540787	0.009262619	68.10927	0.016918	42563.17	0.445806
	0.04081	0.0752	0.065052	0.542682	0.009425284	67.28458	0.017335	44073.05	0.447369
	0.043891	0.08006	0.068615	0.548232	0.009667518	66.18428	0.017916	46962.49	0.451944
	0.046164	0.0833	0.070954	0.554186	0.009779774	65.79113	0.018131	49090.81	0.456852
	0.048861	0.088571	0.074699	0.551657	0.01016731	63.82823	0.019263	51445.8	0.454767
	0.052165	0.095	0.079167	0.549105	0.010617916	61.7141	0.020606	54270.7	0.452663

Table 4.4(i)-4.4(xi): Determination of hydraulic parameters

From the tables it is found that the values of *n* are changing very significantly with respect to flow depths. So now it is required to find out the discharge for all the eleven channels data by using MDCM with the varying n values.

4.10 Effect of '*n*' On MDCM

From the comparison study it is seen that MDCM is the best method among those five methods for predicting discharge by keep n value constant with respect to surface roughness of the channel. Therefore in the present work all eleven data sets are validated by MDCM for discharge prediction by changing the value of *n* with respect to the depth of flow.. From the calculation it is found that the MDCM is overestimating the discharge with a maximum error of 35% for lower depth of flow while for higher depth of flow, the error has been reduced to 2%. So there is a large variation in error is occurring for all depth of flow. Therefore this method needs few modifications.

Khatua (2007) proposed an equation for $\%S_{fp}$ (equation 3.2.12, as shown in chapter-3) for a compound channel section having a width ratio varying from 2-6.67 as

$$\%S_{fp} = 4.105\left[\frac{100\beta(\alpha-1)}{1+\beta(\alpha-1)}\right]^{0.6917}$$

But the equation valid for a constant value of manning's *n*. therefore on the basis of simulation of the experimental data an empirical factor (E_f)is multiplied to it.

$$E_f = \left(1 + (0.25\beta + 1)^{(1-100\beta)}\right) \tag{4.8}$$

So the $\%S_{fp}$ is now re written as

$$\%S_{fp} = \left(4.105\left[\frac{100\beta(\alpha-1)}{1+\beta(\alpha-1)}\right]^{0.6917}\right)E_f \tag{4.9}$$

So the value obtain from equation (4.8) has been put in the equation (3.2.9) and (3.2.10) to get the values of X_{mc} andX_{fp}. The discharge is again computed through the equation (3.2.11) and the results are compared with MDCM and experimental data sets. The error obtained from both the methods is presented in the table 4.5.(i)-4.5(xi).

Table 4.5(i)

Series name	Depth of flow *H* (m)	Manning's *n*	Observed discharge *Q* (m3/s)	Discharge through MDCM	% of error	Discharge through Revised MDCM	% of error
FCF Series-1	0.15899	0.005388	0.2082	0.36895	77%	0.228586	10%
	0.16519	0.006334	0.2337	0.378637	62%	0.233336	0%
	0.17563	0.007633	0.2852	0.3907	37%	0.261201	-8%
	0.18656	0.00853	0.3535	0.437736	24%	0.331313	-6%
	0.19881	0.009041	0.4511	0.52207	16%	0.451171	0%
	0.21411	0.009294	0.6001	0.660719	10%	0.620229	3%
	0.21443	0.00928	0.6046	0.665143	10%	0.625064	3%
	0.25012	0.009647	1.0145	1.058544	4%	1.048342	3%

Table 4.5(ii)

Series name	Depth of flow *H* (m)	Manning's *n*	Observed discharge *Q* (m3/s)	Discharge through MDCM	% of error	Discharge through Revised MDCM	% of error
FCF Series-2	0.15649	0.005492	0.2123	0.346245	63%	0.252167	19%
	0.16873	0.006958	0.2483	0.354987	43%	0.269628	9%
	0.1699	0.007166	0.2492	0.351242	41%	0.27042	9%
	0.17784	0.007802	0.2821	0.367429	30%	0.293044	4%
	0.18676	0.008363	0.3237	0.396214	22%	0.335757	4%
	0.18695	0.008395	0.32382	0.395904	22%	0.33592	4%
	0.19796	0.008874	0.3832	0.444645	16%	0.40206	5%
	0.21355	0.009307	0.48	0.531133	11%	0.506803	6%
	0.24855	0.00952	0.763	0.800636	5%	0.793965	4%
	0.28795	0.009891	1.1142	1.140711	2%	1.139081	2%

Table 4.5(iii)

Series name	Depth of flow *H* (m)	Manning's *n*	Observed discharge *Q* (m3/s)	Discharge through MDCM	% of error	Discharge through Revised MDCM	% of error
FCF Series-3	0.158	0.007218	0.2251	0.296722	32%	0.264499	18%
	0.16627	0.007872	0.2412	0.299077	24%	0.270035	12%
	0.17712	0.008532	0.2676	0.314461	18%	0.286337	7%
	0.18779	0.008868	0.3031	0.34351	13%	0.320486	6%
	0.19804	0.009331	0.3323	0.367321	11%	0.350409	5%
	0.21454	0.009723	0.3922	0.421612	7%	0.411967	5%
	0.2477	0.009705	0.5579	0.577445	4%	0.574455	3%
	0.2484	0.009767	0.5581	0.584956	5%	0.58202	4%
	0.29922	0.009951	0.836	0.853225	2%	0.852699	2%
	0.30014	0.010031	0.8349	0.851885	2%	0.851377	2%

Table 4.5(iv)

Series name	Depth of flow *H* (m)	Manning's *n*	Observed discharge *Q* (m3/s)	Discharge through MDCM	% of error	Discharge through Revised MDCM	% of error
FCF Series-8	0.15796	0.005792	0.1858	0.281377	51%	0.210059	13%
	0.167	0.007046	0.2064	0.30152	46%	0.226227	10%
	0.17653	0.007979	0.23815	0.311474	31%	0.241262	1%
	0.18757	0.008712	0.28406	0.342514	21%	0.288397	2%
	0.20008	0.009292	0.34398	0.391371	14%	0.355588	3%
	0.21483	0.009687	0.42726	0.465878	9%	0.445184	4%
	0.25022	0.009818	0.69018	0.715908	4%	0.710426	3%
	0.29973	0.010221	1.1034	1.116371	1%	1.115431	1%

Table 4.5(v)

Series name	Depth of flow *H* (m)	Manning's *n*	Observed discharge *Q* (m3/s)	Discharge through MDCM	% of error	Discharge through Revised MDCM	% of error
FCF Series-10	0.15803	0.005799	0.2368	0.360451	52%	0.272253	15%
	0.1666	0.006832	0.2627	0.376866	43%	0.297139	13%
	0.17654	0.007779	0.3006	0.389485	30%	0.314824	5%
	0.18701	0.008455	0.3514	0.424746	21%	0.365663	4%
	0.20033	0.009	0.429	0.489967	14%	0.450984	5%
	0.20051	0.009025	0.4292	0.489913	14%	0.451253	5%
	0.21481	0.009445	0.522	0.573401	10%	0.550406	5%
	0.2493	0.009758	0.8071	0.845071	5%	0.838662	4%
	0.2797	0.009969	1.0939	1.123388	3%	1.121219	2%

Table 4.5(vi)

Series name	Depth of flow *H* (m)	Manning's *n*	Observed discharge *Q* (m3/s)	Discharge through MDCM	% of error	Discharge through Revised MDCM	% of error
Knight & Demetriou -1	0.085500	0.008407	0.005200	0.005776	11%	0.00522	0%
	0.094527	0.008305	0.006400	0.007259	13%	0.006788	6%
	0.100263	0.008599	0.007300	0.007984	9%	0.007647	5%
	0.113433	0.008452	0.009450	0.010619	12%	0.010476	11%
	0.125828	0.008732	0.011700	0.012769	9%	0.012711	9%
	0.151100	0.008260	0.017100	0.01939	13%	0.019378	13%

Table 4.5(vii)

Series name	Depth of flow *H* (m)	Manning's *n*	Observed discharge *Q* (m³/s)	Discharge through MDCM	% of error	Discharge through Revised MDCM (m³/s)	% of error
Knight & Demetriou -2	0.096081	0.008217	0.006700	0.00837	25%	0.007627	14%
	0.100930	0.008910	0.008050	0.008867	10%	0.008356	4%
	0.112094	0.008329	0.011150	0.012643	13%	0.012397	11%
	0.125000	0.008293	0.015150	0.016826	11%	0.016732	10%
	0.149312	0.007892	0.023400	0.026926	15%	0.026907	15%

Table 4.5(viii)

Series name	Depth of flow *H* (m)	Manning's *n*	Observed discharge *Q* (m3/s)	Discharge through MDCM	% of error	Discharge through Revised MDCM (m³/s)	% of error
Knight & Demetriou -2	0.095597	0.009256	0.007500	0.008011	7%	0.007056	-6%
	0.102151	0.009800	0.009100	0.009415	3%	0.008822	-3%
	0.114286	0.009632	0.013500	0.013608	1%	0.013369	-1%
	0.127303	0.009957	0.018000	0.017965	0%	0.017882	-1%
	0.153846	0.009991	0.029400	0.029203	-1%	0.02919	-1%

Table 4.5(ix)

Series name	Depth of flow *H* (m)	Manning's *n*	Observed discharge *Q* (m3/s)	Discharge through MDCM	% of error	Discharge through Revised MDCM (m³/s)	% of error
Atbay's Data	0.0538	0.006443	0.012	0.017676	47%	0.014791	23%
	0.0596	0.007624	0.015349	0.01898	24%	0.016038	4%
	0.0641	0.008437	0.018013	0.020807	16%	0.018781	4%
	0.0682	0.008926	0.020953	0.023146	10%	0.021839	4%
	0.0713	0.008934	0.024042	0.026005	8%	0.025056	4%
	0.0686	0.007988	0.023836	0.026253	10%	0.024848	4%
	0.0733	0.008638	0.027085	0.028975	7%	0.028188	4%
	0.0764	0.008799	0.030012	0.031678	6%	0.031128	4%
	0.0788	0.008386	0.034429	0.036034	5%	0.035593	3%
	0.0846	0.008763	0.040052	0.041299	3%	0.041078	3%
	0.0876	0.008551	0.044939	0.046085	3%	0.04592	2%
	0.0923	0.008797	0.050026	0.050952	2%	0.050854	2%
	0.0946	0.008506	0.055037	0.055907	2%	0.055828	1%

Table 4.5(x)

Series name	Depth of flow *H* (m)	Manning's *n*	Observed discharge *Q* (m3/s)	Discharge through MDCM	% of error	Discharge through Revised MDCM (m^3/s)	% of error
Rezai's Data	0.0528	0.007883	0.012	0.013514	13%	0.012846	7%
	0.05556	0.008345	0.01275	0.014687	15%	0.013774	8%
	0.058824	0.008793	0.013758	0.016248	18%	0.015307	11%
	0.0603	0.008519	0.015	0.017	13%	0.016104	7%
	0.0625	0.008929	0.015472	0.018167	17%	0.017373	12%
	0.0667	0.008865	0.0179	0.020529	15%	0.019957	11%
	0.0718	0.008803	0.021	0.023603	12%	0.023253	11%
	0.0762	0.008687	0.024	0.026416	10%	0.026195	9%
	0.08	0.008504	0.027	0.028955	7%	0.028807	7%
	0.08333	0.008583	0.028968	0.031257	8%	0.031153	8%
	0.0852	0.008651	0.03	0.032581	9%	0.032495	8%
	0.0933	0.008811	0.035	0.038552	10%	0.038514	10%
	0.1015	0.009031	0.0399	0.044967	13%	0.044949	13%
	0.1077	0.008896	0.0451	0.050046	11%	0.050036	11%

Table 4.5(xi)

Series name	Depth of flow *H* (m)	Manning's *n*	Observed discharge *Q* (m3/s)	Discharge through MDCM	% of error	Discharge through Revised MDCM (m^3/s)	% of error
NIT Rourkela Data 2013-2014	0.1111	0.009223	0.02919	0.0341	17%	0.03116	7%
	0.1147	0.008867	0.033	0.037666	14%	0.034468	4%
	0.117647	0.009077	0.034403	0.038664	12%	0.035592	3%
	0.125	0.009263	0.039207	0.042807	9%	0.040281	3%
	0.128	0.009425	0.04081	0.044162	8%	0.041934	3%
	0.1334	0.009668	0.043891	0.046882	7%	0.045154	3%
	0.137	0.00978	0.046164	0.048966	6%	0.047523	3%
	0.142857	0.010167	0.048861	0.051353	5%	0.050319	3%
	0.15	0.010618	0.052165	0.054365	4%	0.053684	3%
	0.16667	0.011851	0.058596	0.060326	3%	0.060076	3%
	0.2	0.014651	0.0684	0.069773	2%	0.069734	2%

Table 4.5(i)-4.5(xi) Calculation of percentage of error in discharge by varying the value of Manning's n.

From the table 4.4(i)-4.4(xi) we observed that the percentage of error is found to be less when the empirical factor is used in MDCM. The average absolute errors for Revised MDCM are found to be 5% whereas for MDCM it is observed to be 13%.

4.11 Establishment of linear relationship

Through Revised MDCM, and MDCM the discharge is calculated for all eleven numbers of data sets by considering the variation in manning's n. So a linear relationship is established between the discharge obtained from these methods and the actual discharge obtained from each experimental run. The Fig 4.10(i)-4.10(ii) the linear relationship is presented.

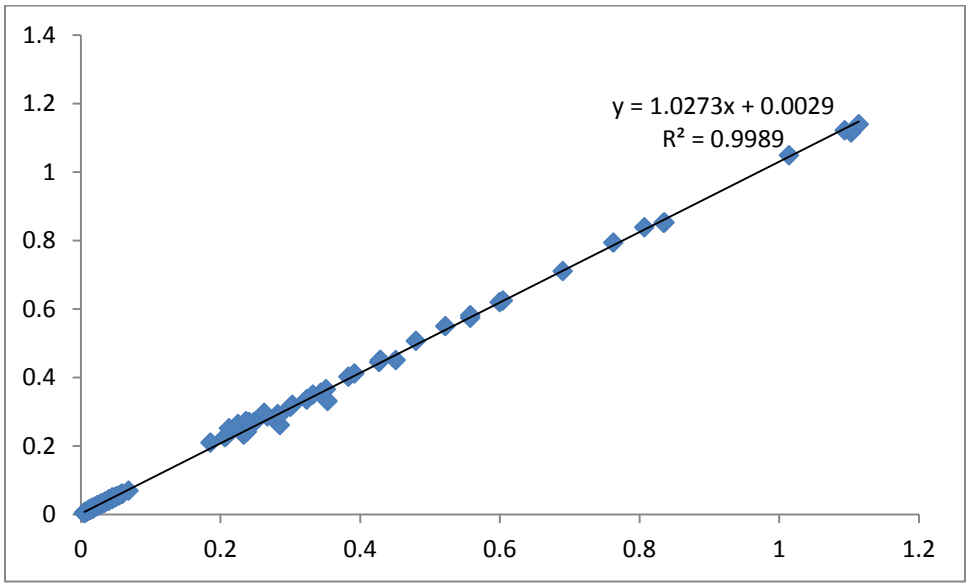

Fig.4.10.(i): Correlation plot of actual discharge and Discharge predicted by Revised MDCM

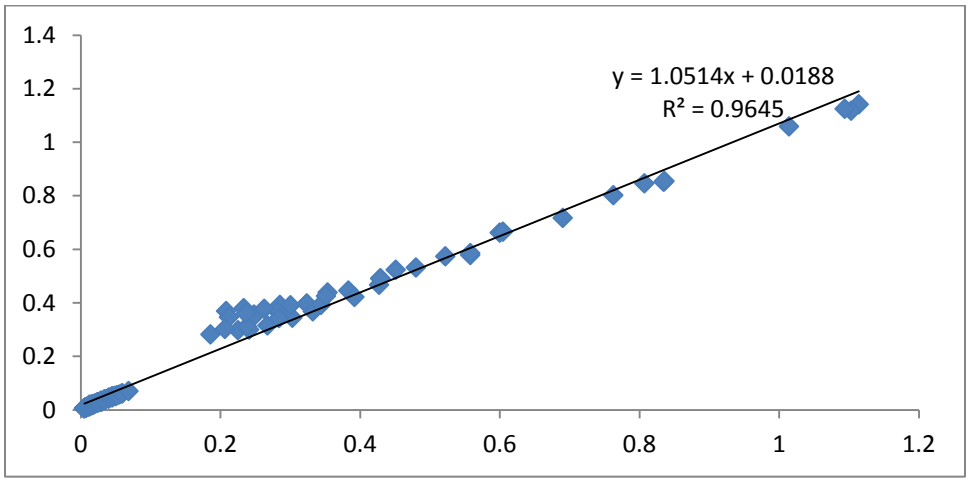

Fig.4.10.(ii): Correlation plot of actual discharge and Discharge predicted by MDCM

5.1 Conclusions

Experiments are carried out to analyze the flow pattern in a straight compound channel having narrow flood plains for four different relative depths. Observations are made at section-1 of the channel (as shown in the figure 3.2) for depth averaged velocity and wall shear data at different depth of flow. Apart from this, eleven data sets are tested through five different methods for predicting discharge and the obtained results are compared with the experimental results (as described in chapter 4). Based on analysis and discussions of the experimental investigations certain conclusions from the present work are drawn below.

- Form the stage discharge curve it is observed that the rate of flow increases with the increase in flow depth. The maximum discharge is recorded as $0.0526m^3/s$ for 0.1487m of depth flow.
- Velocity measurements are made for four relative depths such as 0.15, 0.2, 0.25, and 0.3. Maximum velocity is observed just below the free water surface. This may be due to formation of boundary layer between the free water surface and air which restrict the flow of top layer.
- The depth averaged velocity is measured at a depth of 0.6H and 0.6(H-h) from the free water surface of the main channel and flood plain respectively. From the depth averaged velocity graph it is observed that the depth averaged velocity goes on decreasing with decrease in depth of flow.
- It is observed from the boundary shear stress graphs that, the boundary shear stress at the bed of the main channel remains higher at center while decreasing towards the wall. In the flood plain it is observed to remain lower at its wall while gradually increasing towards the junction of main channel and flood plain.
- From the values of Reynolds number and Froude's number, it is found that the flow type is turbulent for all eleven channels and they are having subcritical flow conditions.

- Discharge has been computed through five different methods. The results are compared with the actual data that has been collected from different sources. The percentage of error for all the methods is found to be more or less than 10%.
- From the absolute error graph it is clearly visible that MDCM is giving better result as compared to other four methods.
- From the comparison study we got that among the three numerical methods, both IDCM and MDCM gives better discharge prediction as compared to DCM as both IDCM and MDCM considers the effect of momentum transfer in terms of interface stress and interface length respectively, at the junction of the main channel and the flood plain whereas DCM does not consider this effect.
- Between MDCM and IDCM, we can say that from the calculation point of view MDCM is much better than IDCM, as it has less number of computational steps for calculation of discharge which leads to less computational error.
- By varying the values of manning's *n* with respect to depth of flow, discharge is computed through MDCM. It is found that MDCM fails to predict the discharge for lower depth of flow. But as the higher depth of it works well.
- Modification is applied to MDCM for predicting discharge for lower depth of flow.
- The discharge is calculated through the Revised MDCM and the results are compared with the experimental discharge data. It is found that the Revised MDCM is doing better discharge prediction as compared to MDCM with a percentage of error of 5%.

5.2 Scope for Future Work

The present research is restricted to straight prismatic channel. The work thereof leaves a broad spectrum for other investigators to explore many intricate flow phenomena such as secondary currents, turbulent intensities and vortices that significantly affects the distribution of boundary shear stress in simple and compound non prismatic straight channels as well as the meandering channel. The determination of discharge, velocity, boundary shear stress calculations involves limited number of data.

The future scope of the present work may be summarized as:

- The work is applied to straight prismatic channels only, while its applicability to other channels such as meandering, curved channel can be be incorporated and tested.
- The present work lacks shear force analysis for trapezoidal straight and meandering compound channel. The percentage of floodplain and main channel shear can be estimated for non-prismatic straight compound channels and models can be developed incorporating present data.
- The current data can be used to validate with data of other investigators.
- The channel here is smooth and rigid. Further investigation for the calculation of discharge, velocity and boundary shear stress may also be carried out for mobile beds and by roughening the channel bed.
- Discharge prediction through SKM is limited to prismatic rectangular straight channel in this work. So SKM can be used for trapezoidal as well as non-prismatic channel and for that some modification is required in the formulae.
- IDCM is restricted to straight prismatic channel only so it can be used for meandering channel by simply modifying the formulae for discharge and velocity calculation.
- By the help of dimensional analysis the given model can be further verified.

REFERENCES

1. Sellin, R.H.J.,(1964**),"**A Laboratory Investigation into the Interaction Between Flow in the Channel of a River and that of its Flood Plain", La Houille Blanche, *No.7, pp.793-801.*
2. Zheleznyakov, G. V. (1965). "Relative deficit of mean velocity of unstable river flow: Kinematic effect in river beds with floodplains." *Proc.14th Congress of IAHR*, Paris, France, 5, 144-148.
3. Ghosh, S. N. and Jena, S. B. (1971). "Boundary Shear Distribution in Open Channel Compound." *Proc. Inst. Civ. Eng.*, London, 49, 417-430.
4. Ghosh, S. N. and Kar, S. K. (1975). "River Flood Plain Interaction and Distribution of Boundary Shear in a Meander Channel with Flood Plain." *Proc. of the Inst. of Civil Engineers*, London, Vol.59, Part 2, December.
5. Yen, C. L. and Overton, D. E (1973). "Shape Effects on Resistance in Floodplain Channels." *J. Hydraul. Div.,* ASCE, 99(1), 219-238.
6. Myers,W. R. C. and Elsawy (1975). "Boundary Shear in Channel with Floodplain." *J. Hydraul. Eng.*, ASCE, 101(HY7), 933-946.
7. Rajaratnam, N. and Ahmadi, R.M. (1979). "Interaction between Main Channel and Flood Plain Flows." J. Hydraul. Div., ASCE, 105 (HY5), 573-588.
8. Wormleaton, P. R., Allen, J. and Hadjipanos, P. (1982). "Discharge Assessment in compound Channel Flow." *J. Hydraul. Eng.*, ASCE, 108(HY9), 975-994.
9. Knight D. W. and Demetriou J.D. (1983). "Floodplain and main channel flow interaction." *J. Hydraul. Eng*., ASCE, 109(8), 1073–92.
10. Knight, D. W. and Hamed, M. E. (1984). "Boundary Shear in Symmetrical Compound Channels." *J. Hydraul. Eng.*, ASCE, Vol.110, Paper 19217, pp.1412-1430
11. Wormleaton, and Hadjipanos, P. (1985). "Flow Distribution in Compound Channels." *J. Hydraul. Eng.*, ASCE, 111 (7), 1099-1104.
12. Myers, W.R.C. (1987). "Velocity and Discharge in Compound Channels." *J.Hydraul. Eng.*, ASCE, 113(6), 753-766.

13. Stephenson, D. and Kolovopoulos, P. (1990). "Effects of Momentum Transfer in Compound Channels." *J. Hydraul. Eng.*, ASCE, 116 (HY12), Paper No.25343, 1512-1522.

14. Shiono, K., Knight, D. W. (1988). "Refined Modelling and Turbulence Measurements." *Proceedings of 3rd International Symposium*, IAHR, Tokyo, Japan, July, 26-28.

15. Shiono, K. and Knight, D. W. (1991). "Turbulent open channel flows with variable depth across the channel." *J. Fluid Mech.*, 222, 617–46.189

16. Ackers, P. (1992). "Hydraulic Design of Two Stage Channels." *Proc. Inst. Civ.Eng., Waters. Maritime and Energy*, December, Paper No. 9988, 247-257.

17. Ackers, P. (1993a). "Stage-Discharge Functions for Two-Stage Channels." The Impact of New Research", *J. Inst. Water & Environmental Management*, 7(1), 52-61.

18. .Ackers, P. (1993b). "Flow Formulae for Straight Two-Stage Channels", *J.Hydraul. Res.*, IAHR, 31 (4), 509-531

19. Myer, W. R. C. and Lyness, J. F. (1997). "Discharge Ratios in Smooth and Rough compound Channels." *J. Hydraul. Eng.*, ASCE, 123 (3), 182-188.

20. Pang, B. (1998). "River Flood Flow and its Energy Loss." *J. Hydraul. Eng.*, ASCE, 124 (2), 228-231.187

21. Bousmar, D. and Zech, Y. (1999). "Momentum transfer for practical flow computation in compound channels." *J. Hydraul. Eng.*, ASCE, 125(7), 696-706.

22. Thrnton, C.I., Abt, S.R., Morris, C.E. and Fischenich, J.C. (2000)."Calculating shear stress at channel-overbank interfaces in straight channels with vegetated floodplains" *J. Hydraul. Eng.*, ASCE. 126(12), 929-936.

23. Patra, K. and Kar, S. (2000). "Flow Interaction of Meandering River with Floodplains." *J. Hydraul. Eng.*, 126(8), 593–604.

24. Liu and James (2000). "Estimating of discharge capacity in meandering compound channels using artificial neural networks," *Canadian Journal of Civil Engineering*, Vol.27, No.2, pp. 297-308,

25. Myer, W. R. C., Lyness, J. F. and Cassells, J. (2001). "Influence of Boundary Roughness on Velocity and Discharge in Compound River Channels," *J. Hydraul. Eng.*, ASCE, 39 (3).

26. Atabay, S. A. and Knight, D.W., (2002). "The influence of floodplain width on the stage-discharge relationship for compound channels", River Flow 2002, *Proc. Int. Conf. on Fluvial Hydraulics*, Louvain-la-Neuve, Belgium, Sept., Vol.1, 197-204.

27. Ozbek , T. and Cebe ,K. (2003). "Comparison of Methods for Predicting Discharge in straight Compound Channels Using the Apparent Shear Stress Concepts." *Tr. Journal of Engineering and Environmental Science*, Tubitak, 101-109.

28. Weber, J. F., and Menéndez, A.N. (2004)) An Performance of lateral velocity distribution models for compound channel sections. River Flow 2004, Proc., Int. Conf. on Fluvial Hydraulics,Vol. I, Balkema, Rotterdam, The Netherlands, 449–457.

29. Tominaga, A., Knight, D. W. (2004). "Numerical Evaluation of Secondary Flow Effects on Lateral Momentum Transfer in Overbank Flows." River Flow- 2004, Taylor and Francis Group, London.

30. Jin, Y.C., Zarrati, A. R. and Zheng, Y. (2004). "Boundary Shear Distribution in Straight Ducts and Open Channels" *J. Hydraul. Eng.*, ASCE, 130(9), 924-928.

31. Prooijen, B.C.V., Battjes, J. A. and Uijttewaal, W.S. J. (2005). "Momentum Exchange in Straight Uniform Compound Channel Flow" *J. Hydraul. Eng.*, ASCE, 131(3),175-183.

32. Guo, J. and Julien, P. Y. (2005). "Shear Stress in Smooth Rectangular Open-Channel Flows" *J. Hydraul. Eng.*, ASCE, 131(1), 30-37.

33. Othman, F. and Valentine, E.M. (2006). " Numerical modelling of the velocity distribution in a compound channel" *Journal of Hydrology and Hydromechanics*, 54, 3, pp.269-279.

34. Proust. S., Rivière. N., Bousmar. D., Paquier. A., Zech, Y. and Morel. R. (2006). "Flow in Compound Channel with Abrupt Floodplain Contraction." *J. Hydraul. Eng.*, ASCE, Vol. 132, No. 9, September 1.

35. Knight, Donald. W., Omran, M. and Tang, X. (2007). "Modeling Depth-Averaged Velocity and Boundary Shear in Trapezoidal Channels with Secondary Flows" *J. Hydraul. Eng*., ASCE, 133(1), 39-47.

36. Khatua, K.K., Patra, K.C. (2007). "Boundary Shear Stress Distribution in Compound Open Channel Flow." *J. Hydraul. Eng*., ISH, 12 (3), 39-55.

37. Huthoff, F., Roos, P. C., Augustijn, D. C. M. and Hulscher, S. J. M. H. (2008). "Interacting divided channel method for compound channel flow." *J. Hydraul. Eng*., ASCE, 134(8), 1158–1165.

38. Mamak, M., (2008). "A comparison of conveyance methods for compound channels". *Kuwait J. Sci. Eng*.35(2B).pp 19-38

39. Seckin, G., Mamak, M., Atabay, S., and Omran, M. (2008). "Discharge estimation in compound channels with fixed and mobile bed" *Sadhana* . Indian Academy of Science .Vol. 34, Part 6, December 2009, pp. 923–945.

40. Khatua, K.K. (2008) . "Interaction of flow and estimation of discharge in two stage meandering compound channels." Ph.D. thesis, NIT, Rourkela, India.

41. Tang, X. & Knight, D.W. (2009). "Lateral distributions of streamwise velocity in compound channels with partially vegetated floodplains" *Sci China Ser E-Tech Sci*, 52(11): 3357─3362,

42. Khatua, K.K. (2009). "Apparent Shear Stress in a Compound Channel" this paper is communicated to HYDRO 2009, CWPRS, Pune

43. Zahiri, A. and Dehghani, A.A. (2009). "Flow Discharge Determination in Straight Compound Channels Using ANNs" World Academy of Science, Engineering and Technology 58 ,pp 12-15`

44. Tang, X., Sterling, M. & Knight, D.W. (2010). "A General Analytical Model for Lateral Velocity Distributions in Vegetated Channels". *Bundesanstalt für Wasserbau*, River Flow 2010 conf ISBN 978-3-939230-00-7, 469-475,

45. Knight, D.W., Tang, X. & Sterling, M. (2010). "Solving open channel flow problems with a simple lateral distribution model" *Bundesanstalt für Wasserbau*, River Flow 2010 conf ISBN 978-3-939230-00-7, pp 41-48.

46. Beaman, F. (2010). "Large Eddy Simulation of Open Channel Flows For Conveyance Estimation". Thesis submitted to the University of Nottingham for the degree of Doctor of Philosophy.

47. Absi, R. (2011). "An ordinary differential equation for velocity distribution and dip-phenomenon in open channel flows" *Journal of Hydraulic Research*, IAHR, Taylor and Francis, Vol. 49, N° 1, pp. 82-89

48. Fernandes, J.N., Leal, J.B., & Cardoso, A.H. (2012). "flow structure in acompound channel with smooth and rough flood plains" *European water* E.W.publication,38. pp 3-12

49. Khatua, K.K., Patra, K.C., and Mohanty, P.K. (2012)."Stage-Discharge Prediction for Straight and Smooth Compound Channels with Wide Floodplains'' *J. Hydraul. Eng*. ASCE 138 (1), 93-99.

50. Yang, K., Liu, X., Cao, S., & Huang, E. (2014). "Stage-Discharge Prediction in Compound Channels" *J. Hydraul. Eng*. ASCE,140(4) 06014001.

APPENDIX-I

List of Publication

- Published "Stage Discharge Prediction in a Prismatic Compound Channel" in *International Journal of Civil Engineering Research*. ISSN 2278-3652 Vol (5), Number 3 (2014), pp. 227-232
- Published "Experimental & Validation of Discharge Prediction Approaches In Straight Two Stage Compound Channels" *International Journal of Engineering Research and Applications (IJERA)* ISSN: 2248-9622. pp 39-44

Accepted for Publication

- Paper "Analysis of Depth Averaged Velocity in Meandering Compound Channels" accepted for *7th International Conference in Fluvial Hydraulics* – River Flow 2014, Lausanne, Switzerland.

APPENDIX-II

SKM Method in MATLAB

The experiments are conducted in NIT Rourkela 2013-2014 (Bandita channel), by considering different water depth and the depth averaged velocity and discharge is calculated for each relative depth. SKM is being used and a program is being written for rectangular compound channel through MATLAB to calculate the depth average velocity, boundary shear stress and discharge for each flow depth. The code for finding out the velocity, boundary shear stress is being written for one relative depth and is given below.

```
clear all
clc
lamdamc ;                                   % all units are in meter
f;                                          %coefficent of friction;
H;                                          %overall depth of water
h;                                          %depth of the main channel
w;                                          %total width of the channel
S;                                          %bed slope of the channel
g;                                          %accelaration due to gravity
taumc;                                      %boundary shear stress in the main channel
taufp;                                      %boundart shear stress in flood plain
Dr=(H-h)/H;                                 % relative depth
B1;                                         %half width of the main channel
B2;                                         %width of the right flood plain
B3;                                         %width of the left flood plain
ro=1000;

%calculation of lamda for flood plain
lamdafp=lamdamc*(-0.2+1.2*(Dr^(-1.44)));

% calculation of gamma for the compound channel
Y1=sqrt(2/lamdamc)*((f/8)^0.25)*(1/H);      %Y1 indicates the gamma value for the main
                                            channel
```

```
Y2=sqrt(2/lamdafp)*((f/8)^0.25)*(1/(H-h));      %Y2 indicates the gamma value for the right flood plain

Y3=sqrt(2/lamdafp)*((f/8)^0.25)*(1/(H-h));      %Y3 indicates the gamma value for the left flood plain

K1=taumc/(ro*g*H*S);
K2=taufp/(ro*g*S*(H-h));
K3=taufp/(ro*g*S*(H-h));
% calculation of secondary current
cgmmamc=ro*g*H*S*(1-K1);
cgmmafp2=ro*g*(H-h)*S*(1-K2);
cgmmafp3=ro*g*(H-h)*S*(1-K3);

% calculation of Beta

betamc=cgmmamc/(ro*g*H*S);
betafp2=cgmmafp2/(ro*g*(H-h)*S);
betafp3=cgmmafp3/(ro*g*(H-h)*S);

% calculation of k

k1=((8*g*S*H)/f)*(1-betamc);
k2=((8*g*S*(H-h))/f)*(1-betafp2);
k3=((8*g*S*(H-h))/f)*(1-betafp3);

 %matrix method
```

$$A = \begin{bmatrix} e^{\gamma_1 B_1} & e^{-\gamma_1 B_1} & -e^{\gamma_2 B_1} & -e^{-\gamma_2 B_1} & 0 & 0 \\ \gamma_1 e^{\gamma_1 B_1} & -\gamma_1 e^{\gamma_1 B_1} & -\gamma_2 e^{\gamma_2 B_1} & \gamma_2 e^{\gamma_2 B_1} & 0 & 0 \\ 0 & 0 & e^{\gamma_2 (B_1+B_2)} & e^{-\gamma_2 (B_1+B_2)} & 0 & 0 \\ e^{-\gamma_1 B_1} & e^{\gamma_1 B_1} & 0 & 0 & -e^{-\gamma_3 B_1} & -e^{\gamma_3 B_1} \\ \gamma_1 e^{-\gamma_1 B_1} & -\gamma_1 e^{-\gamma_1 B_1} & 0 & 0 & -\gamma_3 e^{-\gamma_3 B_1} & \gamma_3 e^{-\gamma_3 B_1} \\ 0 & 0 & 0 & 0 & e^{-\gamma_3 (B_1+B_3)} & e^{\gamma_3 (B_1+B_3)} \end{bmatrix}$$

$$B = \begin{bmatrix} k_2 - k_1 \\ 0 \\ -k_2 \\ k_3 - k_1 \\ 0 \\ -k_3 \end{bmatrix}$$

```
I=A\B;

 y=0.45:-0.05:-0.45;

    for j=1:2

      for i=1:19
      ud(i,1)=y(i);
      taub(i,1)=y(i);
      Q1(i,1)=y(i);
      Q2(i,1)=y(i);
      for i=1:4
      ud(i,2)=(I(3)*exp(Y2*y(i))+I(4)*exp(-Y2*y(i))+k2)^0.5;
      taub(i,2)=(f*ro*ud(i,j)^2)/8;
      Q1(i,2)=ud(i,2)*area1;
      end
      for i=5:10
      ud(i,2)=(I(1)*exp(Y1*y(i))+I(2)*exp(-Y1*y(i))+k1)^0.5;
      taub(i,2)=(f*ro*ud(i,j)^2)/8;
      Q2(i,2)=ud(i,2)*area2;
      end
      for i=11:16
      ud(i,2)=(I(1)*exp(-Y1*y(i))+I(2)*exp(Y1*y(i))+k1)^0.5;
      taub(i,2)=(f*ro*ud(i,j)^2)/8;
      Q2(i,2)=ud(i,2)*area2;
      end
      for i=16:19
      ud(i,2)=(I(6)*exp(-Y3*y(i))+I(5)*exp(Y3*y(i))+k3)^0.5;
      taub(i,2)=(f*ro*ud(i,j)^2)/8;
      Q1(i,2)=ud(i,2)*area1;
      end
   end
```

```
    end
ud
taub
plot(y,ud)
hold on
plot(y,taub);
hold off
 table1=[y,ud];
table2=[y,taub];
fid1=fopen('depth averaged value.txt','w');
fid2=fopen('boundary shear.txt','w');
fprintf(fid1,' m/s \n');
fprintf(fid1,'  %1.5f\n',table1);
fprintf(fid2,' N/m^2 \n');
fprintf(fid2,'%1.5f\n',table2);
fclose(fid1);
fclose(fid2);
```